AD-A118 687 BRISTOL UNIV (ENGLAND) F/G 8/8
THE ROLE OF HILLSLOPE HOLLOWS IN GENERATING RIVER DISCHARGE.(U)
APR 82 M G ANDERSON. DA-ERO-78-G-104
UNCLASSIFIED NL

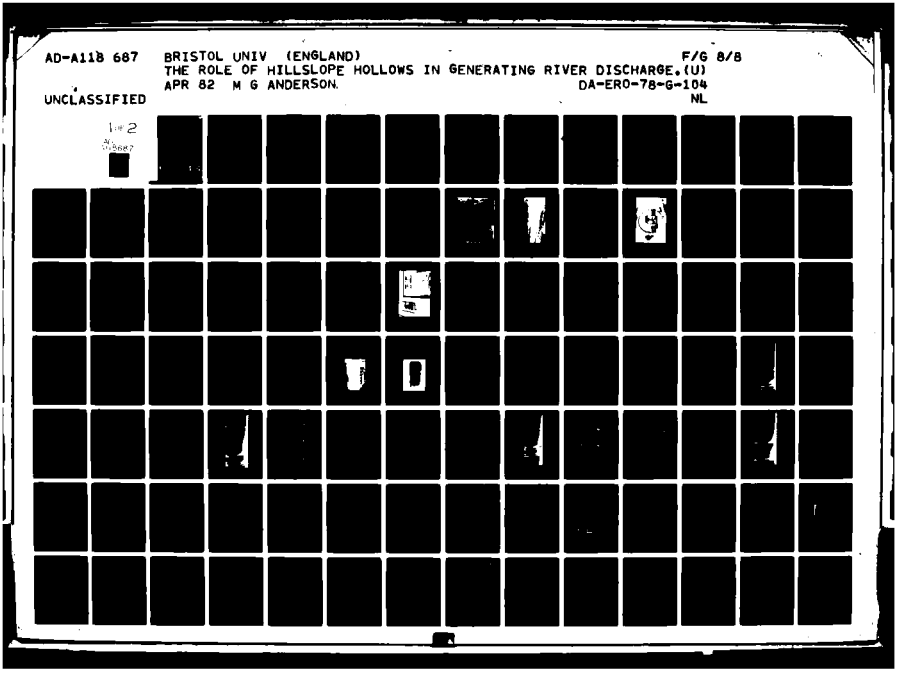

THE ROLE OF HILLSLOPE HOLLOWS IN GENERATING RIVER DISCHARGE

Final Technical Report

by

Dr. Malcolm G. Anderson

April 1982

EUROPEAN RESEARCH OFFICE
United States Army
London England

GRANT NUMBER DA-ERO-78-G-104

Dr. Malcolm G. Anderson

UNCLASSIFIED

SECURITY CLASSIFICATION OF THIS PAGE *(When Data Entered)*

REPORT DOCUMENTATION PAGE		READ INSTRUCTIONS BEFORE COMPLETING FORM
1. REPORT NUMBER	2. GOVT ACCESSION NO. AD-A118687	3. RECIPIENT'S CATALOG NUMBER
4. TITLE *(and Subtitle)* The Role of Hillslope Hollows in Generating River Discharge		5. TYPE OF REPORT & PERIOD COVERED Final Technical Report October 1978 - May 1982
		6. PERFORMING ORG. REPORT NUMBER
7. AUTHOR(s) Dr. Malcolm G. Anderson		8. CONTRACT OR GRANT NUMBER(s) DAERO-78-G-104
9. PERFORMING ORGANIZATION NAME AND ADDRESS University of Bristol Bristol, England		10. PROGRAM ELEMENT, PROJECT, TASK AREA & WORK UNIT NUMBERS
11. CONTROLLING OFFICE NAME AND ADDRESS US Army European Research Office Box 65 FPO New York 09510		12. REPORT DATE April 1982
		13. NUMBER OF PAGES 138
14. MONITORING AGENCY NAME & ADDRESS *(if different from Controlling Office)*		15. SECURITY CLASS. *(of this report)* Unclassified
		15a. DECLASSIFICATION/DOWNGRADING SCHEDULE

16. DISTRIBUTION STATEMENT *(of this Report)*

Approved for Public Release; Distribution Unlimited

17. DISTRIBUTION STATEMENT *(of the abstract entered in Block 20, if different from Report)*

18. SUPPLEMENTARY NOTES

19. KEY WORDS *(Continue on reverse side if necessary and identify by block number)*

Hillslope Hydrology; Modelling; Soil Water

20. ABSTRACT *(Continue on reverse side if necessary and identify by block number)*

This investigation sought to undertake an analysis of soil water movement on shallow, undulating topography with the specific aim of isolating the spatial and temporal nature of hillslope zones contributing preferentially to streamflow in such topography.

With the combined used of data on soil water potentials from the study site and a simulation program designed to replicate soil water movement processes on hillslopes, it was shown that only in relatively restrictive cases of topography/soil/stream gradient configurations, does soil water convergence always

DD FORM 1 JAN 73 1473 EDITION OF 1 NOV 65 IS OBSOLETE

UNCLASSIFIED

SECURITY CLASSIFICATION OF THIS PAGE *(When Data Entered)*

take place into hillslope hollows. The implications of this finding in the context of static indices, hitherto used to identify those hillslope zones that saturate preferentially, is discussed.

It is further shown that relatively minor variations within the shallow topography area studied are capable of enducing significant differences in the hillslope outflow hydrographs. The detailed relationships between soil water convergence zones, in being spatially and temporally dynamic, and variations in the hillslope contribution to streamflow are discussed.

The principal recommendation is the evident need for developing improved simulation procedures for identifying streamflow source areas in shallow topography, as evidenced by the research reported in this investigation.

ABSTRACT

This investigation sought to undertake an analysis of soil water movement on shallow, undulating topography with the specific aim of isolating the spatial and temporal nature of hillslope zones contributing preferentially to streamflow in such topography.

With the combined used of data on soil water potentials from the study site and a simulation program designed to replicate soil water movement processes on hillslopes, it was shown that only in relatively restrictive cases of topography/soil/stream gradient configurations, does soil water convergence always take place into hillslope hollows. The implications of this finding in the context of static indices, hitherto used to identify those hillslope zones that saturate preferentially, is discussed.

It is further shown that relatively minor variations within the shallow topography area studied are capable of enducing significant differences in the hillslope outflow hydrographs. The detailed relationships between soil water convergence zones, in being spatially and temporally dynamic, and variations in the hillslope contribution to streamflow are discussed.

The principal recommendation is the evident need for developing improved simulation procedures for identifying streamflow source areas in shallow topography, as evidenced by the research reported in this investigation.

CONTENTS

Acknowledgements

Dr. P. E Kneale (University of Bristol) was a research assistant on the research program and her help is gratefully acknowledged.

Mr. E. Thomas (University of Bristol) provided advice on selected computer procedures.

Mr. S. Godden and Mr. A. Philopott (University of Bristol) prepared many of the diagrams and plates.

The Word Processing Center and Publications and Graphic Arts Division (Waterways Experiment Station, Vicksburg, Mississippi) aided in the production of the final report, and their assistance and efficiency is recorded with thanks.

Discussions with the following individuals were of particular value at various stages during the project: Dr. R. A. Freeze, Mr. W. E. Grabau, Professor D. Hillel.

PUBLICATIONS

Publications arising from the research program to which at least partial contractural sponsorship is attributed:

1980. Topography and hillslope soil water relationships in a catchment of low relief. Journal of Hydrology, 47, 115-128 M. G. Anderson and P. E. Kneale.

1982. The influence of low angled topography on hillslope soil water convergence and stream discharge. Journal of Hydrology, in press. M. G. Anderson and P. E. Kneale.

1982. Modelling hillslope soil water status during drainage. Transactions Institute British Geographers, in press. M. G. Anderson

1982. Piping and throughflow in humid temperate areas, in Badland Geomorphology and Pipe Erosion, Bryan, R. and Yair, A. (eds). Geobooks, Norwich, in press. M. G. Anderson and T. P. Burt.

PART I

Chapter 1

The Role of Hillslope Hollows In Generating River Discharge

Introduction

1.1 Background

Existing hydrology models do not generally include submodels which accurately portray the detailed soil water processes on hillslopes (1). It is evident from recent empirical findings that this widely recognized omission may present less problems in certain topographies and environments than others from the standpoint of forecasting. For example, on steep permeable slopes, it has been shown that soil water convergence dominantly occurs in topographic hollows (2, 3). Emipirical generalizations are, however, hard to make in the field of hillslope hydrology for three principal reasons:

(a) the significant variations that are found catchment to catchment

(b) the rather piecemeal approach that many field studies have taken to both experimental design and rigor in analysis.

(c) the relative bias there has been towards investigations of hillslope hydrology processes occurring on steeper slopes with permeable regoliths. (Table 1 details some recent principal investigations to demonstrate this point).

In recognition of these general points, the objectives of this research and the experimental design were directed towards soil water processes on shallow topography (point c), specifically to examine convergence and streamflow source area location (point b), and to model these processes over a wide range of environmental conditions (point a).

Table 1.1.

Examples of Previous Studies in Hillslope Hydrology which show that Investigators have Concentrated Primarily on Slopes which are Steeper than 12 Degrees and have Permeable Regoliths

Author	Slope Angle	Permeability and Soils	Location and Notes
Bates and Henry (1928)(4)	22°	Deep permeable soils, particularly on the catchment divides	Wagon Wheel Gap, Colorado
Hewlett (1961)(5)	22°	Permeable sandy loam	Slope model, Coweeta, North Carolina
Pereira et al. (1962)(6)	---	Deep permeable volcanic ash soils	Kenya
Hewlett and Hibbert (1967)(7)	12° - 26°	Granitic sandy loams	Cowetta Watersheds 2, 8, 14, 18, 21, 28 and 36, North Carolina
Whipkey (1965, 1967)(8, 9)	11° - 23°	Coarse sandy loam to fine silt loam	Plot and sprinkler studies of runoff
Ragan (1968)(10)	---	Sandy soils to glacial tills	Forested catchment, Vermont
Dunne and Black (1970)(11)	16° - 45°	Free draining brown podzols and brown sandy loams overlying poorly drained tills and varve deposits	Vermont

(Continued)

Table 1.1 (Continued)

Author	Slope Angle	Permeability and Soils	Location and Notes
Hewlett and Nutter (1970)(12)	18°	Shallow permeable soils overlying bedrock	Whitehall Watershed, Georgia
	22°	Very permeable, deep granitic soils on divides and valley floors	Coweeta Waterhsed 17, North Carolina
Wilson and Lignon (1973)(13)	6°	Sandy loams, saturated hydraulic conductivities of 4.4×10^{-1} to 4.0×10^{-5} cm sec^{-1}	Two plot studies, Clemson Watershed, South Carolina
Weyman (1973)(14)	15° - 23°	Free draining brown earth silty to very stony loam	East Twin Brook, Mendip
Arnett (1974)(15)	14.5° and 17.7°	Free draining brown earths	Plot study, Yorkshire
Knapp (1974)(16)	11°	Free draining podzols, silty clays, peat. Pipes	Plynlimmon, Wales
Harr (1977)(17)	26° - 50°	Highly weathered, coarse volcanic breccias, saturated hydraulic conductivities range between 1.1×10^{-1} to 4.4×10^{-3} cm sec^{-1}	Oregon

(Continued)

Table 1.1 (Concluded)

Author	Slope Angle	Permeability and Soils	Location and Notes
Anderson and Burt (1978)(18)	25°	Free draining, permeable	Bicknoller Combe, Somerset
Burt (1978)(19)		brown earths, saturated hydraulic conductivity 1×10^{-1} cm sec^{-1} to 5×10^{-3} cm sec^{-1}	

Chapter 2

Objectives and Approach

Objectives

This investigation had 4 principal objectives:

(i) to undertake an empirical investigation of soil water movement on shallow, undulating topography with the specific aim of isolating the spatial and temporal nature of hillslope zones contributing preferentially to streamflow in such topography.

(ii) to undertake a simulation of soil water processes on a topographic hollow and spur hillslope configuration, for a wide range of soil characteristics, slope angles and stream gradients. The objective here was thus to seek to define the circumstances under which hillslope soil water accumulates in topographic hollows and those circumstances where more spatially complex patterns of accumulation occur.

(iii) as a result of (ii) to prescribe circumstances under which static, a priori topographically based indices may be appropriate for the identification of hillslope zones that saturate, and contribute to streamflow, preferentially.

(iv) to examine the effect of minor topographic hillslope differences on the hillslope outflow hydrographs.

The overall objective therefore is to provide both a clearer understanding of hillslope flow processes in shallow topography and to illustrate the applications of these findings to hydrology modelling strategies.

2.2. Approach and scope

Given the stated objectives, the report has two principal sections:

Part II (Chapters 3-5) outlines the empirical aspects of the investigation, whilst

Part III (Chapters 6-7) reports the results of the simulation procedures. The research program was thus divided into two principal phases:

Phase 1 involved the site and instrumentation selection and the acquisition of soil water data over a 2-yr period, together with associated streamflow and ancillary data.

Phase 2 involved in part the writing of a computer simulation model to evaluate environmental controls on hillslope soil water drainage. This model was then calibrated and tested on the study site data. Subsequent extension to other non-instrumented areas of the catchment was undertaken to evalate the importance of topographic hollow and spur slope sectors in contributing to streamflow.

It is important to place this approach in the context of work done in this specific field.

The inter-relationships between the major variables which control hillslope runoff processes have been described schematically by Dunne (1978)(20), Figure 2.1. In areas where Hortonian overlandflow does not dominate the hydrograph, the variable source area concept exerts a significant control on streamflow.

Although the variable source area concept, established in the 1960's, has been investigated generally, and a wide number of case studies of catchment processes has been made, in 1978 Dunne reports "that the spatial and temporal occurrence of runoff processes is less well understood" in humid temperate areas, as compared with overland flow, although the general controls on runoff can be detailed. This is primarily due to the lack of empirical investigations at suitable temporal and spatial scales of soil water physics in small catchments. In a number of studies precipitation has been related to runoff without detailed investigation of the soil water processes, although soil water is assumed to play a significant role in the generation of discharge. The importance of the zone of 'saturated' soil, or soils, with high soil water potentials, along the stream in generating throughflow is central to the variable or partial source area concept (Hewlett and Hibbert, 1967)(7), but examination of the fluctuations in the saturated area during precipitation and drainage have been limited

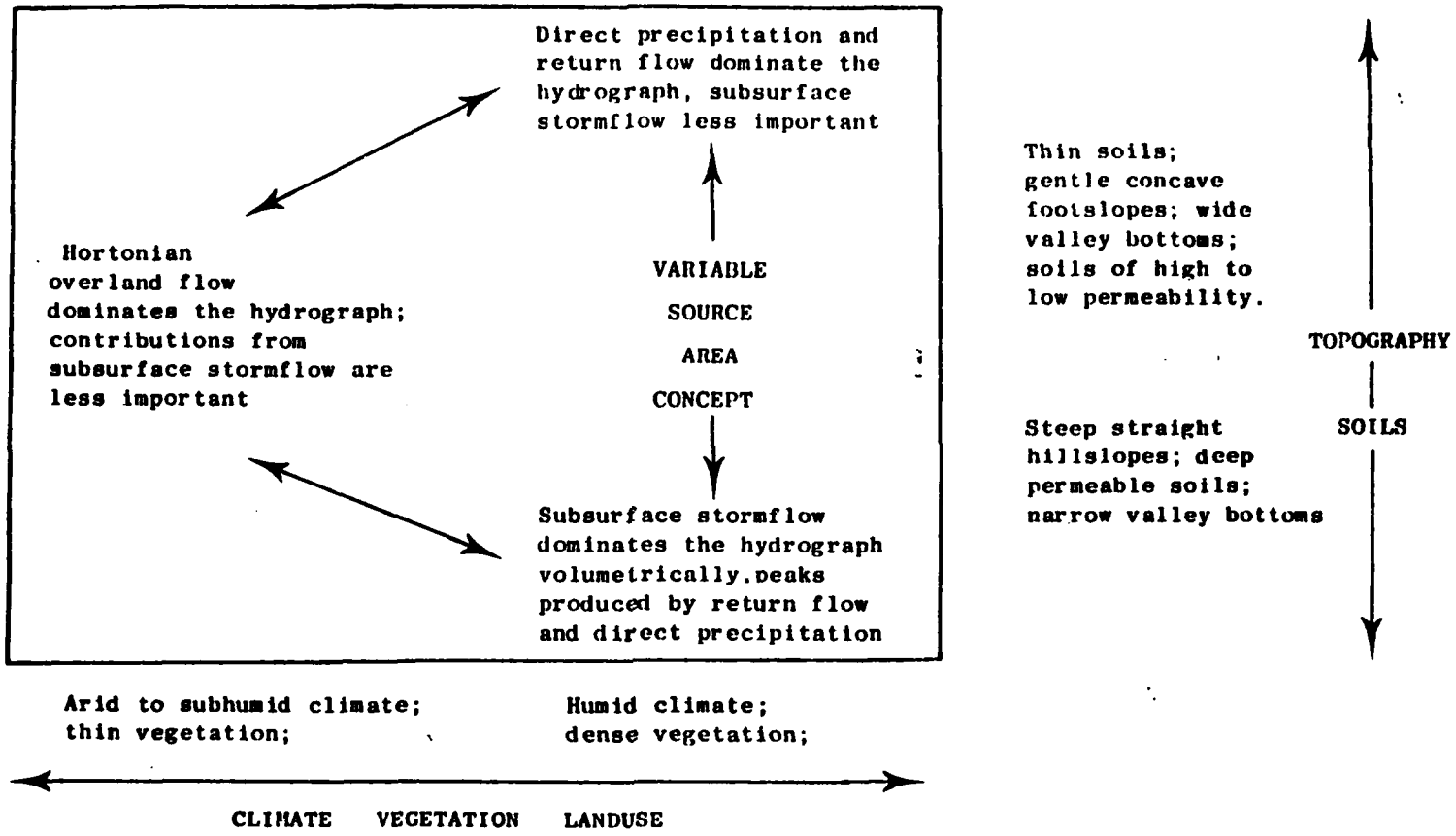

Figure 2.1. Schematic illustration of the occurrence of various runoff processes in relation to their major controls, (after Dunne 1978) (20).

where manual tensiometers were employed (Weyman, 1973)(14). Although Wilson and Lignon (1973)(13) used an automatically recording system of tensiometers for their plot studies, continuous recording of soil water potentials has not been a feature of hillslope hydrology studies until more recently (Anderson and Burt, 1977(2)

The importance of slope morphology in controlling the flow of water in hillslopes has been considered implicitly by Kirkby and Chorley (1967)(21) with their discussion of the role of contour curvature, and explicitly by Anderson and Burt (1978)(3) on a steep permeable regolith.

Results obtained by Anderson and Burt showed that the saturated wedge of soil at the foot of the slope controls the discharge of hillslope water to the stream. The wedge expands to its maximum extent coincident with the peak of the delayed throughflow pulse, then the saturated wedge drains slowly supplying water to the stream, but it never disappears. This was true even during the summer of 1976 where there was a five-month period without effective rainfall (Burt and Anderson, 1980)(22).

Furthermore, it was shown that it is the topographic hollows on these slopes which are the most important areas in supplying the secondary throughflow peaks. On these steep slopes (26°) the total soil water potential equation is dominated by the elevation potential component. Consequently, the direction of soil water flow is primarily downslope converging into the centre of the hollow. Kirkby and Chorley (1967)(21) considered zones of saturation would occur preferentially on slopes with concave contours and concave profiles. Anderson and Burt (1978)(3) were able to show that hollows provide the major source of hillslope soil water discharge when compared with straight slope and spur sections, and that the hillslope contours could be used to identify these areas. Recognizing the dominance of elevation potential in total potential calculations on steep hillslopes, we suggest that contours can be used as surrogates for equipotential lines on steep, permeable slopes, and that a flow net can be constructed based on the contours alone. The divergence or convergence of the flow lines would indicate whether or not a zone of saturation was likely to be preferentially developed, and hence the most important variable source areas of hillslope discharge could be identified.

There is no indication as to whether in areas of low relief the topography of the area will similarly significantly affect the distribution of the saturated

wedge or that hollow areas are the major source areas for throughflow. In lower-angled slopes the elevation potential will not play as significant a role in its effect upon total potentials as it does on steep slopes. Therefore, soil water convergence is more likely to be affected by other local variables. It is the general purpose of this investigation to examine this assertion using the two phase approach outlined.

PART II

Chapter 3

Soil Water Monitoring: Field Site and Instrumentation

3.1. Introduction

The relative sparsity of empirical evidence on soil water processes on shallow topography has already been noted (Table 1.1). This fact combined with the potential complexities of spatial and temporal variations of stream source areas as such hillslopes (Section 2.2) makes it especially important not only that further empirical evidence be obtained, but that such evidence should be part of a larger experimental design that would facilitate the realistic testing and calibration of soil water simulation procedures. Thus the field site experimental design outlined in this chapter sought to provide sufficient resolution in both these aspects - compatible with the two phase research approach already stated (Section 2.2).

3.2. The field site

Figure 3.1 shows the general location of the site, whilst Figure 3.2 provides a detailed aerial view of the catchment, and a view of the shallow topography at the instrumented site (Figure 3.2B).

Geology

Bedrock: Keuper Marl, overlain by clay loam soils. These soils are fine, stoneless clay loams with fine pores and well aerated by worm channels. A clear bedrock-soil interface does not occur on this material because the soil horizons grade into the unweathered Marl. This can be seen in the lower stream reaches.

Land use: pasture.

Topography: The catchment exhibits generally shallow relief (12°) with gently undulating topography (hollow and spur). The catchment was divided into 4 subcatchments on the basis of the topography to which the stream hydrological response was to be subsequently related (see Figure 3.1):

Subcatchment	Hillslope angle	Slope topography
Source to D	4°	straight
D - C	2° - 6°	hollow and spur
C - B	6° - 10°	straight
B - A	6° - 10°	spur and hollow

3.3. Monitoring streamflow

The experimental demands for very accurate streamflow data in terms of both the stage and the timing of changing stage made special demands on the instrumentation in this area. This section describes the layout and the testing of a set of electrical stage records which monitored the streamflow. Five weirs were installed at the site, four on the main channel and the fifth on a tile drain tributary. The stream is incised by up to five metres in its lower reaches and is two to five metres wide. This channel width meant that weirs A, B, and C had to be constructed in wood. These were approximately 5 m wide by 1 m deep with a standard 90° 'V' notch. Weir D is located in a narrower channel. This weir again with a 90° 'V' notch was constructed from plastic with dexion supports. At weir E on the drain a metal 1/2 90° 'V' notch weir was employed. The 'V' notches used at each weir were tooled to the British standard. Regular tests were undertaken to ensure that the weir calibrations were stable.

Weirs A and B were installed with Munro stage recorders. These drum recorders had 1:1 gearing, and eight day clock charts. It was impossible to

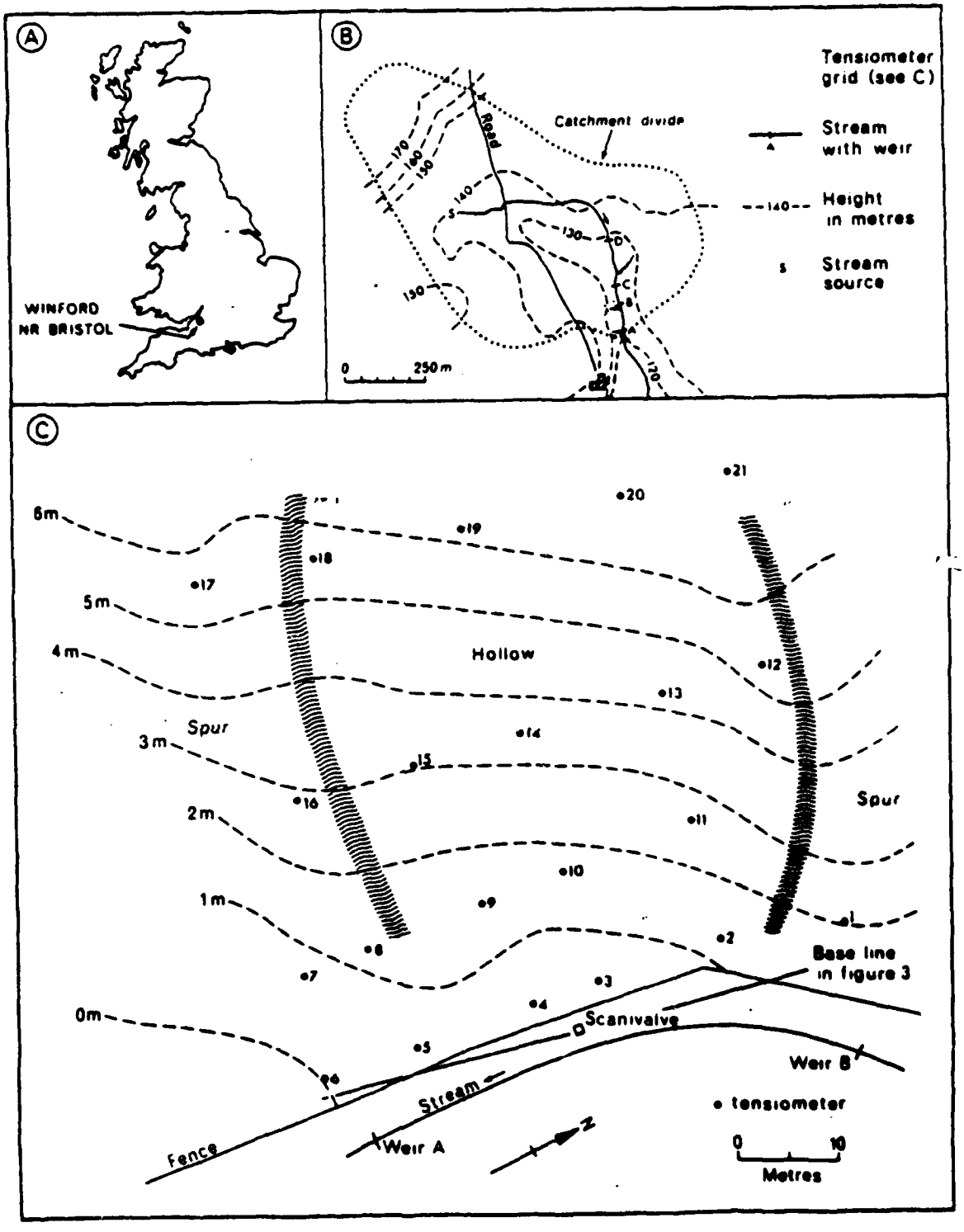

Figure 3.1. Study Site

Figure 3.2A. Aerial View of Study Site.

Figure 3.2B. View looking north across instrumented hillslope sector (See Figure 3.2A)

synchronize the charts because of the gearing and although stage may be read very accurately the time when a change in stage occurs cannot be read to better than ± 15 minutes.

For these reasons electrical stage recorders were used at all of the weirs. (Anderson and Burt 1978, (23) Anderson and Kneale 1980)(24).

Figure 3.3 shows the design of the electrical stage recorders. The float in the stilling well is connected by copper wire to a very light aluminum screw-threaded wheel. This wheel in turn is attached to a low torque 10 k potentiometer. As the float rises, the wheel turns and the potentiometer resistance increases. The potentiometer output is converted to a suitable electrical signal, and the necessary circuit is powered by a 1.25 V dry battery. The output is to a multichannel chart recorder.

The electrical stage recorder at each of the five weirs were connected by three-core telephone cabling to a six-channel 'Miniscript' recorder. The recorder scans each channel in turn for a 10 second period, so that each channel is read once every minute. The chart speed of 10 mm hr^{-1} allowed the time of rise or peak flows to be determined to within three minutes.

The power demand for this instrumentation is very low. The batteries powering the timing circuit were changed at six-monthly intervals but were not discharged at the time they were changed. The miniscript recorder required a 24 volt d.c. input but the consumption here was also very low and batteries were changed at four to six weekly intervals.

Tests were undertaken with this instrumentation because the calibration problems had not previously been investigated, and in the case of this field site, the telephone cable lengths were quite considerable (800 metres from weir D to the recorder).

A series of tests were undertaken at each weir where the mV output was measured for a range of stage values at both the stage recorder and at the chart recorder. The results of these tests for four different stage values at each weir are given in Figure 3.4.

This shows the output in mV both when the chart recorder is connected to that channel and when it is reading other channels and is therefore disconnected. From the results, it is clear that

(i) a slight voltage drop occurs at the stilling well recorder when the chart recorder is connected.

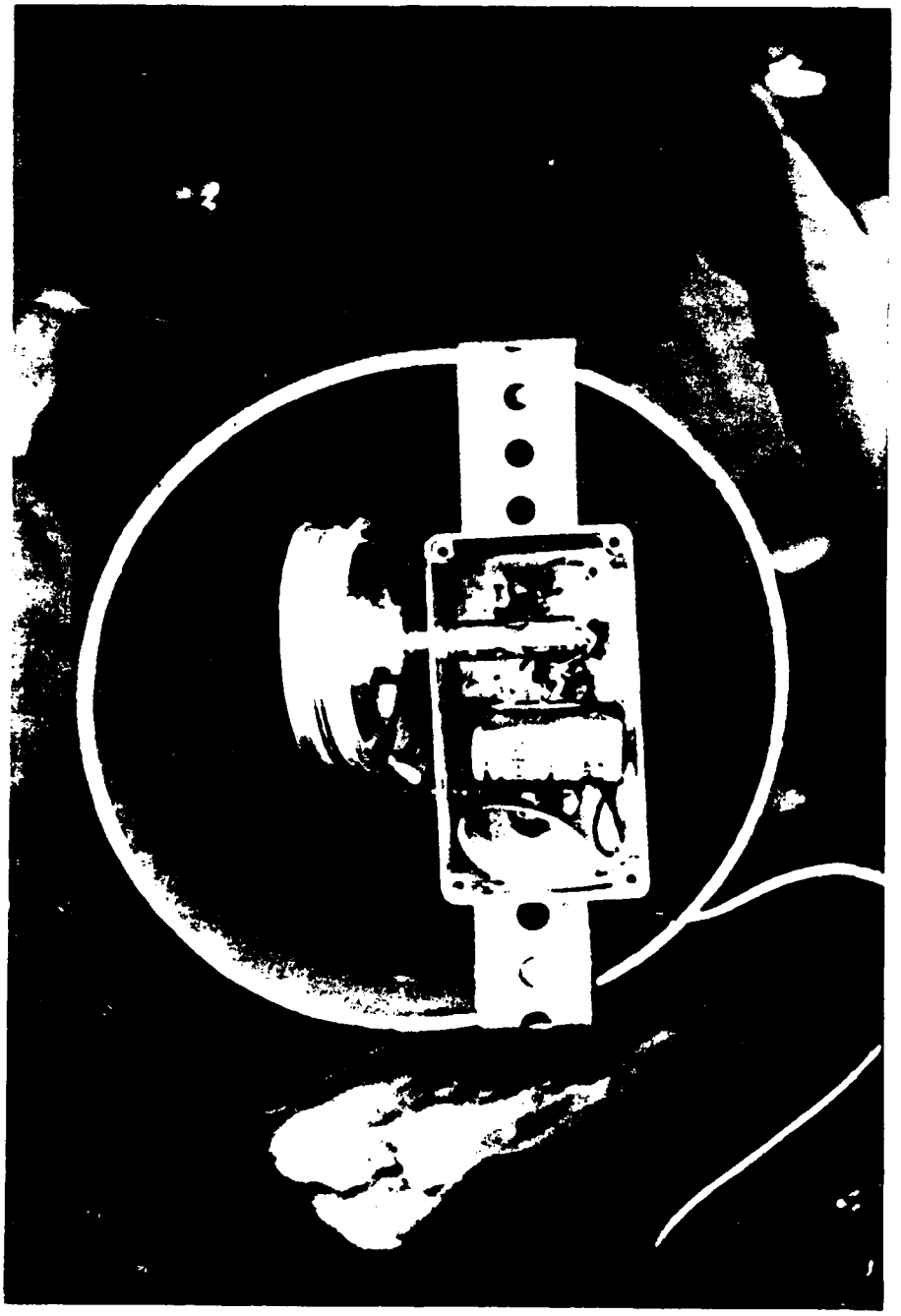

Figure 3.3. View of electrical stage recorder mounted on the stilling well.

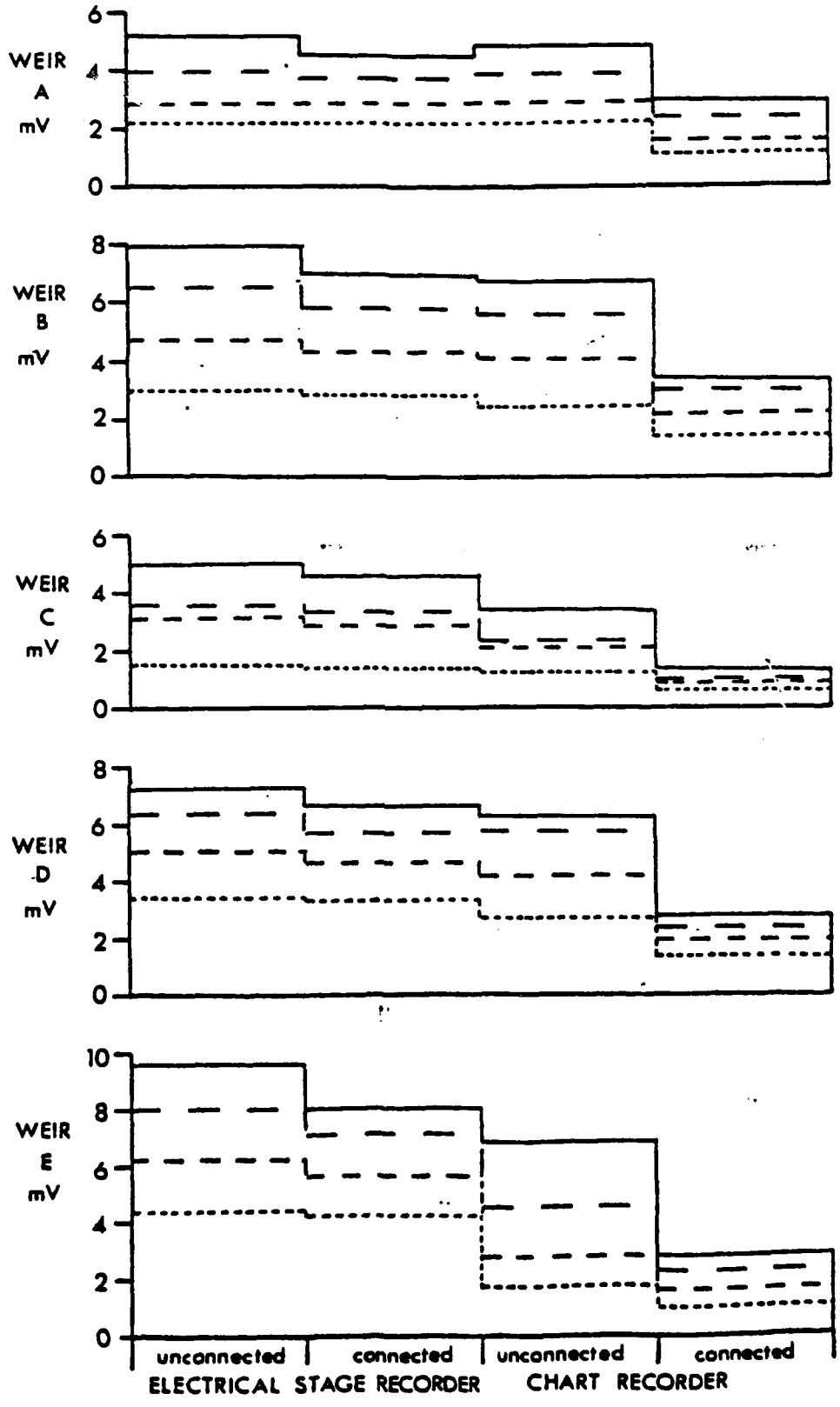

Figure 3.4. mV outputs at the electrical stage recorder and chart recorder for 4 different stages at the 5 weirs. Shown is the change in output caused by effecting different connections.

(ii) A larger voltage drop over the cable length to the chart recorder occurs which is greatest when the stage recorder is connected to the chart recorder. The reasons for these losses are

(i) That the dry battery powering the electrical stage recorder circuit is on continuous load through the circuit. Although the drain on the battery is minimal, when the chart recorder is connected this load is increased and a reduced output is recorded. This loss becomes greater with increasing voltages; that is, higher stage values. The electrical stage recorder therefore under-reads a given rise in stage.

(ii) The cable length induces a certain amount of impedence in the system because the voltages that we were concerned with were very low; in the range 0 to 6 mV. This caused the reduction in the mV output values at the chart recorder, which were very carefully calibrated and accounted for.

Figure 3.5 shows the calibration curves established for each of the five weirs. These were checked at regular intervals and the actual stage at each weir was measured during each visit so that the record was constantly checked and re-calibrated when necessary.

3-4. Monitoring soil water potentials

For monitoring soil water potentials 800 cm, the tensiometer is relatively widely used. Table 3.1 details those principal investigators using standard tensiometric methods. Accordingly it is only necessary here to highlight one or two specific points for the purpose of this investigation. It was desirable that soil water potentials should be continuously and automatically recorded, thereby facilitating maximum resolution of the zones of soil water convergence and divergence. The development of differential pressure transducers (facilitating the registering of both positive and negative pressures) has eliminated the earlier problems of slow response times and the requirement of bourdon gauge tensiometers (negative pressures) and piezometers (positive pressures). In addition, the transducer output is readily monitored and recorded on a range of data logging devices. Transducer-tensiometer systems have been used in a wide variety of laboratory studies of soil water movement. Further studies have coupled the ceramic cups to hydraulic lines which are then themselves coupled to a Scanivalve fluid switch. The Scanivalve has one outlet port with a read line to the transducer. Each inlet port (coupled to a ceramic

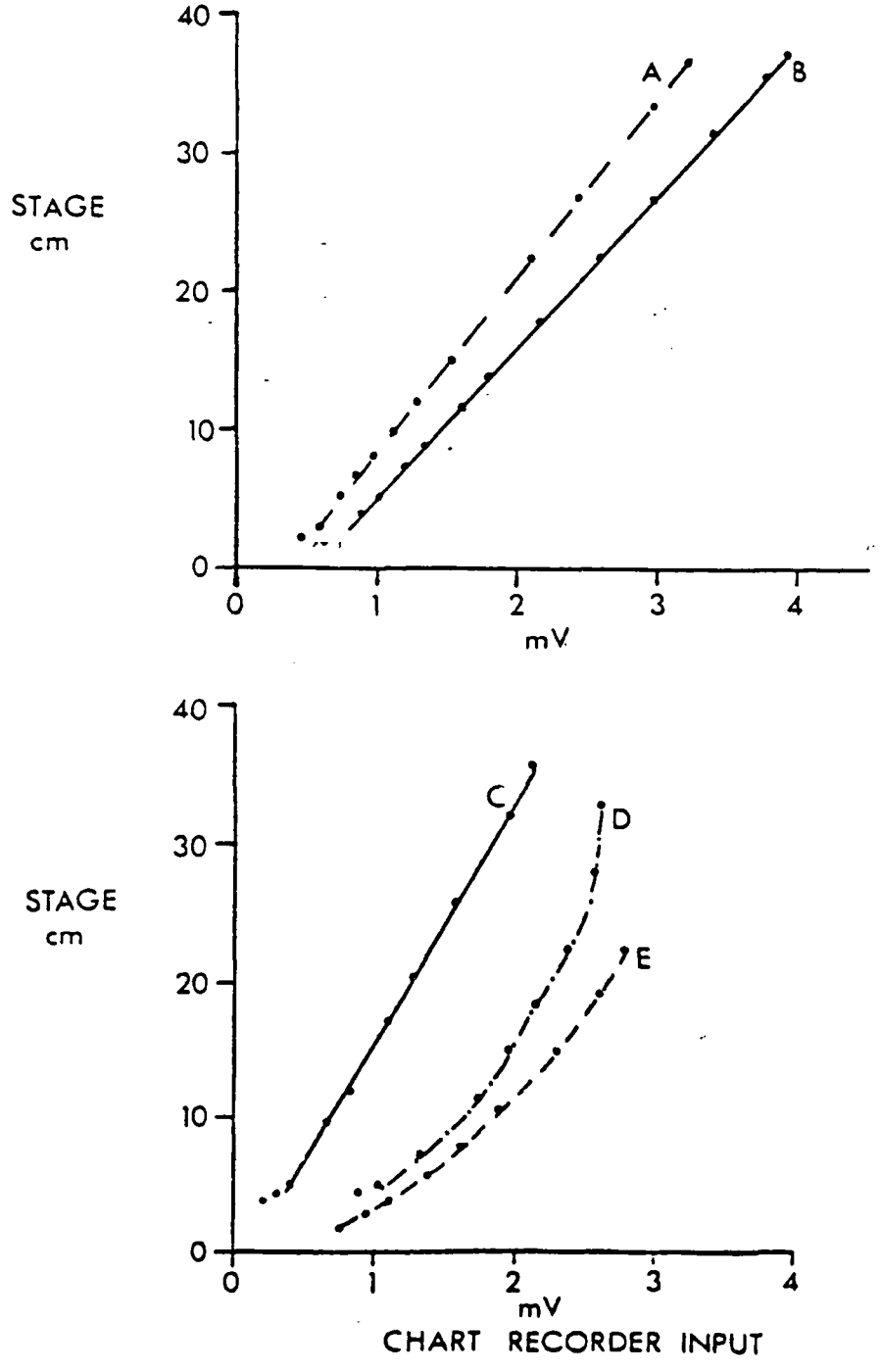

Figure 3.5. Calibration curves for the electrical stage recorders (Figure 3.3) at the 5 weirs.

pot via a hydraulic line) is then connected in turn to the outlet port by the rotation of the switch. Employing a Scanivalve thus reduces the number of transducers and simultaneous data channels needed for output. Several studies have been reported in which such a system has been used. However there has been very limited application of such methods to field soil water potencial monitoring despite the excellent response times reported by studies examining both practical applications and reporting theoretical response functions. The diagramatic layout of the Scanivalve tensiometer system used for this study is shown

Table 3.1

Selected Tensiometer Installations

Field installations (>0°C)
Anderson and Burt (1977)(2)
Anderson and Kneale (1980)(24)
Rice (1969)(25)
Williams (1978)(26)
Watson (1967)(27)
Harr (1977)(17)
Field installation (<0°C)
Colbeck (1976)(28)
Ingersoll (1980)(29), (1981)(30)
McKim et al. (1976)(31)
Reviews of tensiometric techniques
Ingersoll (1981)(30)
McKim et al. (1980)(32)
Schmugge et al. (1980)(33)
Response times (empirical and theoretical)
See table

in Figure 3.6. The tensiometers were constructed from 1 bar ceramic porous cups glued to a 5 cm long perspex cylinder. The uppermost end of the cylinder housed a rubber bung with twin holes to allow entry to the 'de-airing' and 'reading' lines. This arrangement facilitated the direct entry of the hydraulic lines into the water reservoir above the ceramic pot, and this minimized the number of inline couplings. Whilst such ceramic pots should theoretically withstand suctions of up to 1 atmosphere, in practice air entry occurs in the range of suctions of 700-800 cm of water. The hydraulic lines are standard piezometer tubing, being impervious to air and water. The system as designed for field installation (Figure 3.6), allowed de-airing to be accomplished readily by the unclamping of the de-airing line at the surface, and the application of a de-aired water supply to the transducer outlet of the Scanivalve at a pressure commensurate with the elevation/pressure combination at the pot.

The Scanivalve which was used had 24 ports, of which 2 were taken in establishing pressure/suction references to calibrate each cycle of readings, leaving 22 to be coupled to ceramic pots. This has become a standard field installation for the author's soil water monitoring projects and has been widely reported. The pressure transducers used (type MPT117) were differential with a pressure range of +2 atmosphere to -1 atmosphere corresponding to an output range +200 mV to -100 mV. The excitation voltage of 8VDC was supplied from a 30 amp hour lead acid battery (12VDC) through a voltage regulator unit. In this manner the transducer performance and operation is theoretically unimpaired as the supply voltage drops from an initial 12V to 8.5V. The accuracy of the transducer system is theoretically high, since a very low volumetric displacement is required to register large pressure changes. For the transducers used here, a 0.05 cm^3 volume change accompanied a 1 atmosphere pressure change. Thus tensiometric systems are the obvious choice for such a study having the following advantages and disadvantages as reviewed by Schmugge et al.(33):

Advantages:

1. low cost
2. ease of design and construction
3. ease of tensiometer emplacement
4. information can be obtained on moisture distributions under saturated and unsaturated conditions in near real time

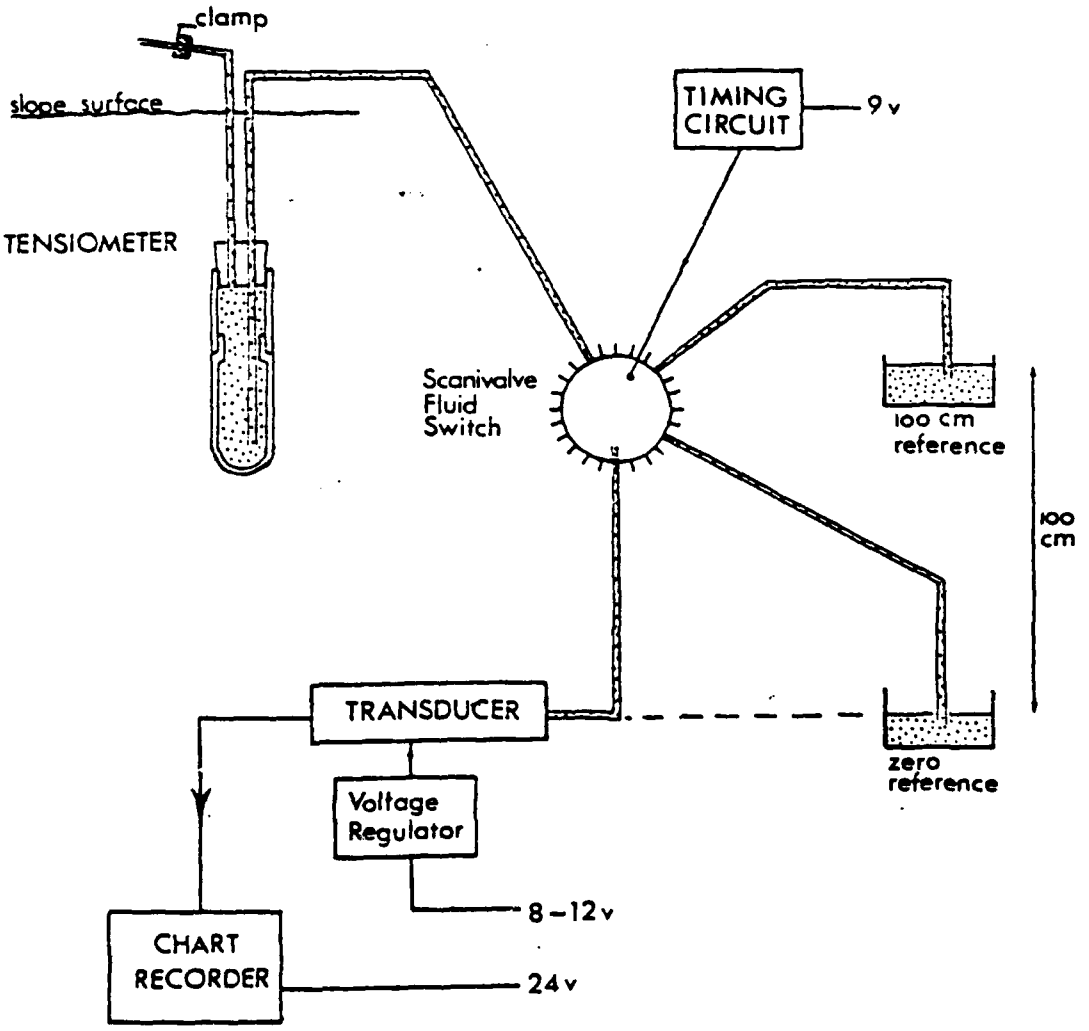

Figure 3.6. Diagrammatic illustration of the Scanivalve-tensiometer system.

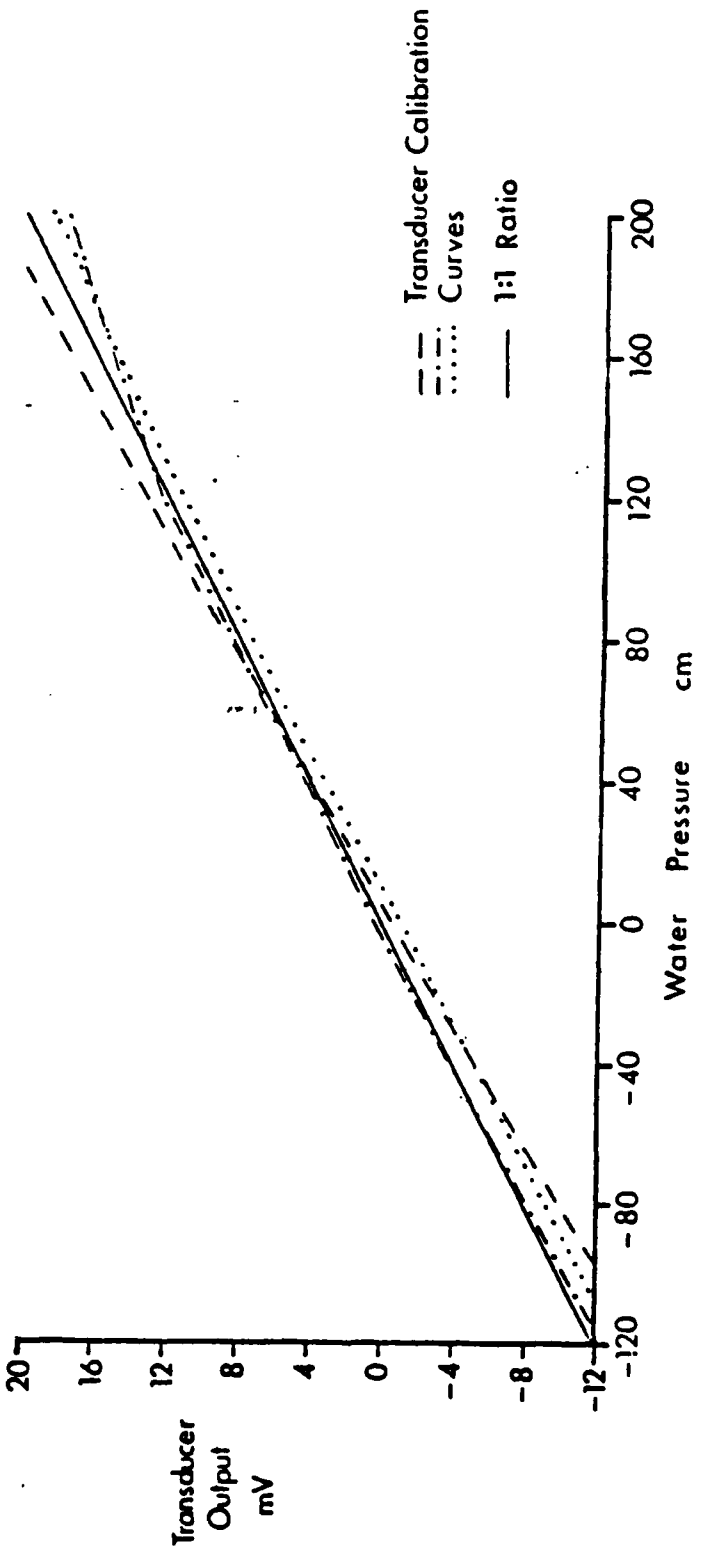

Figure 3.7. Calibration curves for 3 tranducers in the range of greatest non-linearity

5. systems can operate over large periods with proper maintenance

6. with transducer-tensiometer system response is very rapid

7. ethylene glycol solution can be used for freezing conditions

8. differential pressure transducers allow for positive and negative soil water potential readings.

Disadvantages:

1. only indirect measurement of soil moisture content is provided.

2. tensiometers can be easily damaged during installation

3. tensions only as low as - 850 cm can be recorded

4. output from pressure transducer systems can drift electronically in the field.

Regarding the disadvantages, the one salient to the discussion of equipment specification is (4): namely that of drift and transducer calibration problems. It is of course essential that accurate calibration curves be obtained for each unit. Calibration curves (those suctions between - 120 cm and +200 cm water shown here) for 3 units used in this study are shown in Figure 3.7. It is evident that none of the 3 units exhibited a true linear calibration and it was found necessary to undertake laboratory tests for calibration, since the manufacturers stated curves were not always of sufficient precision. Incorporation of the references in the cycle of readings combated the drift problem in transducer output, which in any case was found to be a very small and acceptable amount (0.1%).

The transducer output was recorded on a JJ CR552B chart recorder. Although the above system had been employed successfully at a number of locations by the author, the current consumption of the system was high (0.3 amp hours). This was a restrictive element in remote site operation. Accordingly, a microprocessor based system was designed to overcome this problem (Figure 3.8). The transducer and Scanivalve are shown mounted in the Scanivalve enclosure. The microprocessor unit shown here has a thermal printer (cassette output as a recording mode, although available, was not used here for ease of field reading). The unit is fully programmable allowing the number of tensiometer to be read to be pre-set, together with the dwell time, and an interval time between each cycle of readings. The transducer calibration curve (Figure 3.7) is programmed into the unit and with the references incorporated, is self compensating for electronic drift. For each tensiometer, 3 readings are made at equally spaced

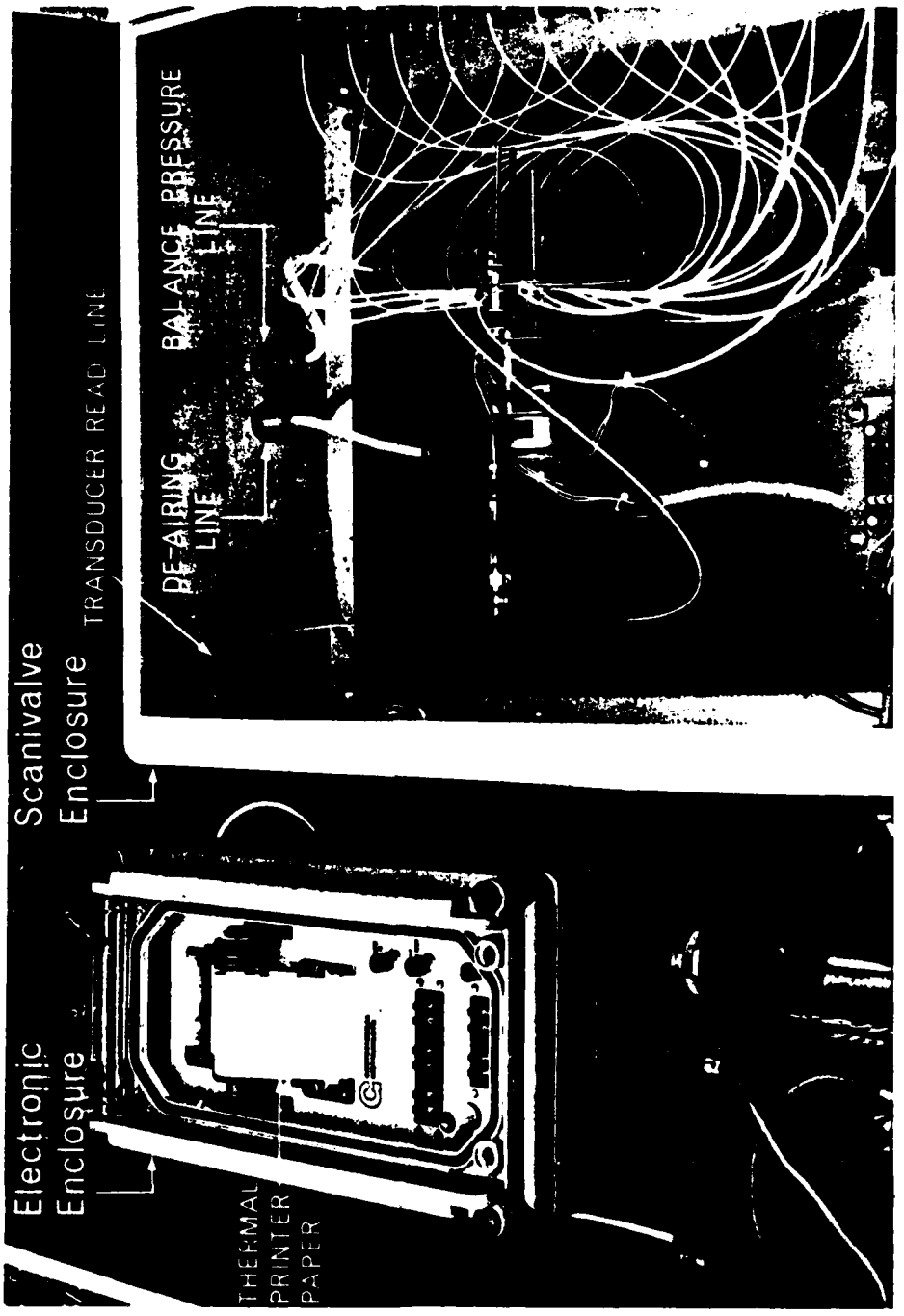

Figure 3.8. Scanivalve system and programmable data logger.

intervals during the dwell time. This facility allows drift in the reading (due, in most cases where it occurs, to air entry in the hydraulic lines) to be identified and the line de-aired as necessary. The power supply required is a 12VDC rechargeable maintenance free battery, allowing up to 4 weeks continuous operation. The microprocessor unit has in addition an automatic shut down facility, turning the system off when the battery has drained to 11V thereby preventing undue (and damaging) discharge to the battery.

Transducer - Tensiometer Response Times

There have been a number of empirical and theoretical investigations of the response times of tensiometers monitored by transducers to changing pressures. The results of eight investigations are summarized in Table 3.2. Although these tests are not directly comparable, they show response times of the order of one to ten minutes but these are dependant on the properties of the tensiometer tip, the soil and the degree of soil saturation.

In theory, the response time of a tensiometer to an instantaneous change in pressure is limited by the conductivity of the material of the cup alone. This can be measured by changing the pressure when the tensiometers is placed in water so that there is a perfect hydraulic contact between the fluid inside and outside the cup. Tests of this type by Klute and Peters (1962)(34) showed a response time of 20-30 seconds. Watson (1965)(27) performing a similar test in laboratory conditions demonstrated that the delay caused by the porous cup was 0.02 seconds but that the whole system took 1 second to respond because of the time the chart recorder took to register the changed input. Williams (1978)(26) calculated the theoretical response time of his transducer-tensiometer system to a changing water pressure as 0-2 second. He also showed that the presence of soil around the tensiometer pot can reduce the response time of the system by a factor of five as compared with the response time in water. This is because the hydraulic contact between the fluid filled tensiometers and the water in the soil matrix is not perfectly continuous and this contact is reduced as the soil drains. At very high tensions where the soil is unsaturated, the water contact may be broken and air entry into the pot occurs. To ensure the best possible seal between the pot and the soil, very careful installation is required. At the sites instrumented in this study, hand augering of a hole the same dimensions as the tip was used and the tensiometer pushed firmly into place.

Table 3.2.

Response Time of Transducer-Tensiometer Systems

Authors	Date	Cup Material	Cup Air Entry Value	Transducer Sensitivity	Empirical	Theoretical	Soil Material	Response Time	Level of Accuracy
Klute, A. and Peters, D. B.(34)	1962	fritted glass	---	$3x10^{3}$ mb.cm^{-3}	E		---	1 sec	---
Watson, K. K.(27)	1965	ceramic	86cm water	$1x10^{2}$ psi.cm^{-3}	E		sand	0.1 sec	---
			1300cm water	$1x10^{2}$ psi.cm^{-3}	E		sand	29.6 sec	
Watson, K. K. & Jackson, R. J.(35)	1967	ceramic	1300cm water	$5x10^{-5}$ cm^{3} $mbar^{-1}$		T	---	9.1 sec	---
Young, N. C.(36)	1968								
Fitzsimmons,D. W. & Young, N. C.(37)	1972	porvic (polyvianl chloride)	---	$3x10^{4}$ mb.cm^{-3}	E		depending on material & satura-tion	1 sec to 60 sec	---
Williams, T.H.L. (26)	1978	ceramic	1000cm water	$1x10^{-4}$ $cm^{3}mbar^{-1}$		T	---	1 sec	---
Boels, D. et al (38)	1978	ceramic	---			T	heavy clay-wet	60 sec	1%
							-medium	98 sec	1%
							-dry	154 sec	1%
							sandy clay-wet	60 sec	1%
							loam-medium	125 sec	1%
							-dry	450 sec	1%

To determine the actual response times of the instrumentation used in this study to changes in soil water pressures, a laboratory experiment was undertaken. This employed exactly the same soil water monitoring instrumentation as that used at the field sites and identical installation procedures were used for the tensiometer emplacement.

To allow the pressures to be changed instantaneously a standard 4 in. triaxial cell testing rig was adapted. The equipment used in the tests is shown in Figure 3.9. Extra holes were drilled in the top plate to take the tubing from the tensiometer to the transducer (1). The t-junction used at point C allowed the cell pressure to be regulated and it was monitored continuously by the second pressure transducer. The mercury pots normally used to apply changing pressures in triaxial tests were modified to allow the relatively small changes in pressure experienced in the field to be applied. Pressures used for the tests ranged from 0 to +500 cm water.

The soil material selected for the test was Oxford Clay. This material had an hydraulic conductivity value of 1×10^{-6} cm sec^{-1}. It was some of the least permeable material encountered in the study period and as such can be assumed to show the "worst case" response time to changing pressures.

An undisturbed 4" core sample was extracted from the field and a tensiometer installed in the centre of the clay. The tubing to the tensiometer was filled with distilled, de-aired water in the normal way and then the sample was placed in the triaxial cell. The soil water pressure was thereby monitored by the tensiometer via transducer No. 1, and the cell pressure by transducer No. 2. The output from the two transducers was recorded by digital voltmeters and a two-channel chart recorder.

Prior to the tests, the sample was left to saturate at zero pressure, a process which took a number of weeks because of the very low permeability of the material.

For the tests, the cell pressure was instantaneously raised from zero pressure to for example +100 cm water and the time for equilibration was recorded. The cell pressure was then returned instantaneously to zero and the equilibration time noted. This test was repeated with instantaneous pressure changes of up to +500 cm water. The mean values of the results of a series of replicate tests of this type are shown in Figure 3.10.

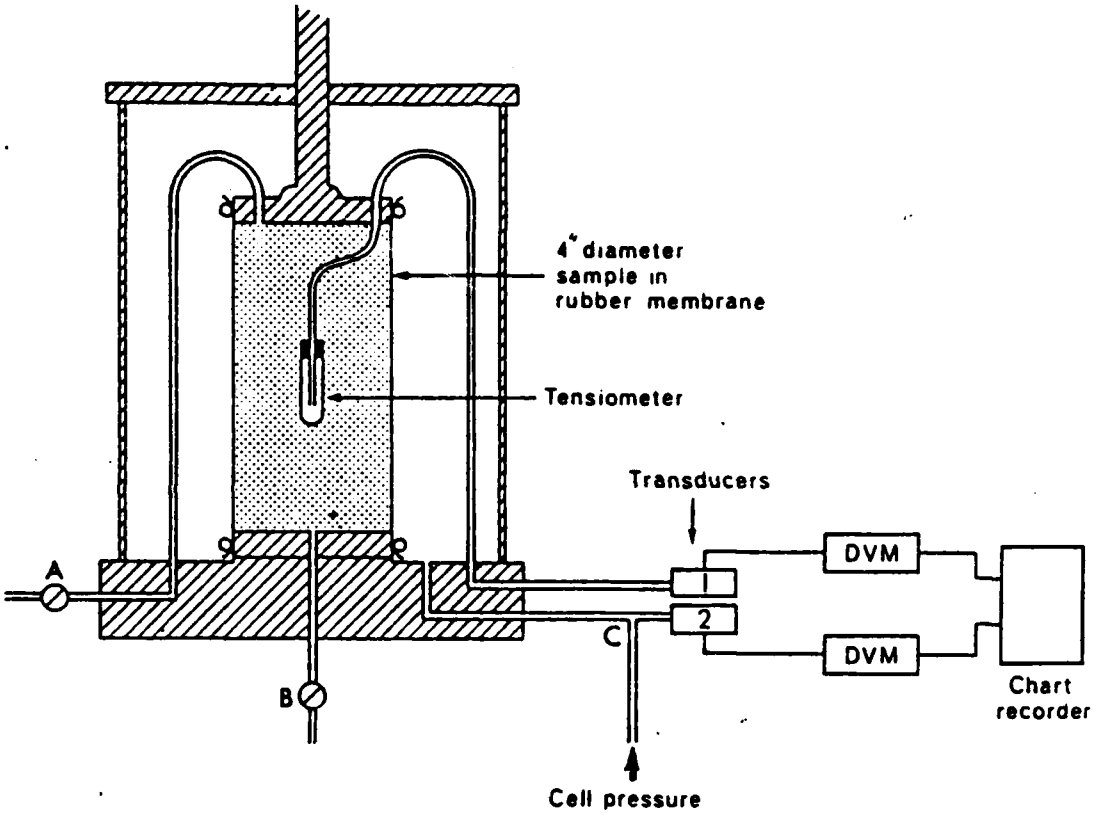

Figure 3.9. Laboratory equipment used to test the response time of the tensiometer-transducer system (Figure 3.6).

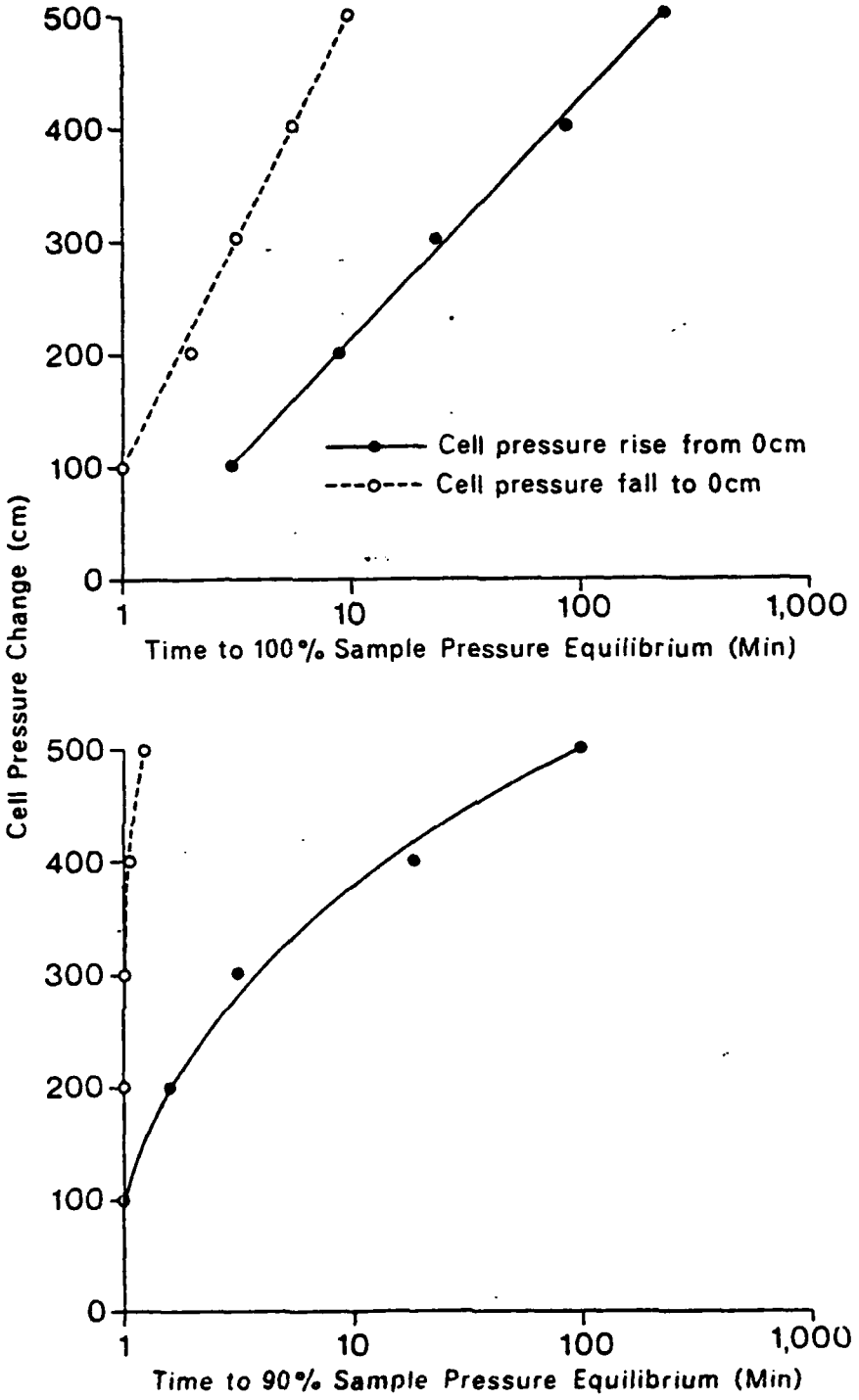

Figure 3.10. Results of the tests measuring the response time of the transducer-tensiometer system to instantaneous changes in pressure, using the equipment shown in Figure 3.9.

Where the changes in cell pressure were small, zero to +50 cm of water, the response of the instrumentation was near instantaneous. Where larger pressure changes were induced a measurable lag time was introduced into the system, which in the case of a $50KNm^2$ pressure change took slightly in excess of two hours. In the field of course, changes in pressure occur very much more slowly so these results with very impermeable clay are satisfactory.

The lag time observed at higher pressure changes suggests that not all the air had been removed from the soil sample and that it was not fully saturated. This is comparable with the field situation, where a measured zero pore water pressure does not imply total material saturation. Isolated pockets of air are to be expected in the zone below the zero pore pressure line.

These results from this very impermeable clay compare well with the theoretical response time calculated by Williams (1978)(26) and furthermore indicate that connection times of two or four minutes for each tensiometer to the transducer are more than adequate enough to allow the correct field pressures and tensions to be recorded.

3.5. Complete instrumentation layout

The equipment layout in the catchment is shown in Figure 3.11. Two Scanivalve tensiometer systems (44 tensiometers) were installed on a hillslope hollow and adjacent spurs - see Section 3.4 and Figure 3.12. This configuration was considered satisfactory from the standpoint of facilitating detailed monitoring of soil water convergence and divergence in shallow topography. Electrical stage recorders (Section 3.3, Figure 3.3) were installed to provide a continuous and time synchronized record of streamflow. Precipitation was recorded by an autographic raingauge (Figure 3.2). The complete system was powered by mains voltage (240VAC) stepped down to the appropriate voltages (24 and 12VDC) to power the recording systems (Figure 3.11).

3.6. Hydraulic conductivity determinations

This section outlines the tests undertaken to determine the hydraulic conductivity characteristics of the slopes, to provide an input therefore to the modelling of soil water potentials (Chapter 6). Field infiltration tests were undertaken using 30 cm double ring infiltrometers. The distribution of values obtained for the instrumented slope area (Figure 3.12) provided a mean value of 1×10^{-4} cm sec^{-1}. It is noteworthy that there is a significant variation however in the infiltration values. Other workers have found similar

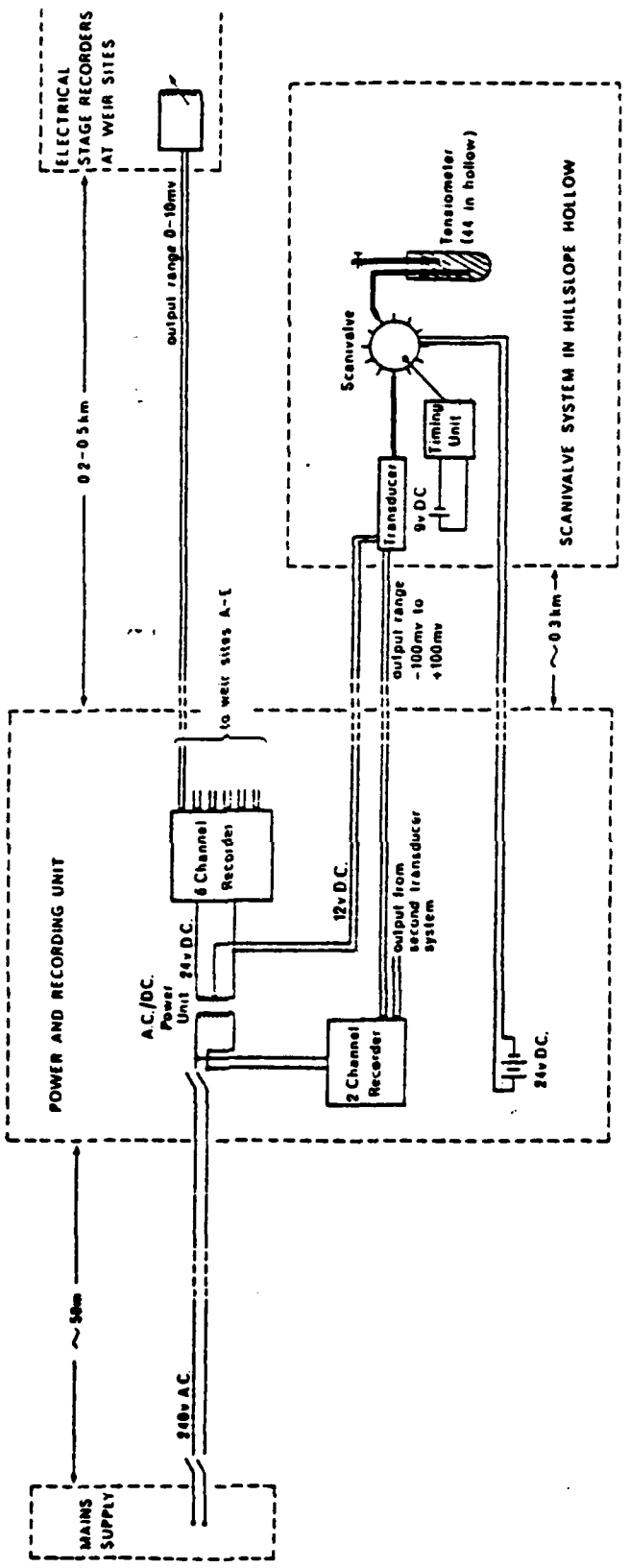

Figure 3.11. Diagrammatic illustration of the field equipment layout.

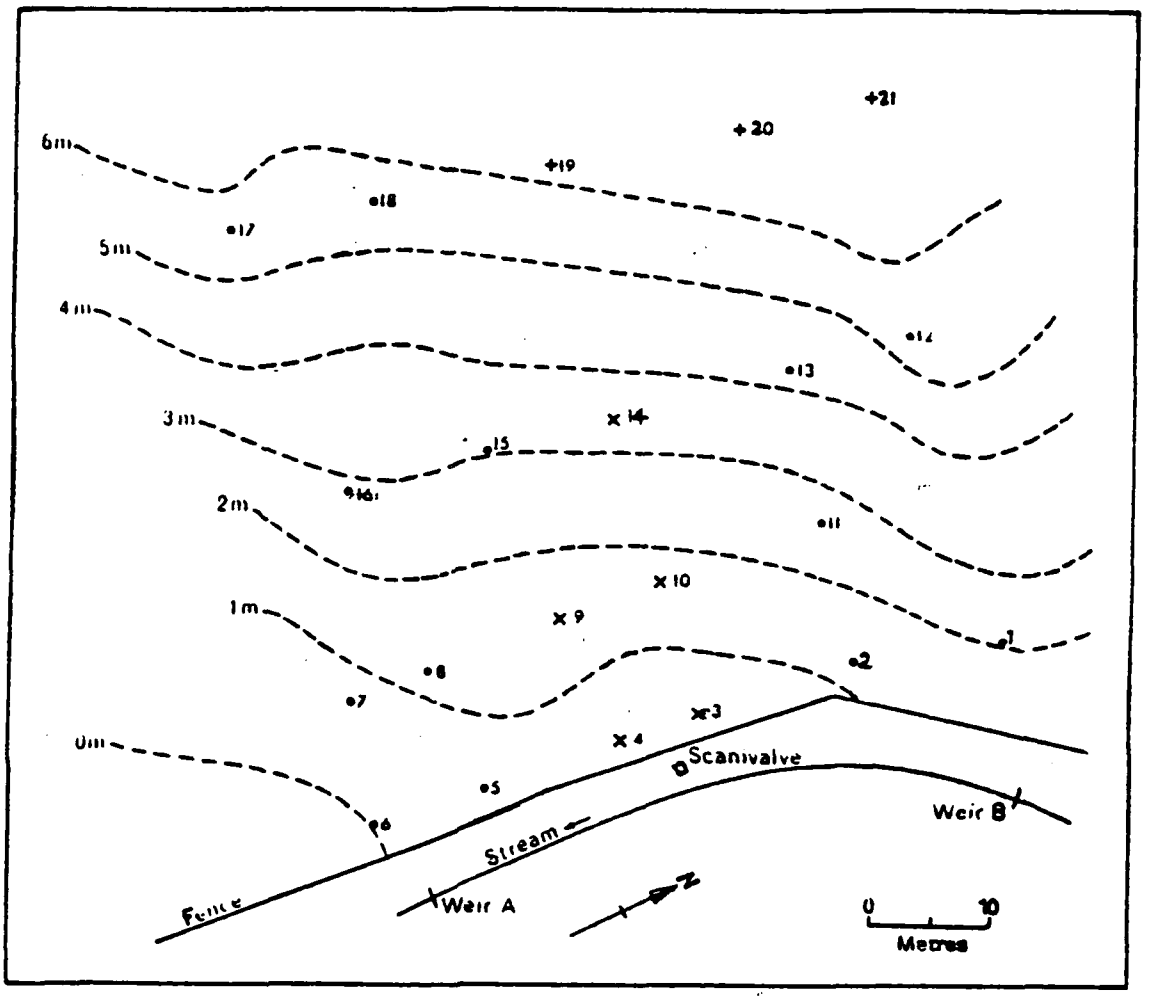

+ **Tensiometers at 40cm depth**

• **Tensiometers at 40cm and 80cm depth**

× **Tensiometers at 40cm, 80cm and 150cm depth**

Figure 3.12. Location and depths of the tensiometer on the study slope (Figure 3.1).

results. Constant head and falling head permeameter tests were also undertaken using undisturbed cores giving results that concurred with these from field tests.

Accepting a saturated hydraulic conductivity (K_s), together with the use of a suction-moisture curve, facilitates the establishment of the K (θ) - θ curve. Several widely used procedures are available for this estimation. These procedures are 'standard' and mostly rely upon the referencing of such a procedure to a measured K_s value.

For this study Campbell's (1974)(39) method was adopted. Suction-moisture curves were established from undisturbed cores. The method assumes that a straight line can be fitted to the log-log plot of the suction - moisture curve (gradient b). Using then the relationship given by Campbell:

$$K = K_s \, (\theta/\theta_s)^{2b+2}$$

where K = hydraulic conductivity cm sec^{-1}

K_s = saturated hydraulic conductivity cm sec-1

θ = volumetric water content

θ_s = volumetric water content at saturation

b = slope of regression line fitted to the logged data of the suction moisture curve.

Figures 3.13 and 3.14 show the suction moisture curve and derived hydraulic conductivity curve using Campbell's method. Of course, because of the keyed relationship to K_s, then any variation in K_s produces a corresponding change in the K(θ)-θ curve. We have already noted the variation in K_s found to exist and the examination by several workers of the static spatial heterogeneity in this variable. (For ease of referencing in this report, the terms 'saturated wedge' and 'zones of saturation' refer to those sectors of the hillslope where the soil water potentials exceed 0 cm. It is to be noted that on the replicate suction-moisture curves run on the field cores, the air entry values were approximately 105 cm).

Techniques are available for an examination of the detailed 3 dimensional soil structure. X-radiography has been demonstrated to be able to identify zones of compaction, discontinuities and root zone depths in undisturbed core samples. In this study, an attempt was made to quantify the radiograph image for making a comparison before and after rolling of a section of the catchment was undertaken. Figure 3.15 shows a photograph of a typical soil sample together

with its radiograph. Figures 3.16-3.19 show microdensitometer scans down the radiographs for two time periods. Optical density decreases with increasing soil density. The evident trend from these plots is for the upper 10-15 cm of the profile to be more compacted on the second sampling period after rolling. The profile below this depth however remains comparatively unaffected. It was hoped that such quantification of x-radiography results would have provided a relatively quick, reliable, depth integrated picture of variations in structure which could be calibrated by field hydraulic conductivity determinations. However, the types of structural changes implied by Figures 3.16-3.19 were insufficient to be recorded in any statistically significant manner as corresponding to changes in hydraulic conductivity. The mean field K_s remained at 1×10^{-4} cm sec^{-1} throughout the period. Kneale (1980)(40) has a discussion of the associations attempted between radiography, structure, and K_s.

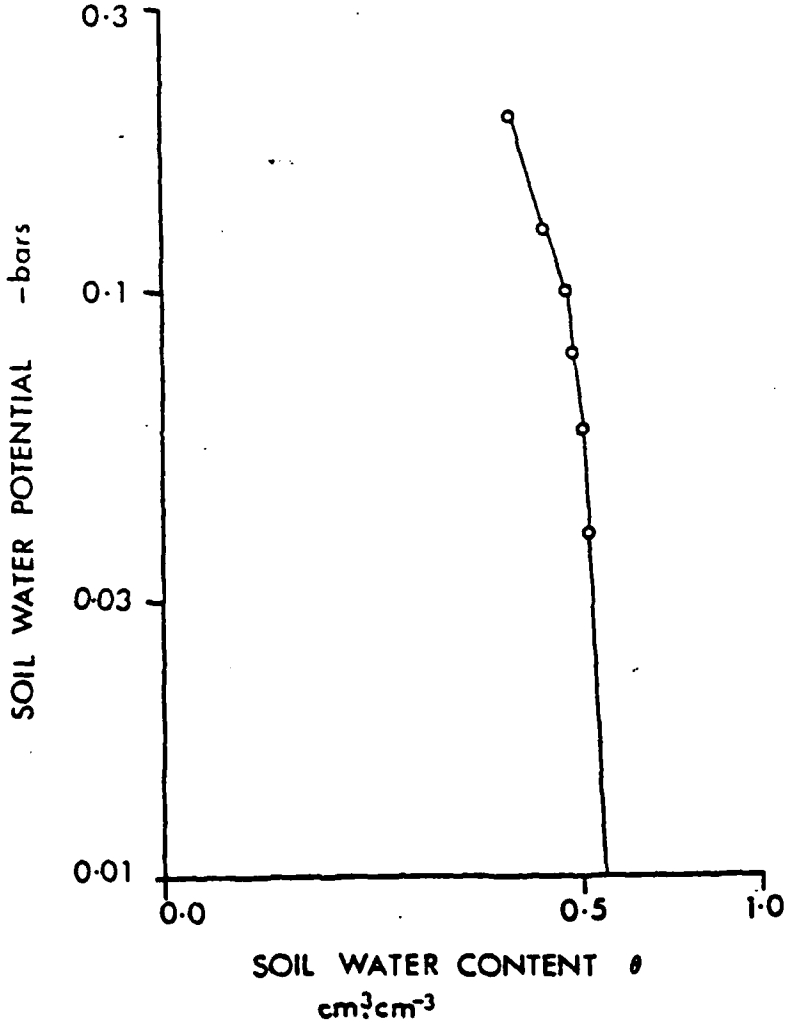

Figure 3.13. Laboratory determined suction-moisture drying curve.

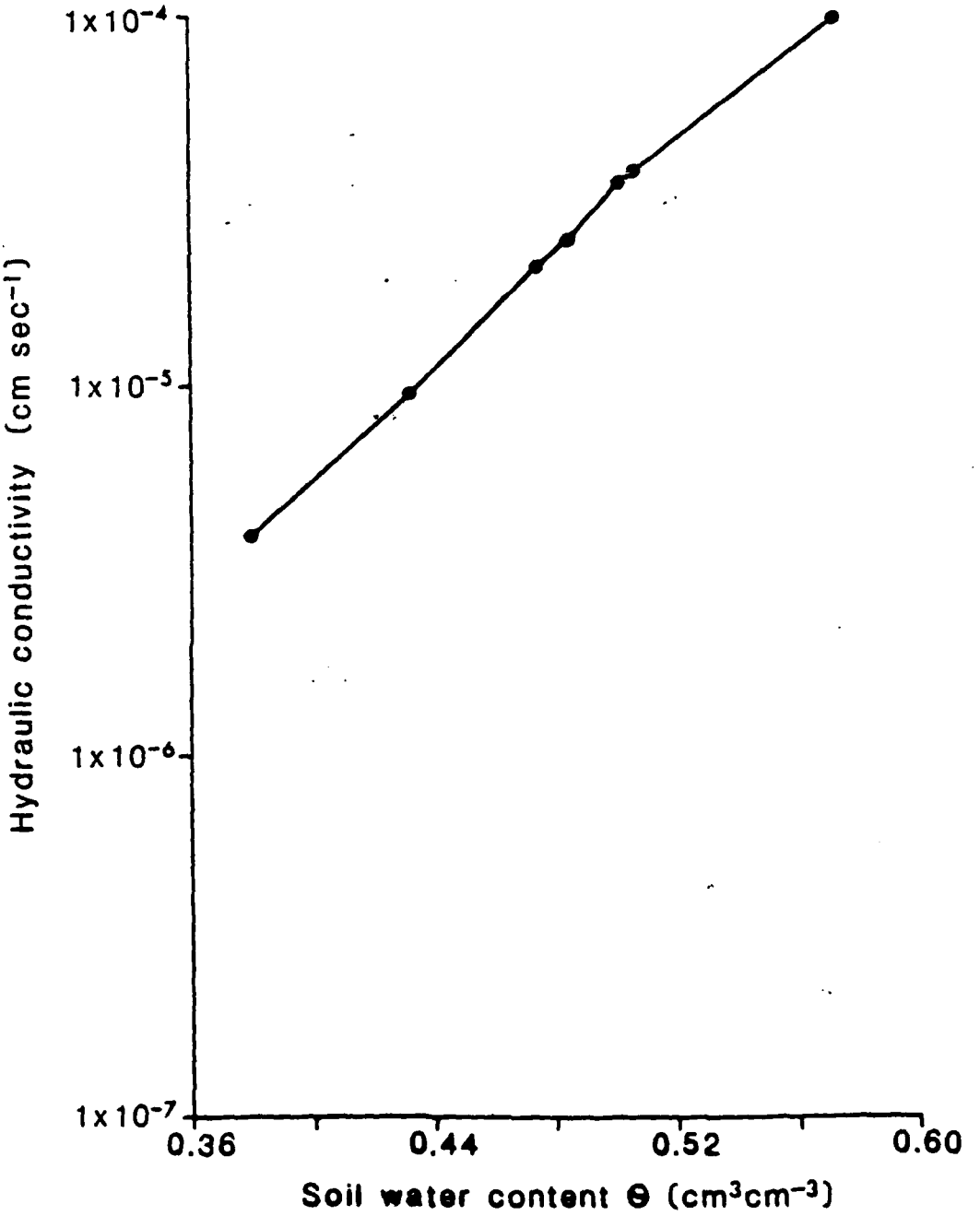

Figure 3.14. K-θ relationship calculated using Campbell's (1974)(39) method.

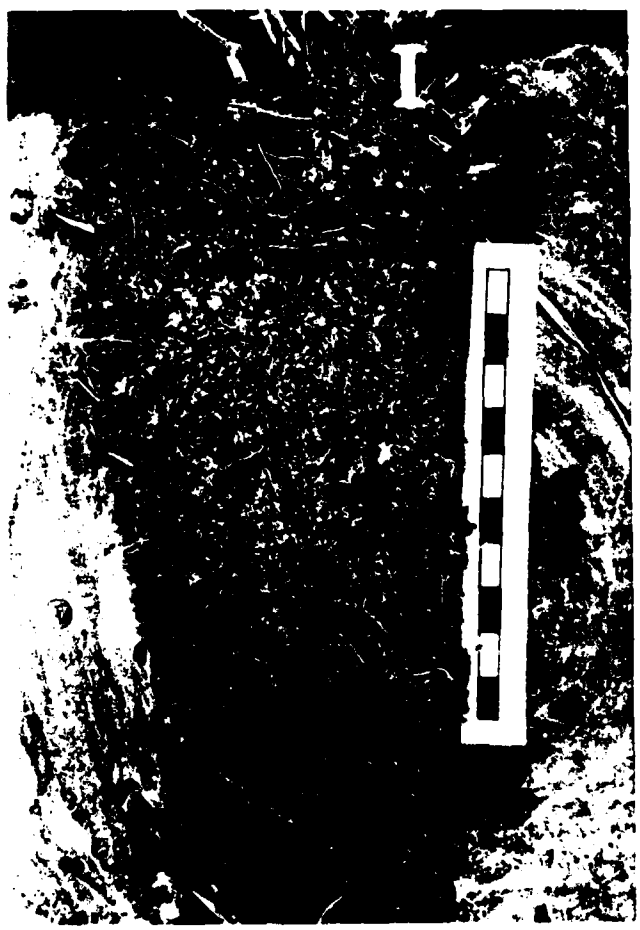

Figure 3.15A. Soil sample used to illustrate X-ray method - See Figure 3.15B.

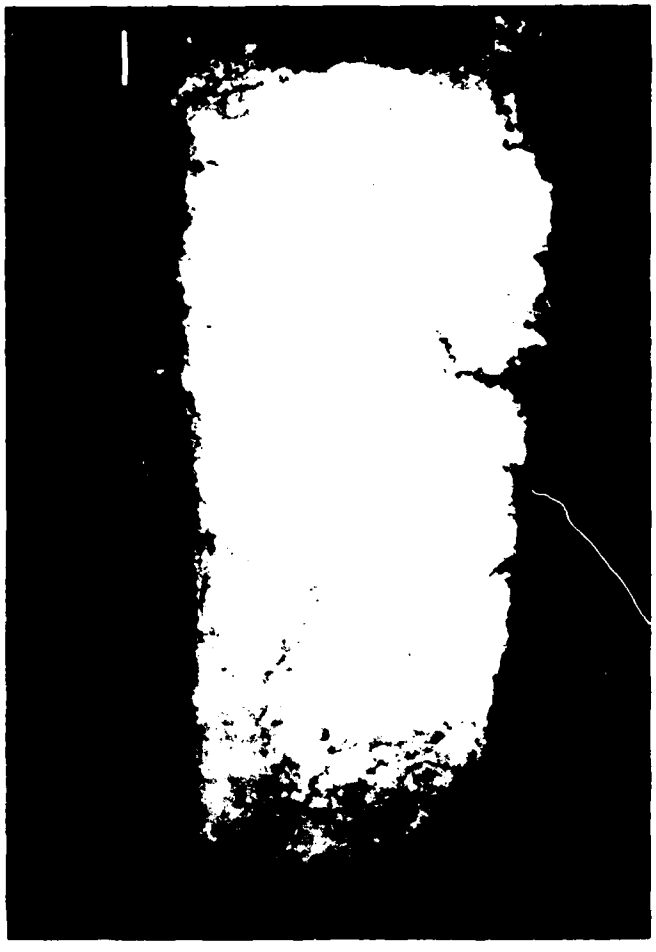

Figure 3.15B. Radiograph of soil sample shown in Figure 3.15A.

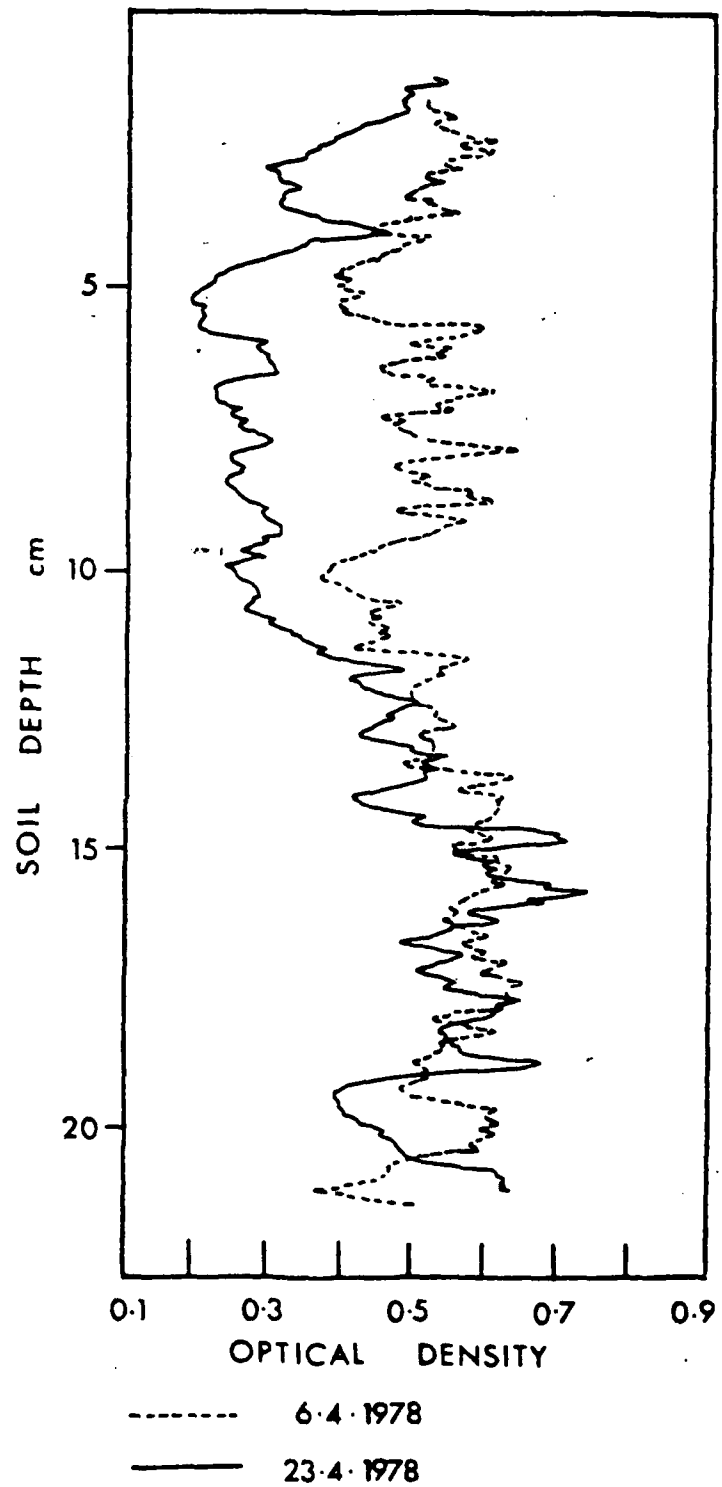

Figure 3.16. Microdensitometer scans of the radiograph at site 1 for 2 different times.

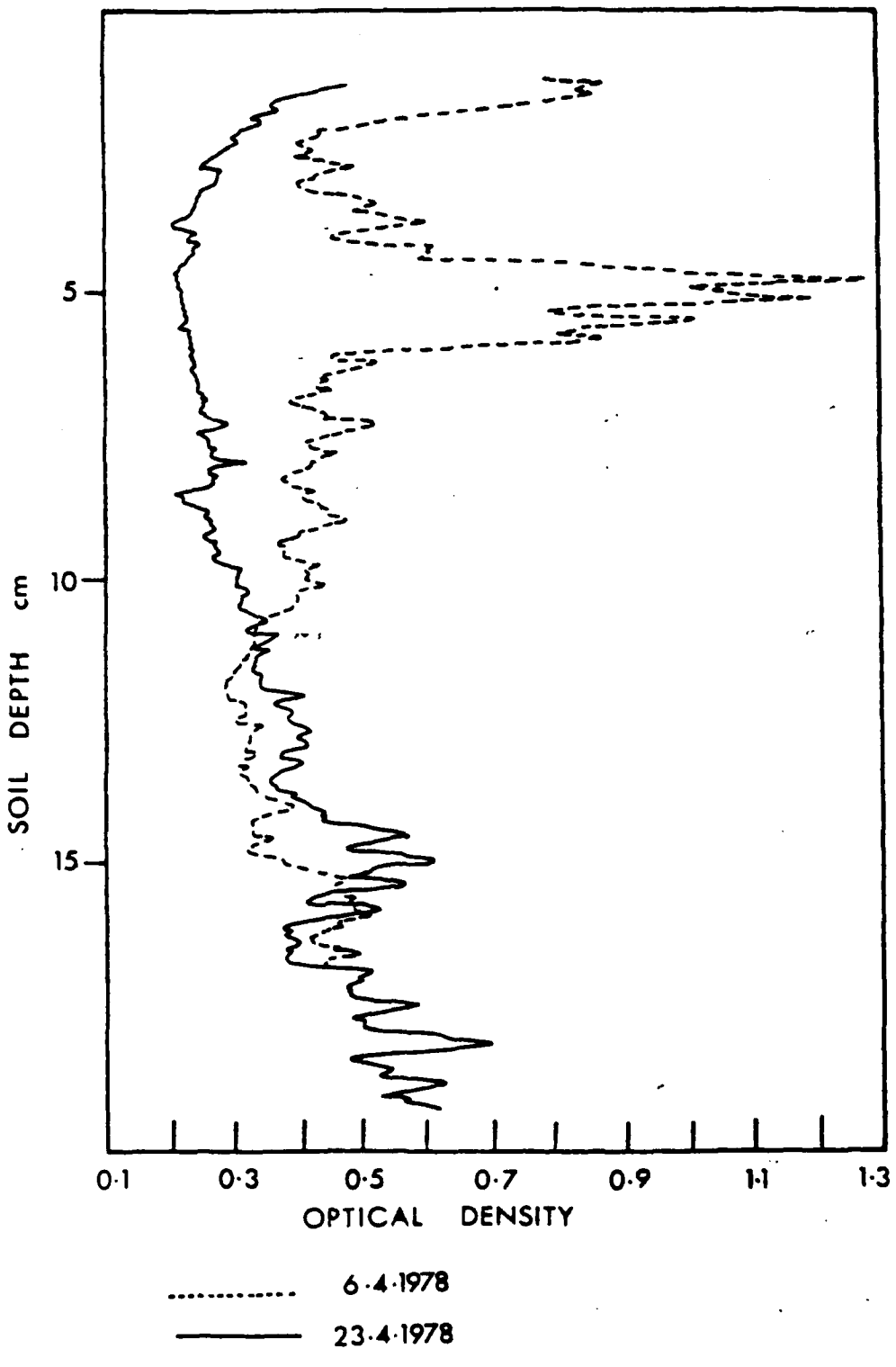

Figure 3.17. Microdensitometer scans of the radiograph for site 2 at two different times.

SITE 3

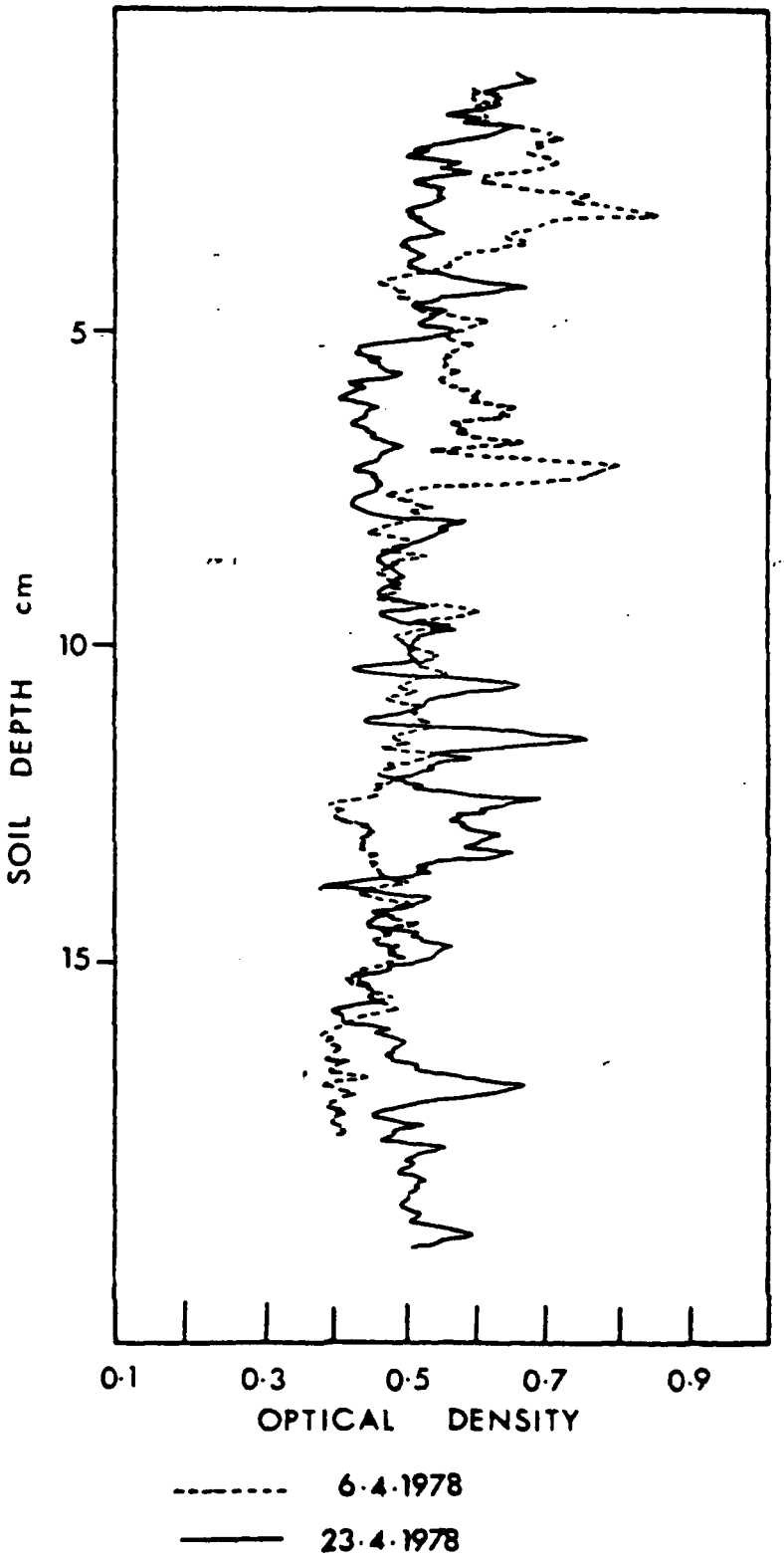

Figure 3.18. Microdensitometer scans of the radiograph at site 3 for two different times.

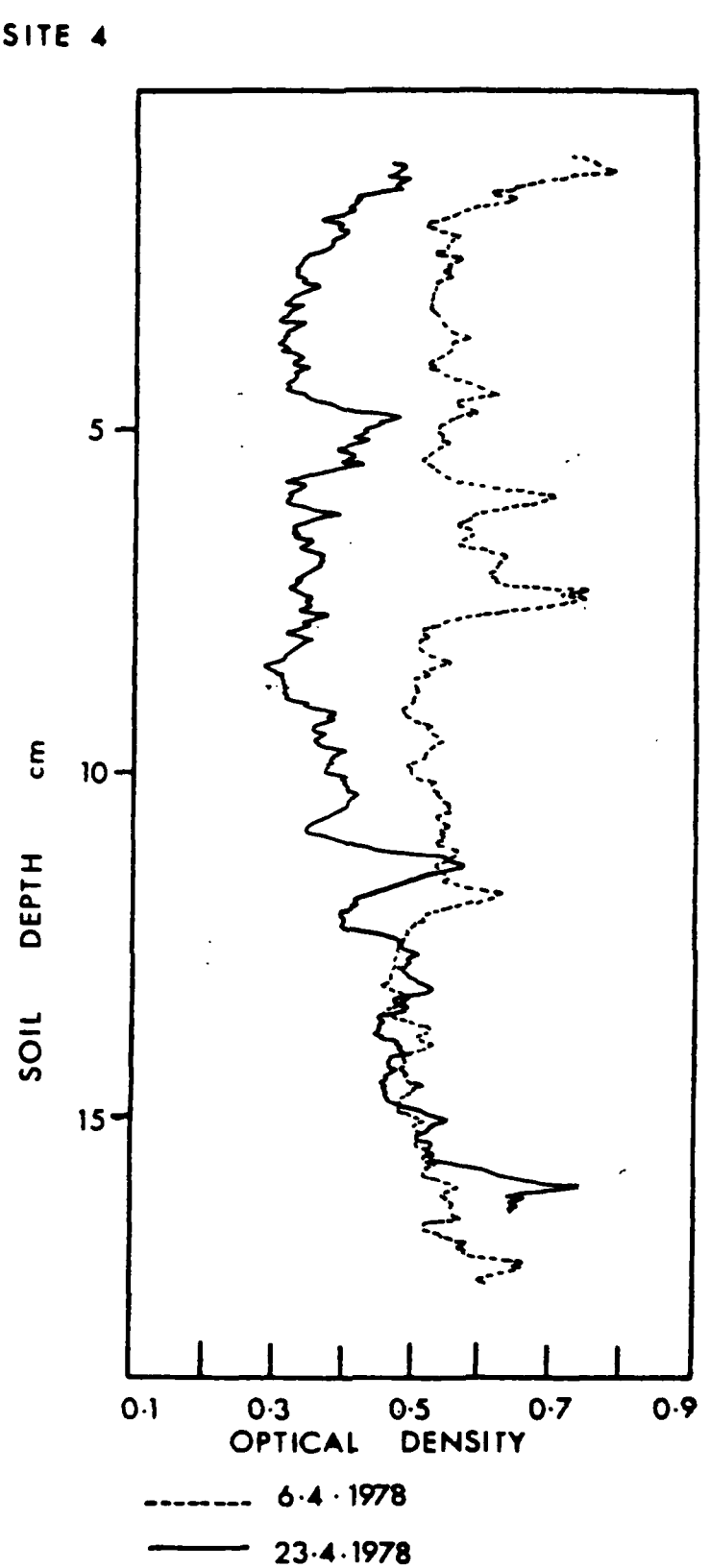

Figure 3.19. Microdensitometer scans of the radiograph for site 4 at two different times.

Chapter 4

Soil Water Convergence on Shallow Topography - Empirical Results

4.1. Introduction

The size and position of the saturated wedge at the foot of a slope is a function of the local hydraulic conductivity, hydraulic gradient and topographic features. The position of the saturated wedge is important in that it is the process control on the volume of the throughflow discharge from the slope.

Earlier studies by Hewlett and Hibbert (1963)(41), Weyman (1973)(14), and Knapp (1974)(16) assumed the saturated wedge to be a short lived phenomenon. Weyman 1973 states that 'baseflow is likely to be dominated by unsaturated lateral flow on the slope since the saturated zone can be expected to contract rapidly once rainfall has ceased.' The inference that unsaturated flow is the key process in hillslope discharge was based on the results of Hewlett and Hibbet's (1963) draining plot studies where initial rapid discharge was thought to be from saturated soil followed by which slower unsaturated drainage. The recent experiments and theoretical calculations by Anderson and Burt (1977)(42) have shown this idea to be incorrect. We showed in that study that a small saturated wedge of soil was maintained at the foot of the slope while drainage is occuring. Hewlett and Hibbert failed to detect the presence of the wedge because their tensiometers were not close enough to the outflow point. Similarly Weyman's manually read tensiometers failed to identify the saturated wedge at the foot of the natural slope as the controlling factor in hillslope discharge.

Detailed instrumentaiton of a 26° slope by Anderson and Burt (1978)(3) showed the presence of the saturated wedge to be a long lasting, stable feature in the slope hydrology. The wedge was observed throughout the period of the summer 1976 when there was no significant precipitation input in a period of 3 months.

The saturated wedge was observed to expand and contract dynamically in response to precipitation inputs. The maximum expansion of the saturated wedge was co-incident with the occurrence of the secondary throughflow peak in the channel discharge and back calculations confirmed this pulse to be produced by the hillslope throughflow discharge. However the slope sites examined in the papers referred to so far have in common the fact that the slopes are very steep

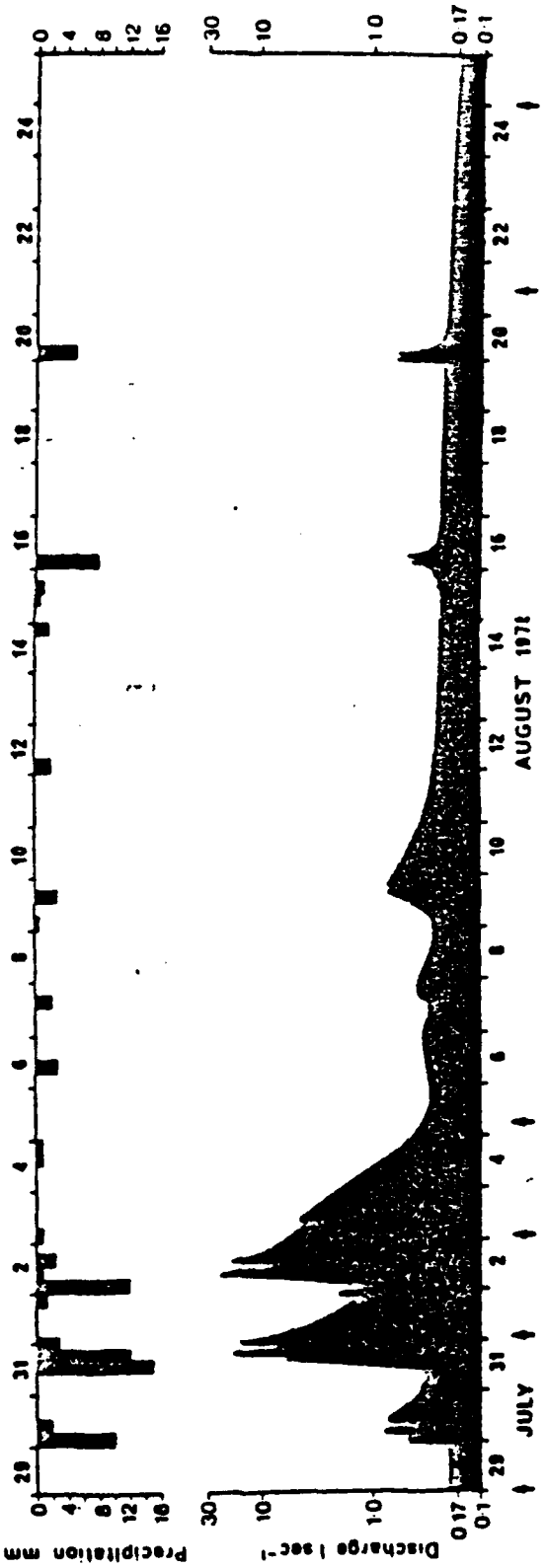

Figure 4.1. Precipitation and discharge at weir A, 29 July to 25 August 1978.

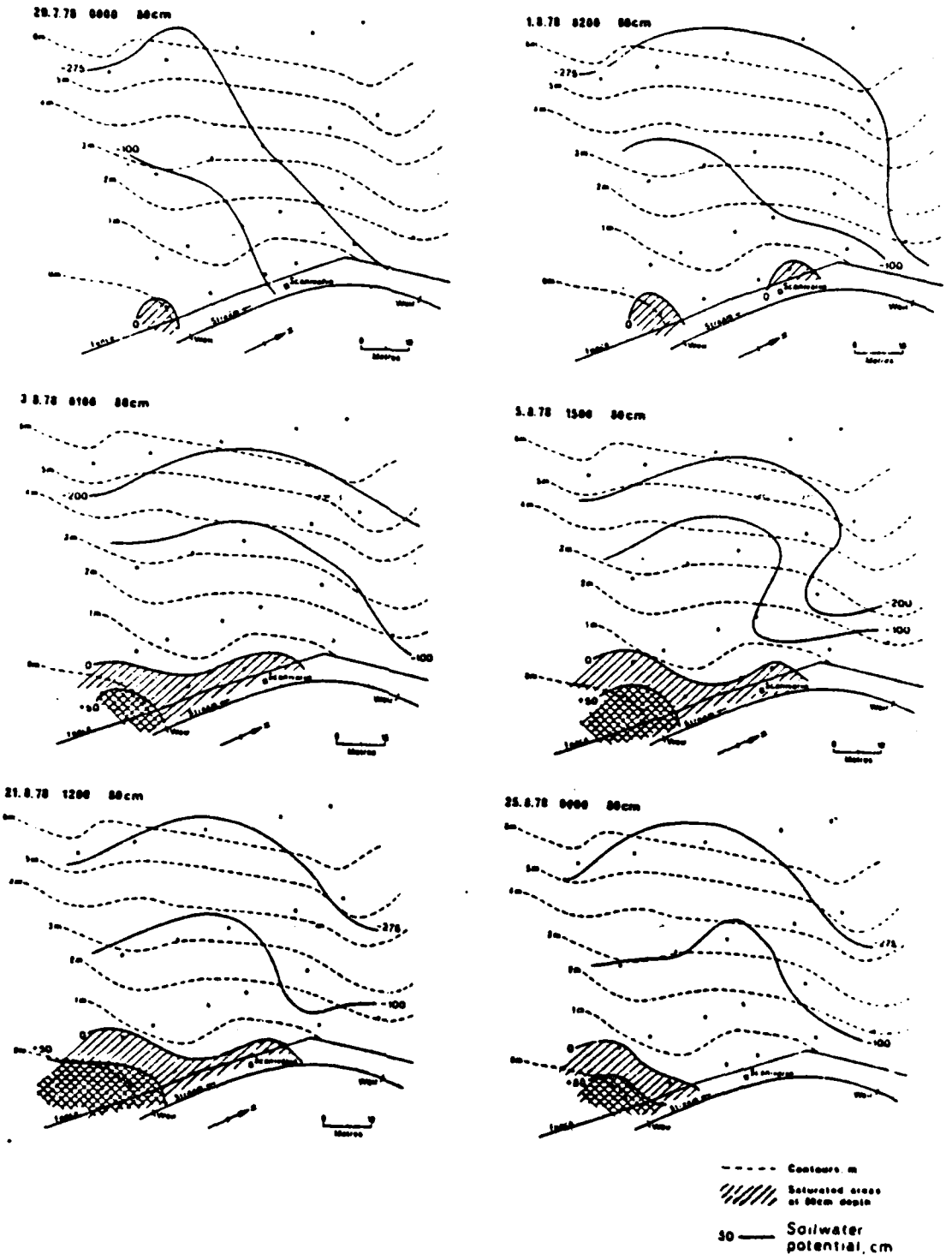

Figure 4.2. Soil Water potential maps, 29 July to 25 August 1978.

and the soils relatively permeable. In this chapter, the development of the saturated wedge at the foot of a relatively shallow channel sideslope is described and then compared with the results of previous observations from more steeply sloped sites.

The development of the saturated wedge is described for storms of both winter and summer types.

4.2. Summer storms and hillslope soil water potentials

The first example is taken from the precipitation events in July and August 1978. The hydrograph for weir A and six hourly precipitation are shown in Figure 4.1, together with arrows to indicate the times for which soil water potential maps have been drawn (Figure 4.2).

All the soil water potential maps presented here are drawn for the tensiometers at 80 cm depth. Lines of equal potential have been interpolated, and the areas which show positive pore water pressures shaded.

From the data in Figures 4.1 and 4.2 it can be seen that prior to precipitation on the 30.7.1978, streamflow is very low ($0.19\ \ell.sec^{-1}$) following dry weather in the previous two months and the slope shows only a very restricted area of positive soil water potentials occurring at 80 cm depth on the downstream spur. On 1.8.78 (02.00), the end of the first precipitation event, the potentials in the centre of the hollow responded first. The area around tensiometer number 3 (t3) showed positive pore water pressures. The general wetting of the slope, by unsaturated throughflow was seen in the retreat of the -100 cm and -275 cm lines of soil water potential across the slope. Forty-eight hours later, 3.8.1978 (01.00), after the second rainfall event, the two areas of saturation amalgamated and t6 registered pressures greater than 50 cm. On 5.8.1978 (15.00) the area of positive potentials reached its maximum extent, t7 recorded positive pore pressures, and although the upstream spur did not record positive potentials at 80 cm depth, the pattern of the potentials indicates that the spur was wetter when compared with the earlier time periods.

The pattern of soil water potentials remainded farily stable from 5.8.1978 until 21.8.1978. The rainfall events on the 9th, 16th and 20th had minor effects on the soil water status. By 21.8.1978 (12.00) the saturated wedge had started to drain, t4 registered 0 cm pressure, so that with drainage the centre of the hollow (around t3) retained positive potentials and for a few hours the pattern was similar to that on 1.8.1978 (02.00). The hollow centre at 80 cm depth

then drained, with the area of positive potentials retained around t5, 6 and 7 on the downstream spur. A month after rainfall, these positive potentials were still observed on the downstream spur with t6 still showing pressures in excess of 50 cm. It was three weeks after rainfall before the flow in the stream had returned to the pre-storm levels.

Figure 4.3 shows the daily precipitation and discharge at Weir A for the period 12th August to 29th September 1979. The large precipitation events on the 14th to 19th August and 23rd August are followed by a month of relatively dry weather through to the end of September. Soil water potential maps are constructed for six occasions during this period (Figure 4.4). The flow on the 12.8.1979 at 0.54 $.sec^{-1}$ is higher than at the start of the 1978 events previously described, a function of heavy rainfall in the preceeding weeks, and there are positive soil water potentials at 80 cm depth both in the centre of the hollow and on the downstream spur. In this example, both t2 and t3 are registering positive pore water pressures. On the 17.8.1979 (10.00) the two areas of positive potentials at 80 cm depth have amalgamated, and t6 is now showing pressures in excess of 50 cm. The size of the zone of positive potentials expands to a maximum on the 1.9.1979 (06.00), with t8 nearly at zero pore pressure. On the 9.9.1979 (00.00) the area of positive potentials is focused on the downstream spur. The pattern established at this point remains constant through the next two weeks and then the wedge slowly contracts to the position shown on the 29.9.1979 (15.00), by which time flow has decreased to 0.28 $.sec^{-1}$. So a month after rainfall a small area of positive potentials still exists in the centre of the hollow, at 80 cm depth, and a larger area of positive pressures are present on the downstream spur. Both the area of positive potentials and the level of streamflow at this time are greater than earlier in the year, in spite of there being almost no effective rainfall for a month.

The shape of the saturated wedge and the manner in which it fluctuates can be best explained by the examination of the total soil water potentials, and the construction from these of orthogonals to the total potential lines. In the absence of vertical infiltration, this method allows the primary direction of soil water flow to be determined. In this study, this procedure is validated by the 105 cm air entry characteristic of the suction-moisture curve (Section 3.6) and the low sustained suctions (<100 cm) over much of the hillslope (See Figures 4.4, 4.8 and 4.11). (3)

Figure 4.5 and 4.6 shows the orthogonals constructed for four of the periods during the 1978 and 1979 events. The pre-storm pattern established on 29.7.1978 (00.00) shows that flow is directed evenly across the slope. This is altered by the 1.8.1978 (02.00) where convergence of flow into the centre of the hollow is clearly seen, accounting for the preferential growth of the saturated area in the centre of the hollow already observed. This pattern then slowly alters to that shown for the 3.8.1978 (01.00) where the zone of convergence has moved somewhat downstream, and is now concentrated on the downstream spur, causing the area of positive potentials at 80 cm depth to extend from the centre of the hollow across to the downstream spur. This shift in the focus of convergence leads to the area in the centre of the hollow draining with respect to the spur, so that after a prolonged period without rainfall the tensiometers at 80 cm depth in the centre of the hollow are recording negative pressures, and on the 25.8.1978 the flow net has assumed a similar pattern to that which existed in late July.

The starting position of the flow net on the 13.7.1979 (00.00) is different from the 1978 event with the centre of the hollow already recording positive potentials. Flow is again converging down the centre of the hollow and from the upstream spur into the centre of the hollow at t3. On the 17.8.1979 (10.00) the direction of convergence has again been deflected downstream away from the centre of the hollow with positive potentials across the hollow to the downstream spur at 80 cm. By the 29.9.1979 (15.00) the original pattern of flow has been reinstated, with flow off the upstream spur feeding the centre of the hollow, and positive potentials on the downstream spur fed from the upslope area and the centre of the hollow.

In summary then the orthogonals indicate that the saturaged wedge is developed at the foot of the slope initially in the hollow but then increasingly on the lower spur and that the focus of convergence migrates from the topographic hollow to this lower spur.

This effect is in marked contrast to the patterns of flow paths recorded by Anderson and Burt (1978)(18) where the zone of positive potentials is always found in the centre of the topographic hollow. On that steep-angled slope the flow lines are concentrated into the centre of the topographic hollow during summer events, and they are not affected by the downstream gradient of the slope.

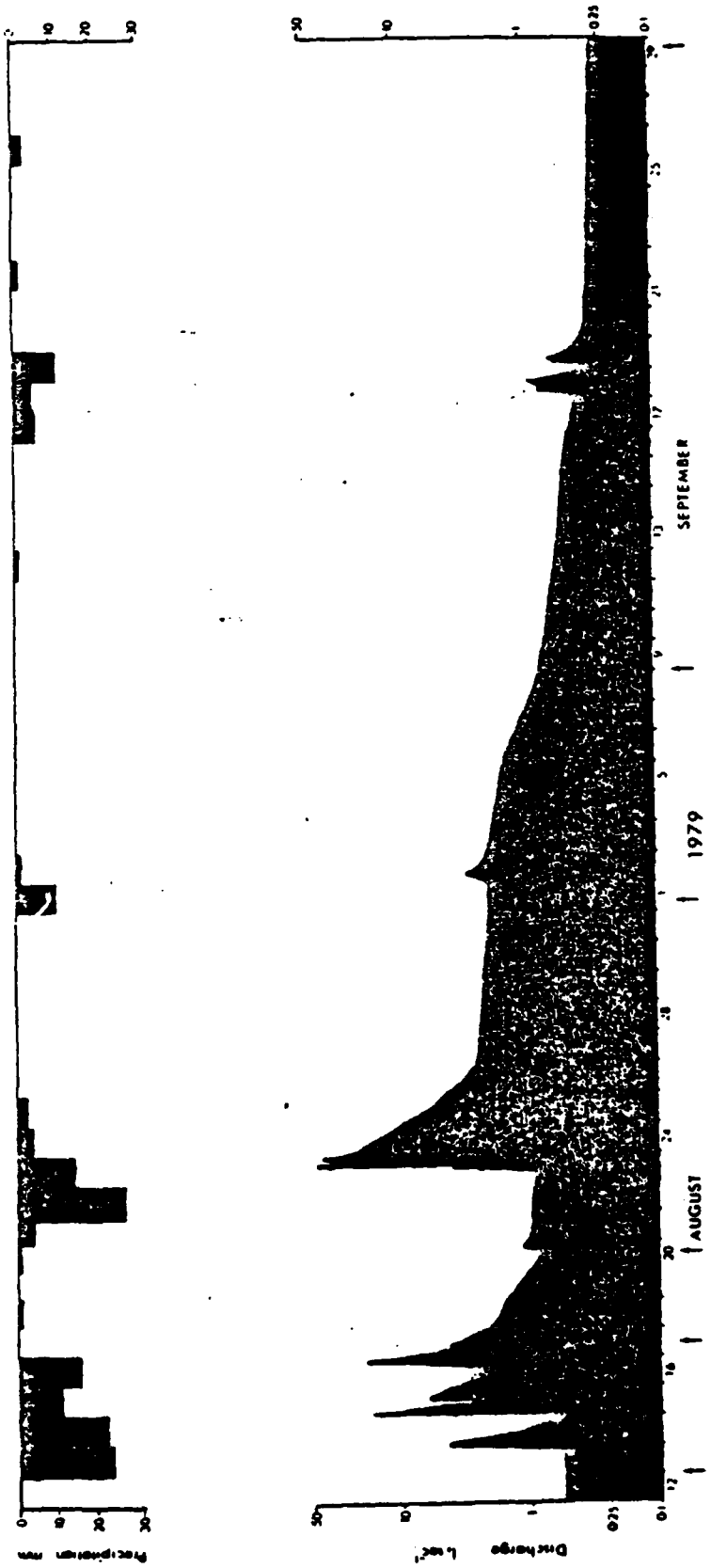

Figure 4.3. Precipitation and discharge at weir A, 12 August to 29 September 1979.

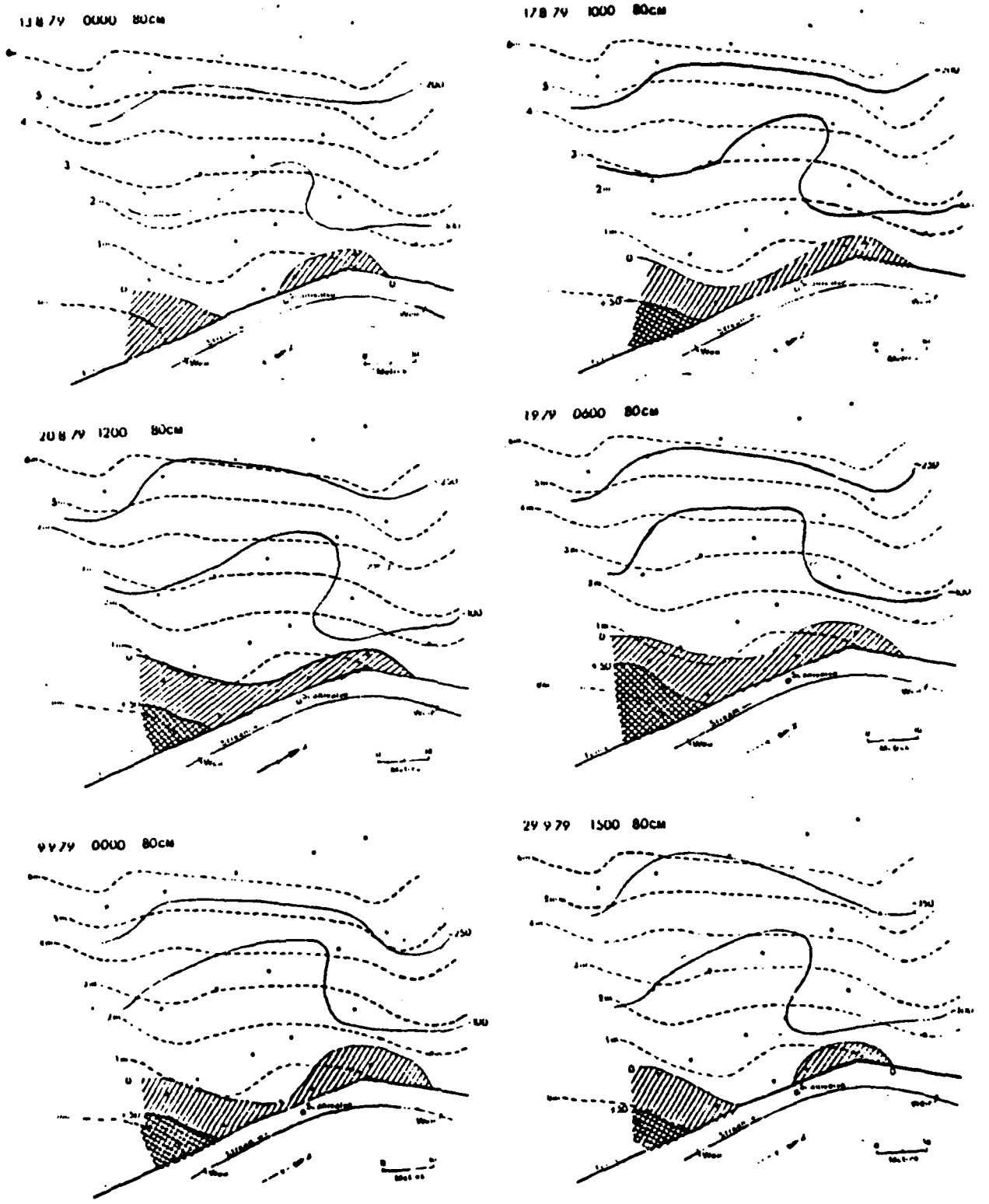

Figure 4.4. Soil water potential maps, 13 August to 29 September 1979.

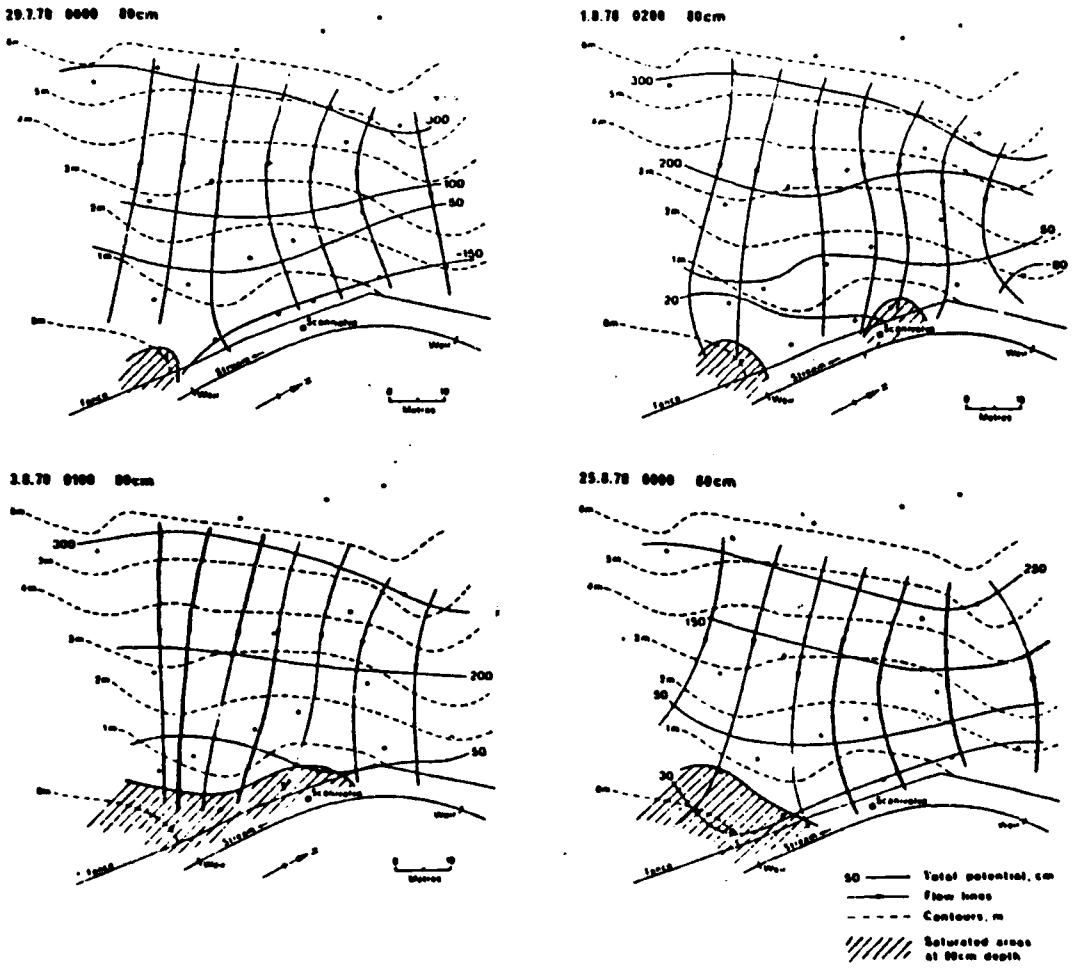

Figure 4.5. Flow nets for the period 29 July to 25 August 1978.

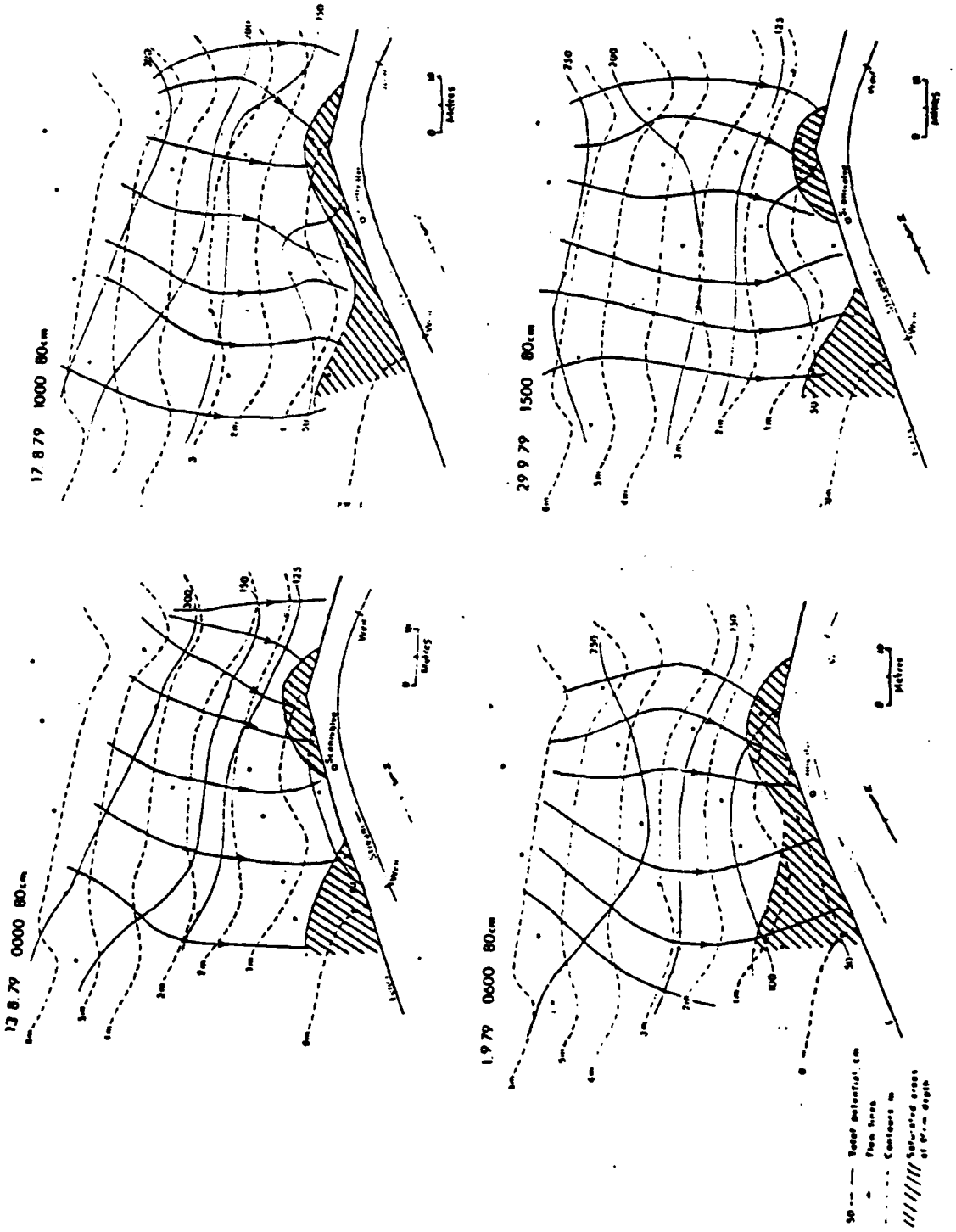

Figure 4.6. Flow nets for the period 13 August to 29 September 1979.

4.3. Winter storms and hillslope soil water potentials

The soil water potentials observed during the winter months are considerably higher than those previously described for the summer period, and the flow regime is also increased. During the winter months, there were very few rainfall events which were followed by a reasonably long recession period uncomplicated by subsequent precipitation. The event of 24th to 27th March 1979 was followed by a nine-day recession period before further significant rainfall occurred.

The discharge for this period, together with six-hourly precipitation totals are shown in Figure 4.7. The maps of soil moisture at 80 cm depth for five selected periods are shown in Figure 4.8. Prior to rainfall on 24.3.1979 (15.00) flow is already established at $6\ell.sec^{-1}$ and there is an extensive region of positive potentials across the foot of the hollow with t2 and t8 registering positive pore water pressures. The zone with potentials greater than 50 cm is more extensive than was seen in the summer events with t3 in the centre of the hollow reading +75 cm.

The hollow responds almost immediately to precipitation, the zone of positive potentials has expanded considerably on the 25.3.1979 (14.00), preferentially in the hollow centre. By the 28.3.1979 (00.00) the zone has extended onto both spurs with t1 registering positive pressures. On the 29th the zone of positive potentials reaches its maximum extent. The -100 cm potential on the 28.3.1979, highlights the existence of a wedge of low tensions in the centre of the topographic hollow extending upslope to t18 and t19. On the 31.3.1979 (00.00) the zone of positive potentials is already starting to contract, although the hollow centre is still exhibiting high soil water potentials, as is the downslope spur. The foot of the upstream spur (t1) is again registering small soil water tensions at 80 cm depth. By April 5th the hollow has drained considerably with pressures in excess of 50 cm now found only around the downstream spur at 80 cm depth. The area of the slope which has pore water pressures in excess of 0 cm is still more extensive than was observed for either of the summer events examined.

As with the summer events, the pattern of soil water potential variation, and the position and extent of the zone of pore water pressures is best explained in terms of the flow net adjustments over the storm and recession periods (Figure 4.9). On 24th March, the flow net reveals that there is a strong convergence into the centre of the hollow, in the vicinity of t3, t4 and t9. Twenty-four hours later the zone of convergence has moved across the hollow so that

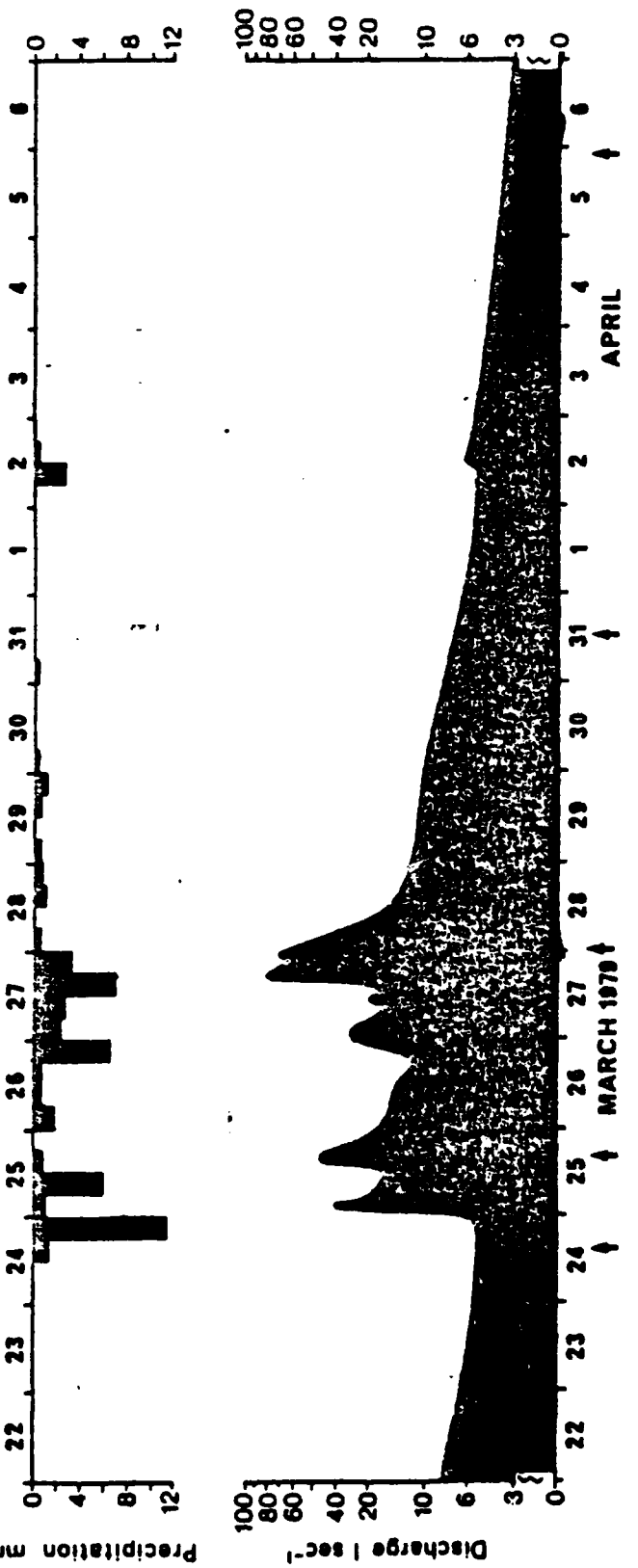

Figure 4.7. Precipitation and discharge at weir A, 22 March to 6 Arpil 1979.

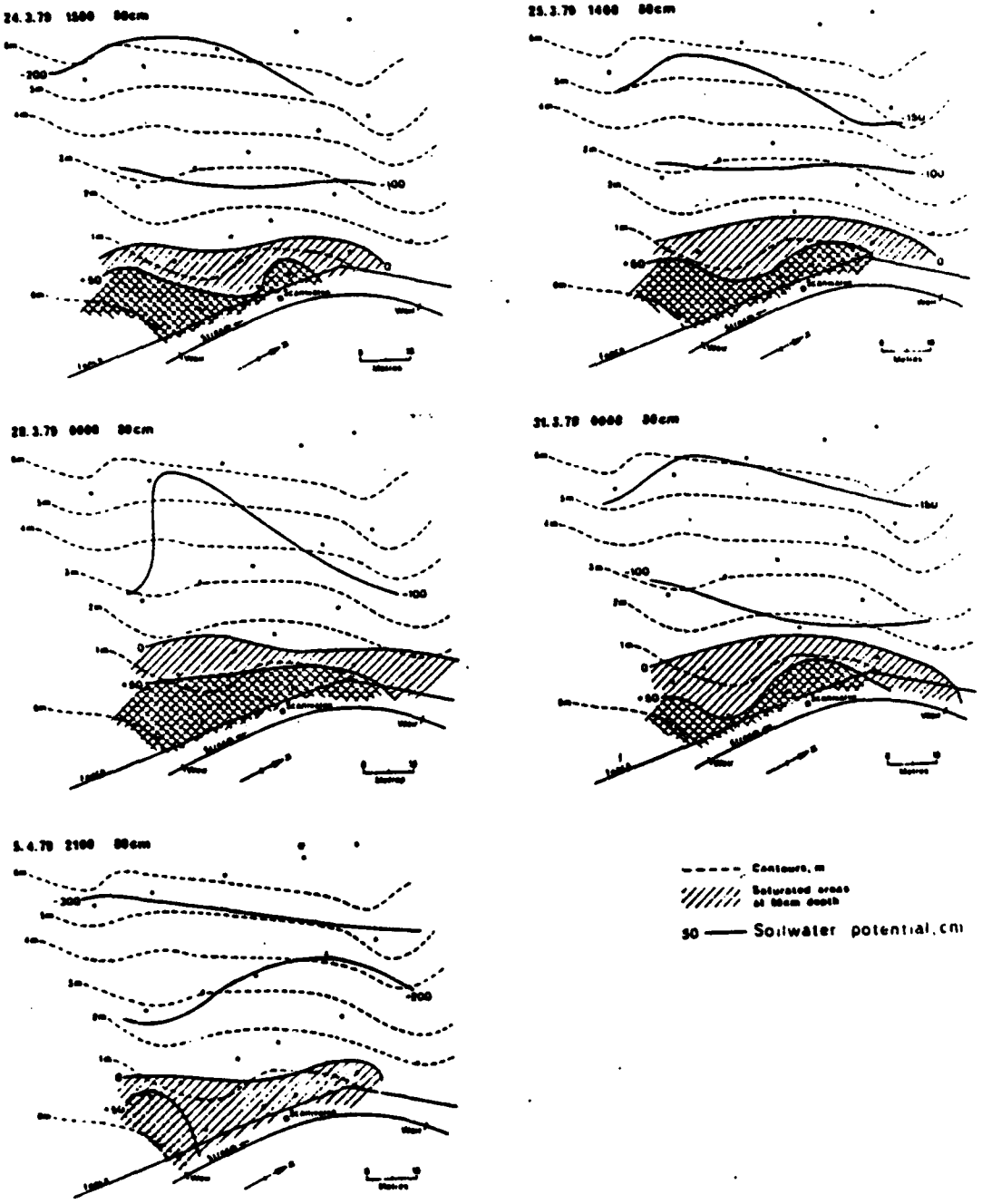

Figure 4.8. Soil water potential maps, 24 March to 5 April 1979.

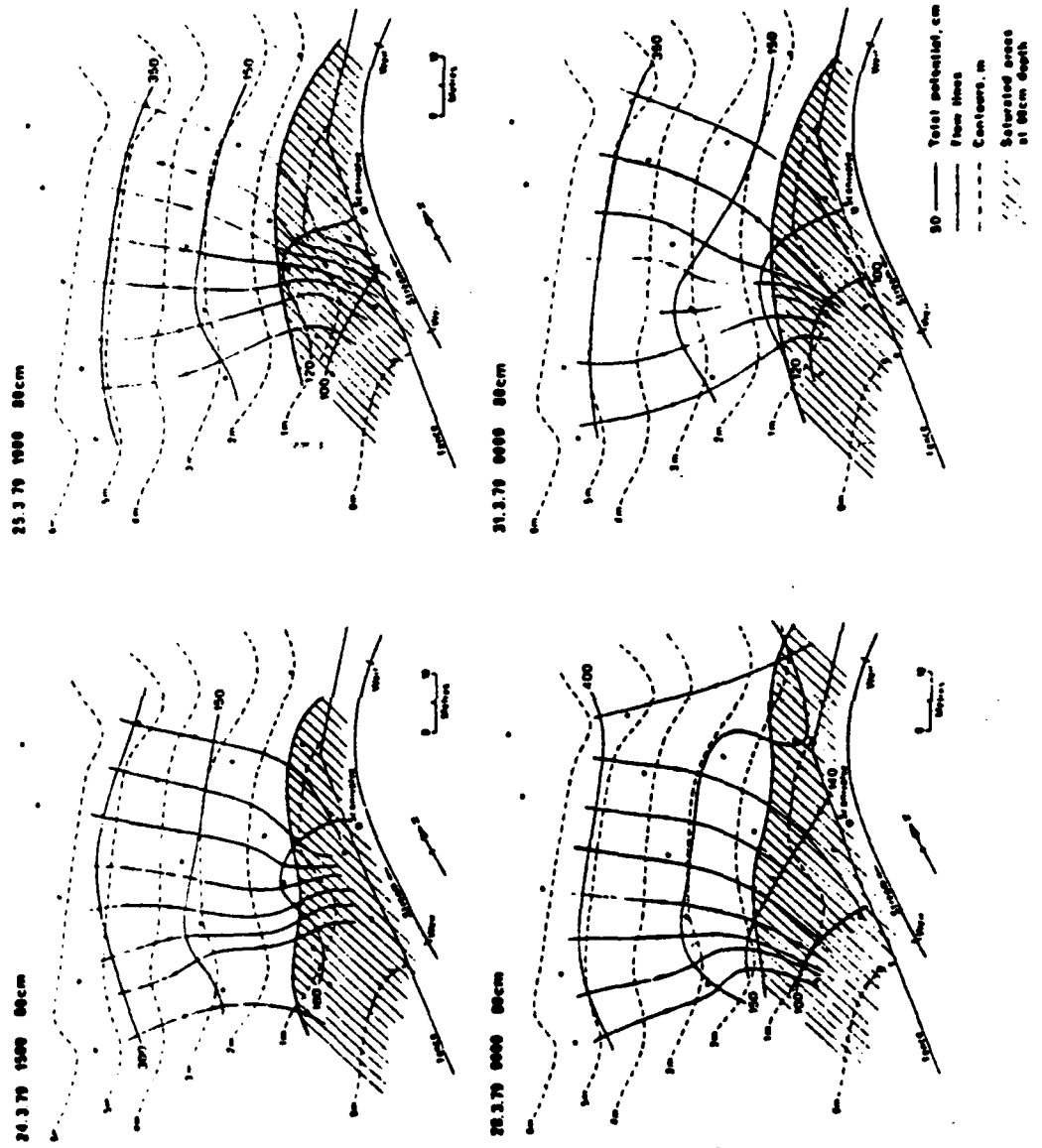

Figure 4.9. Flow nets for the period 24 March to 31 March 1979.

flow from the topographic hollow and the downstream spur slope is feeding the area at the foot of the downstream spur, from t4 and t9. The upstream spur is feeding down to the foot of this spur at t1 leading to the development of positive potentials here on 28.3.1979 (00.00). During the recession period, the pattern of the flow slowly returns to a state similar to that on the 24.3.1979, with the flow converging to the centre of the hollow and the downstream spur. During this winter event it can be clearly seen that the area of positive potentials is greater than during summer events, but more importantly that the response of the soil to precipitation is more immediate.

An interesting contrast to this storm is provided by the precipitation events during the period April 7th to 12th, 1979. These give an example of the disparity that can occur in the soil moisture and runoff response as a consequence of precipitation of different intensities. Figure 4.10 shows the six-hourly precipitation totals together with the runoff hydrograph for Weir A. Prior to precipitation, streamflow was established at $3.2\ell.sec^{-1}$. The precipitation on 8th April was of low intensity, averaging about $1mm.hr^{-1}$ with two short periods of more intense precipitation producing the streamflow peaks of $11\ell.sec^{-1}$ and $17.5\ell.sec^{-1}$. The recession on the 9th and 10th is markedly different from those previously described. The streamflow is maintained at the relatively high level of $9\ell.sec^{-1}$ by almost continuous low intensity precipitation during these two days. When precipitation ceases, the volume of recession flow falls quickly. The storm event on 12th April was very intense with some 8mm falling in a period of 70 minutes. This generated the very marked peak in streamflow of $18.3\ell.sec^{-1}$, and is followed by a rapid recession during which there was no additional precipitation.

Soil water potential maps are constructed for four time periods during these events, (Figure 4.11) at times indicated by the arrows on Figure 4.10. The soil water potential response to rainfall is nearly synchronous, as is to be expected from the previous discussion of the March event, although potentials in the centre of the hollow do not reach +50 cm because the total precipitation is much smaller than for the March 1979 events.

On 9.4.1979 (02.00) the area of positive potentials is at its maximum with t8 showing a small pressure (+6 cm), and flow is predominantly towards the centre of the hollow. As the preceeding storm analyses have shown, this pattern then alters so that the main flow direction is towards the downstream

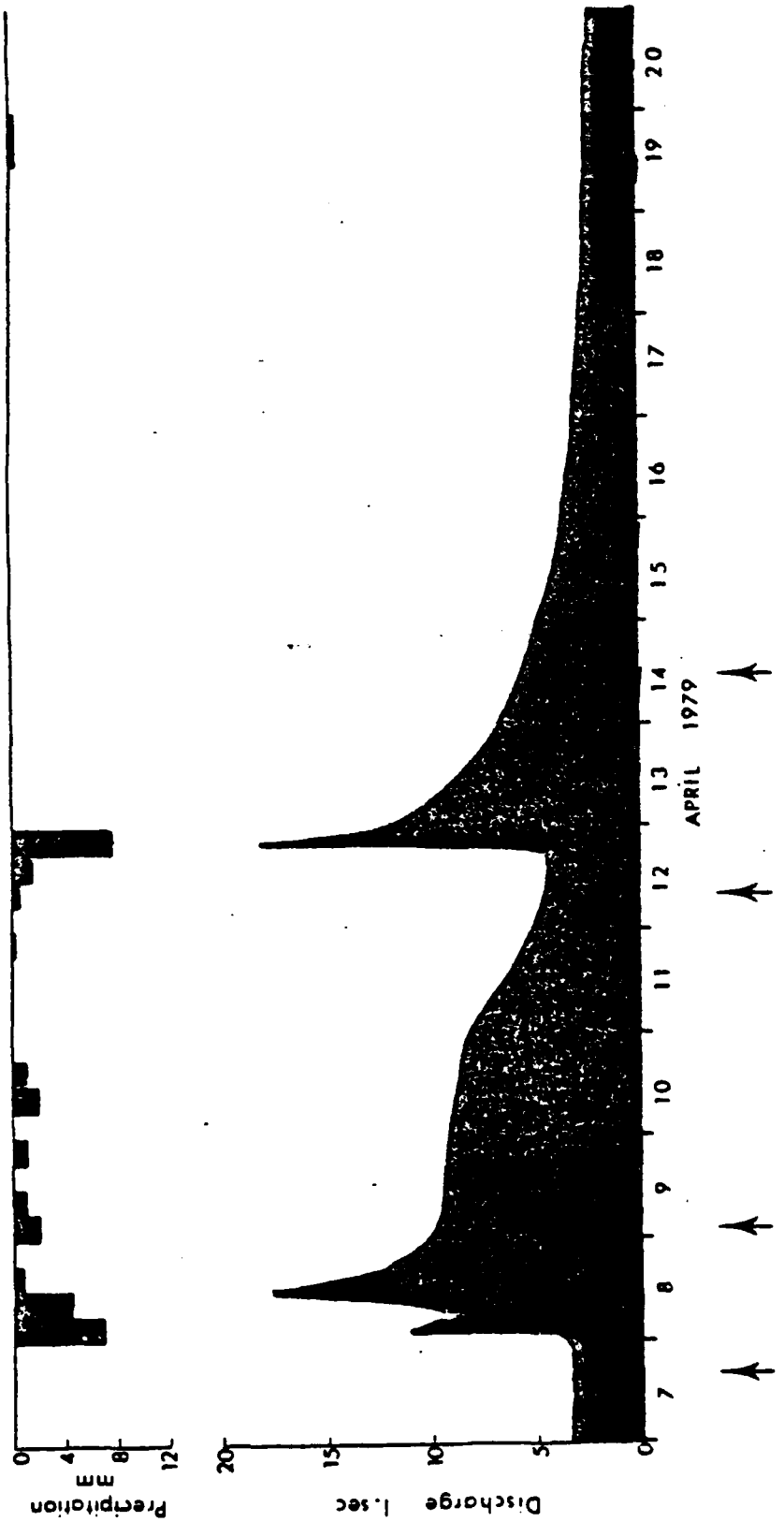

Figure 4.10. Precipitation and discharge at weir A, 7 to 20 April 1979.

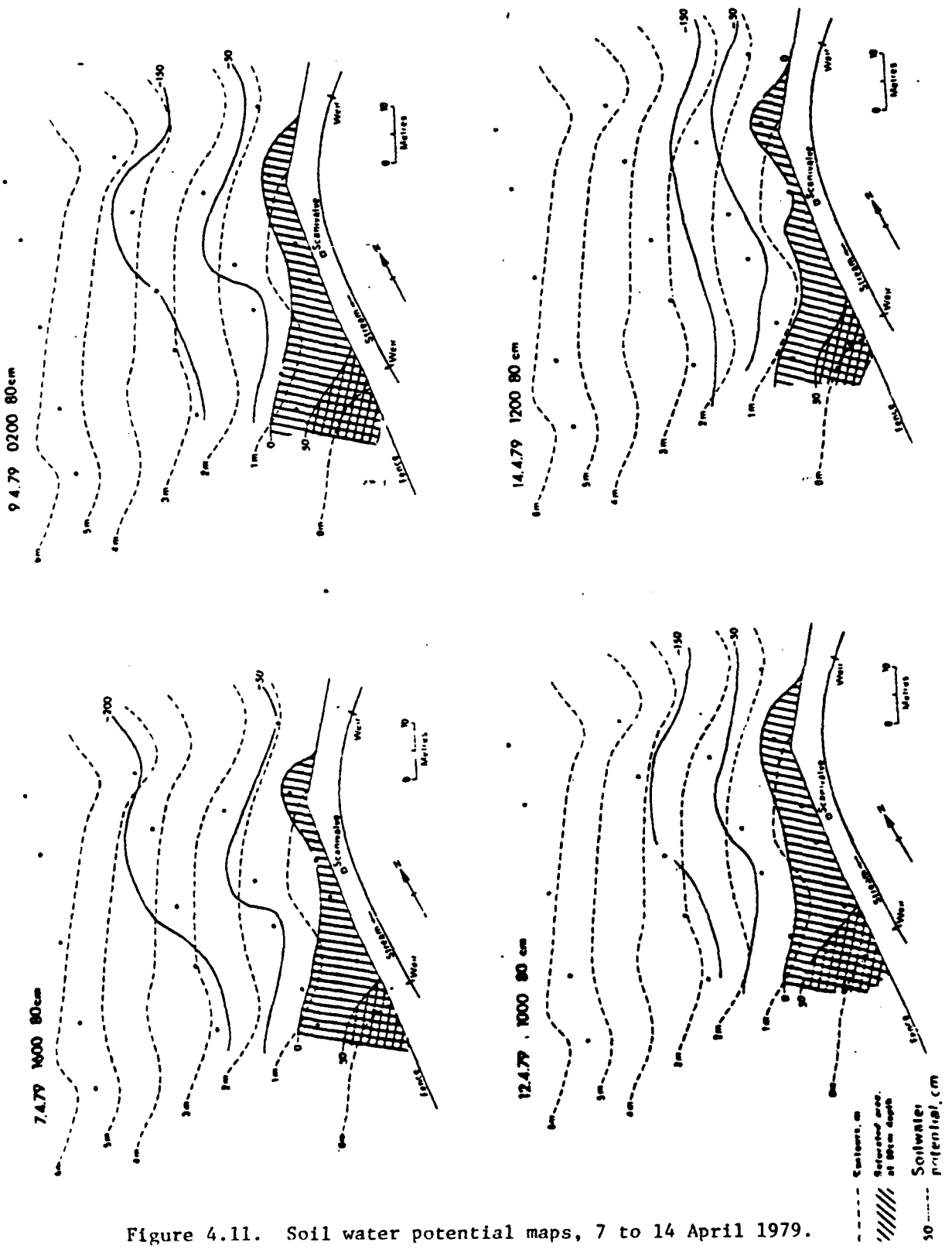

Figure 4.11. Soil water potential maps, 7 to 14 April 1979.

spur, and this is exemplified by the increased area with potentials greater than +50 cm in this region on 12th April.

On 14.4.1979 (12.00) flow is $5.8\ell.sec^{-1}$, but the soil moisture map for this time shows that the slope has continued to drain. Tensiometer number 6 is now the only one recording pressures above 50 cm and in the centre of the hollow tensiometer 3 is registering slight tensions. The pattern of the soil water potentials is therefore essentially similar to that prior to rainfall on 7th April.

These events show how important low intensity precipitation can be in maintaining higher flows in the stream, and in sustaining high soil water potentials. There is very little change in the soil water potential maps between the 9th and the 12th April whereas the results from the previous analysis of the 'winter' storm suggest that there should have been contraction of the wedge of positive potentials. Further, the effect of very high intensity rainfall on this catchment is important in terms of the peak flow. Rainfall of this type runs off quickly overland, unable to infiltrate into the clay soil because of its low hydraulic conductivity, causing a high peak which is followed by a rapid recession, with the pre-storm streamflow levels re-established within 48 hours. The soil water potential maps show that the slopes continued to drain during this period so that this event had no practical effect on the soil water status in the slope. A smaller wedge of positive pressures existed after the intense precipitation event than before (12.4 to 14.4.1979), unlike the growth of the saturated area with less intense precipitation from the 7th to 9th April, 1979.

4.4. Summary

The development and the movement of the saturated wedge across the hillslope hollow on this very shallow slope gives substantial empirical support to observations from two less detailed previous studies. Firstly, Beven (1978)(43) reports on the distribution of saturated areas within the Crimple Beck catchment. In that basin the saturated areas are shown to expand and contract during and between storm rainfall in a manner which reflects the complexities of soil and topography. The dynamic changes in the contributing areas are conditioned by very minor changes in topography. The change in the pattern of the positive soil water potentials across the shallow slope (see for example Figure 4.8) is supportive of this general statement.

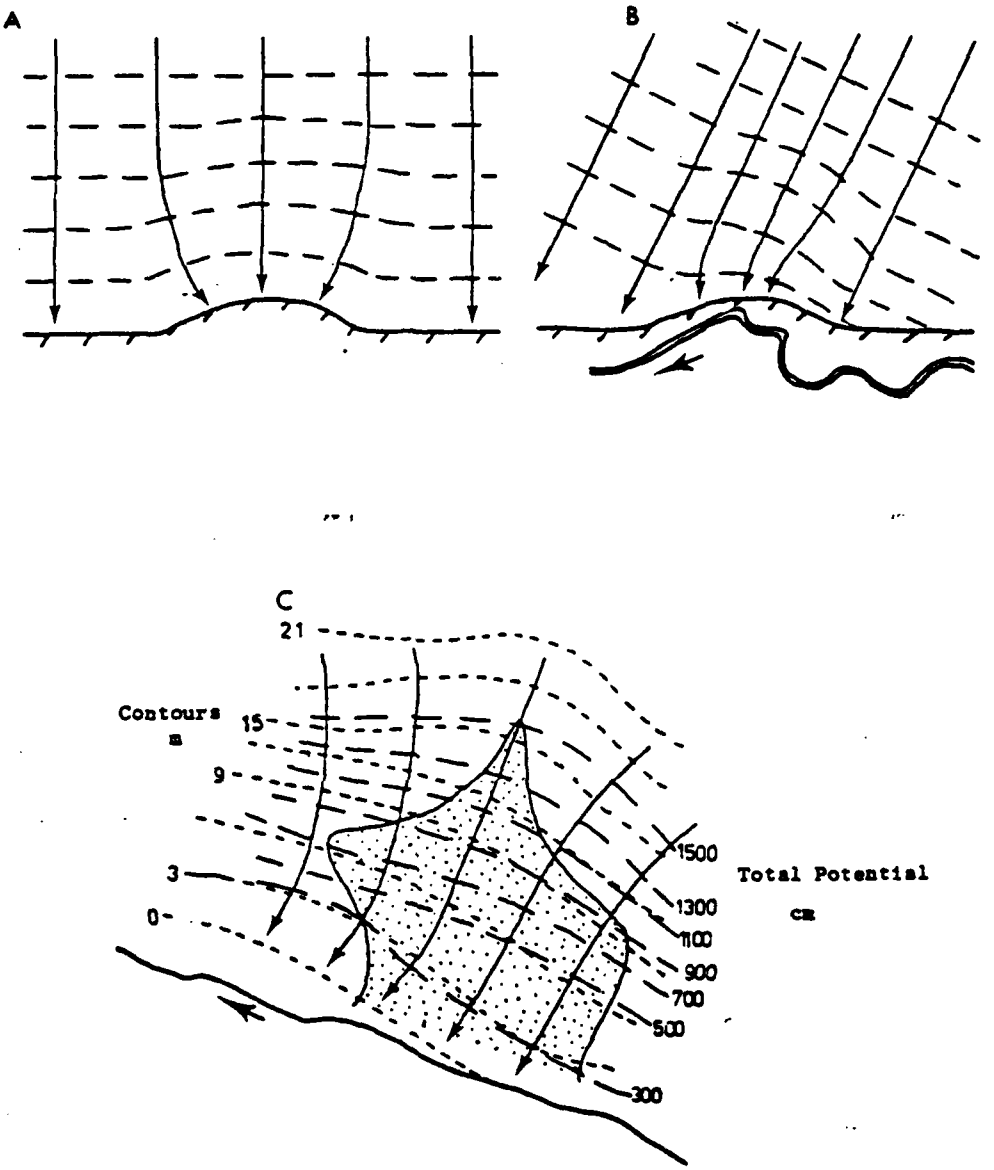

Figure 4.12. A and B Theoretical path of flow lines based on elevation potential. C Convergence of flow lines into a topographic hollow. (From Anderson and Burt 1978)(18).

Secondly, Dunne (1969)(44) hypothesized that the presence of a down stream gradient could cause the direction of the orthogonals to the total potentials to be deflected in downstream directions, as for example in Figure (4.12 a and b).

On the shallow slope reported here, the elevation potential is small in comparison with variatons in soil water potential. For example, the difference in elevation between the hollow centre and the upper spur is 125 cm, whereas the soil water potentials range over 560 cm during the year. Consequently the development of saturation in different parts of the slope affects the total flow pattern.

This is not the case on very much steeper slopes where elevation is much more important. Kirkby and Chorley (1967)(21) suggested that zones of soil saturation would develop preferentially on slopes which have concave contours and slope profiles. Empirical results from detailed tensiometers measurements on a 26° slope confirmed this hypothesis. The hillslope hollows were shown to be the major source areas of throughflow discharge because the saturated wedge was developed there (Anderson and Burt (1977)(2), (1978))(3). Orthogonals to the total potential lines for summer and winter storms showed that <u>at all times</u> the focus of convergence was towards the centre of the hillslope hollow. No movement across the hollow was detected despite a downstream gradient in excess of 5°.

Since the elevation potential dominates the total potential calculation on steep hillslopes, Anderson and Burt suggest that the contours alone may be substituted for mapped total potentials in the calculation of the general direction of hillslope soil water flow. The presence of diverging contours would therefore indicate less saturated soils than areas of converging contours. For this case the close agreement between natural contours and total potential is indicated in Figure 4.12C, which also shows the zone of positive soil water potentials developed in the instrumented hollow after a storm event. The dominance of elevation is clearly seen here where the elevation potential exceeds 2100 cm and the soil water potentials over the slope range over less than 100 cm.

Using the contours as a surrogate for total potentials in the shallow slope case would not of course be adequate. Figure 4.13 plots the position of the orthogonals to the contours. The main flow direction is into the hollow centre and there is divergence on the downstream spur. This is in marked contrast to the actual position as mapped in Figures 4.8 and 4.11 where convergence

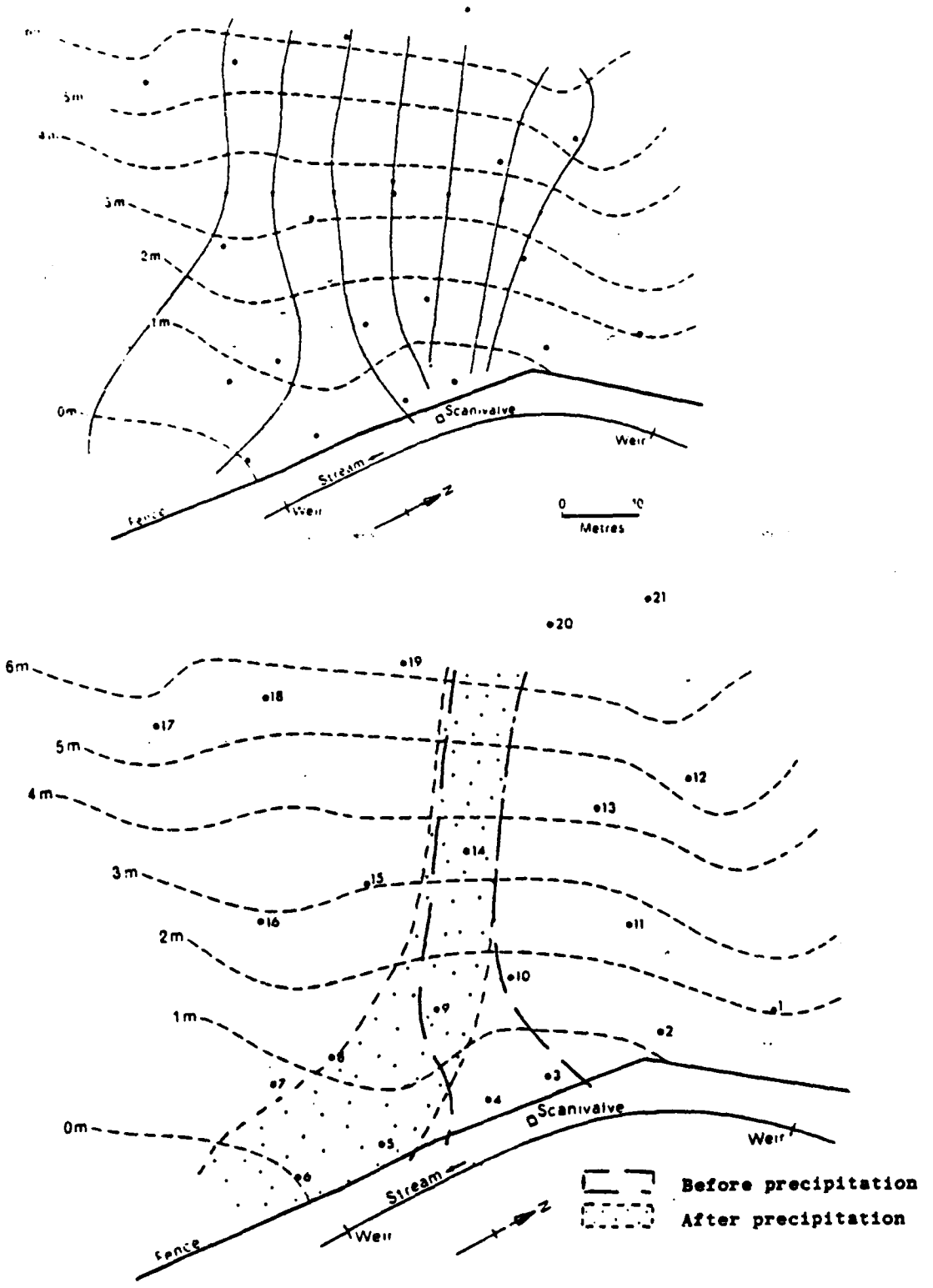

Figure 4.13. A Flow lines based on contours for the study slope
B Path of flow lines in the centre of the hollow before and after precipitation.

to the hollow occurs before the storm followed by the migration focus of the saturated area on the lower spur.

In summary therefore the empirical study of soil water potentials has shown:

(i) that zones of saturation in shallow topography are not confined to hillslope hollows

(ii) that the size and location of such zones are heavily dependent upon the detailed relationships between topography and soil-water potentials, the latter being a function of time during the storm.

(iii) that source areas for streamflow contributions in shallow topography present a much more complex temporal and spatial pattern than source areas in steeper topography.

Chapter 5

Appraoches to Identify Soil Water Convergence Zones in Shallow Topography - Empirical Evidence

5.1. Introduction

In chapter 4 the empirical data from the study slope was used to map the position of the saturated wedge and the migration of the focus of convergence was examined in a qualitative manner. In this chapter the empirical data ia analyzed in greater detail in order:

(1) that the controls on the migration could be delineated

(2) to predict the focus position at the slope foot

(3) to examine and optimize the original soil water sampling frame

(4) to consider alternative indirect methods of identifying the saturated wedge.

In order to quantitatively analyze the soil water data, the soil water total potentials at 80 cm depth for eighty-one periods between May 1978 and July 1979 were used. This data covered two summer storm periods and the winter of 1979. From these data soil water potential maps were drawn using the Ginosurf package program.

5.2. Focus movement mechanisms

The major part of this analysis relates to the plots of total potential. On these maps, orthogonals to be total potential lines were constructed by hand to show the direction of flow. From these orthogonals, the position of the focus of soil water convergence at the foot of the slope was thereby determined. Focus position accuracy by this method is of the order of ± 2m. For example, Figure 5.1 shows the position of the total potential and the orthogonals to the total potentials for three times during a March 1979 storm event.

Immediately prior to the start of precipitation, the focus is at 22m, close to the centre of the topographic hollow. Twenty-one hours later as rainfall stops, the focus has moved to a position at approximately 5m on the downstream spur, while three days later it has returned to the centre of the hollow.

Although the focus can be seen qualitatively to move in Figure 5.1, the mechanism causing migration needs closer examination.

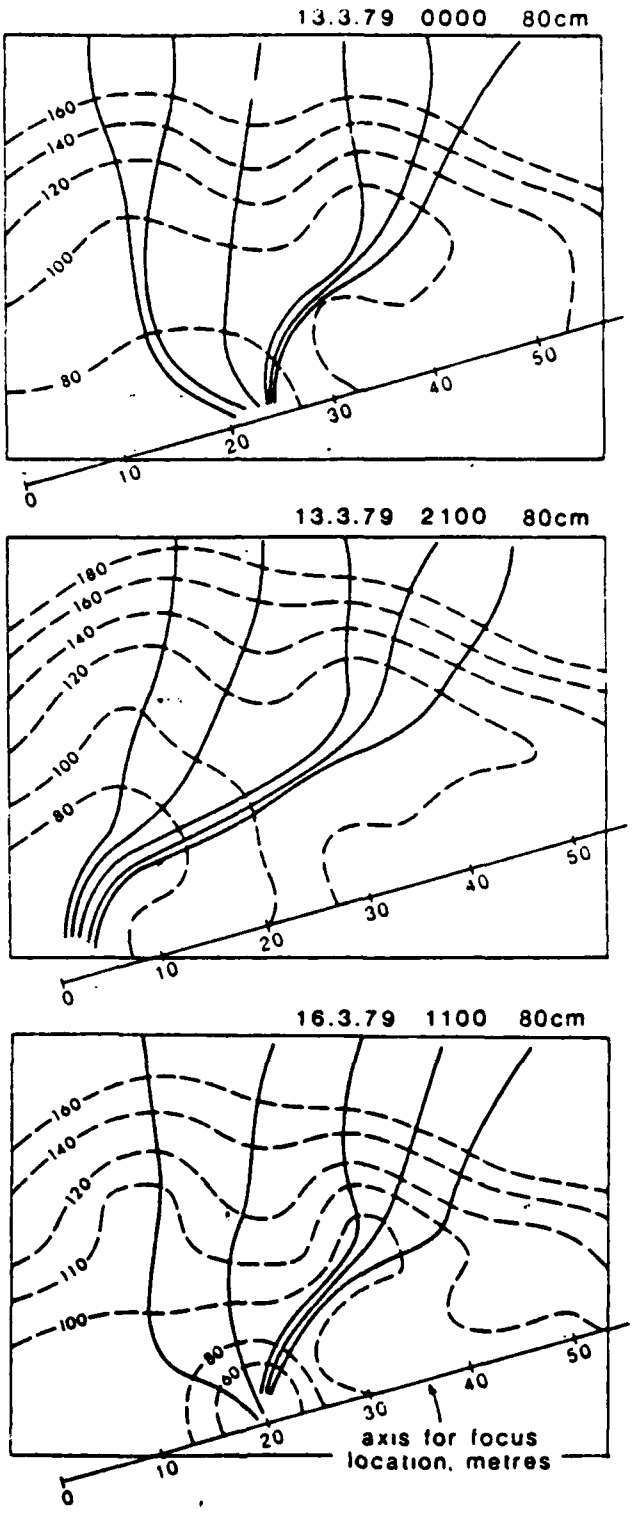

Figure 5.1. Orthogonals to total potential lines during a precipitation event in March 1979.

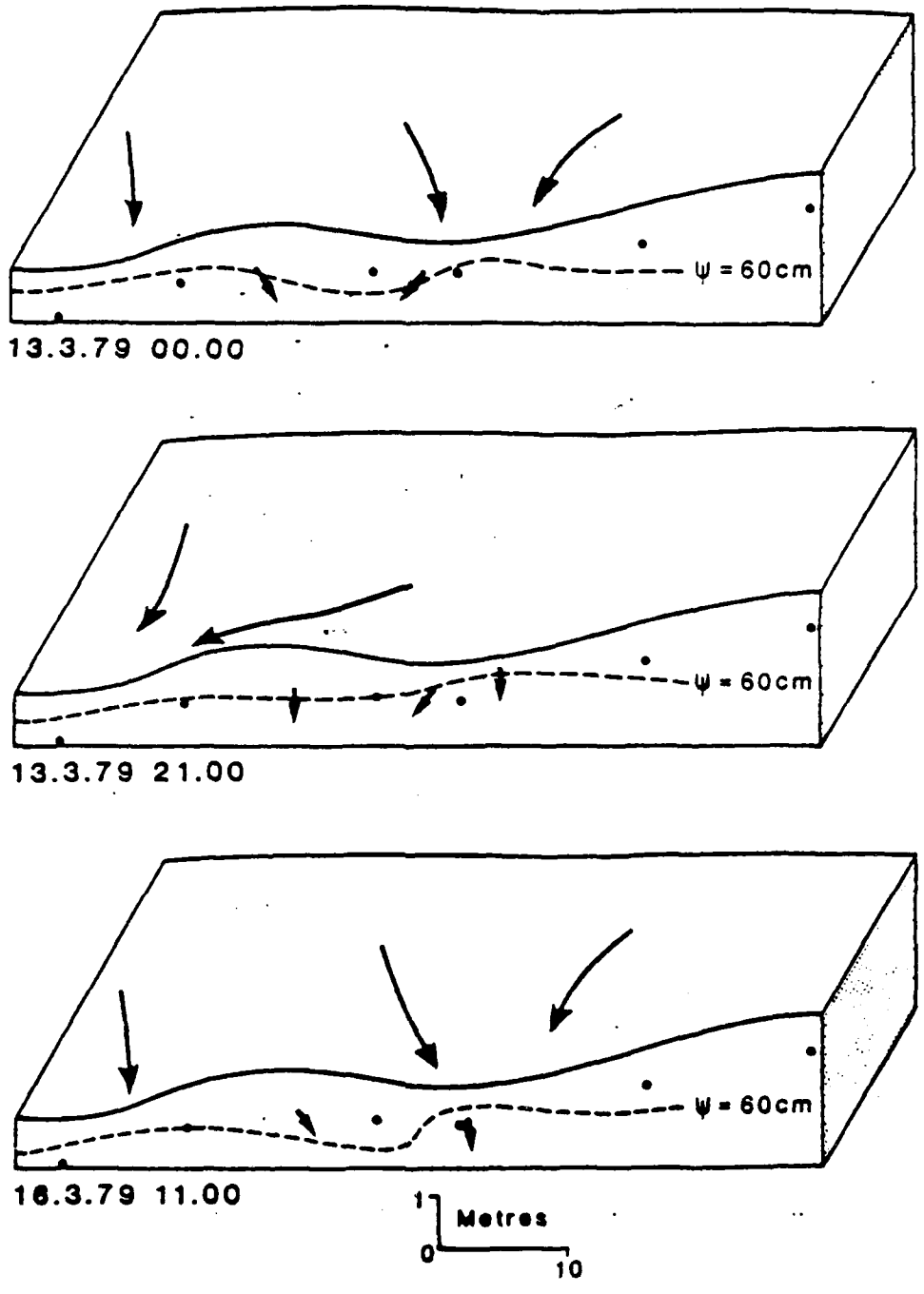

Figure 5.2. Changes in dominant convergence in plan and section, together with the 60 cm soil water potential contour in section during storm (a) Figure 5.3.

To illustrate the mechanisms involved Figure 5.2 shows the position of the soil water potentials in section for the same time slices as the previous figure together with the orthogonals to the total potentials in both section and plan. The stages of development for the March 1979 event are:

(1) 13.3.1979, 00.00. The focus of covergence is directed down the centre of the topographic hollow and the soil water potentials are raised under the hollow. The relative height of the 60 cm soil water potential beneath the hollow creates or causes the flow moving down the hollow to be deflected laterally under the downstream spur.

(2) 13.3.1979, 2100. The deflection of water to the area under the spur has raised the Ψ = 60 cm line right across the slope such that it is almost horizontal. The soil water potential difference between the hollow centre and downstream spur is therefore unimportant in determining the soil water flux and the driving potential becomes the difference in elevation between the hollow centre and the lower side of the downstream spur. Consequently, the focus of convergence moves right across the slope.

(3) 16.3.1979, 11.00. The convergence plan returns to its initial position because there is continuous drainage from the area under the hollow and lower spur to the stream. However the hollow has a much larger source area of throughflow than the area under the downstream spur which can only saturate up as a result of "spill over" effects from the hollow. The preferential lowering of the soil water potentials under the downstream spur causes the focus to be re-established in the hollow centre.

This example shows that the relationship between the elevation potentials and soil water potentials is in a very fine balance in this type of slope. The location of the focus is of course very important because it can determine the major sources areas of throughflow discharge and could control the location of source areas for return overlandflow. At the study site, the preferential saturation at the surface, occurrence of overlandflow and detention storage on the lower spur has been observed in the period following winter precipitation events.

5.3. Focus prediction

The position of the focus at the foot of the slope was mapped for a series of storm events at all times of the year. The pattern of focus migration across the slope shown in Figure 5.1 is plotted up for three storms in Figure 5.3.

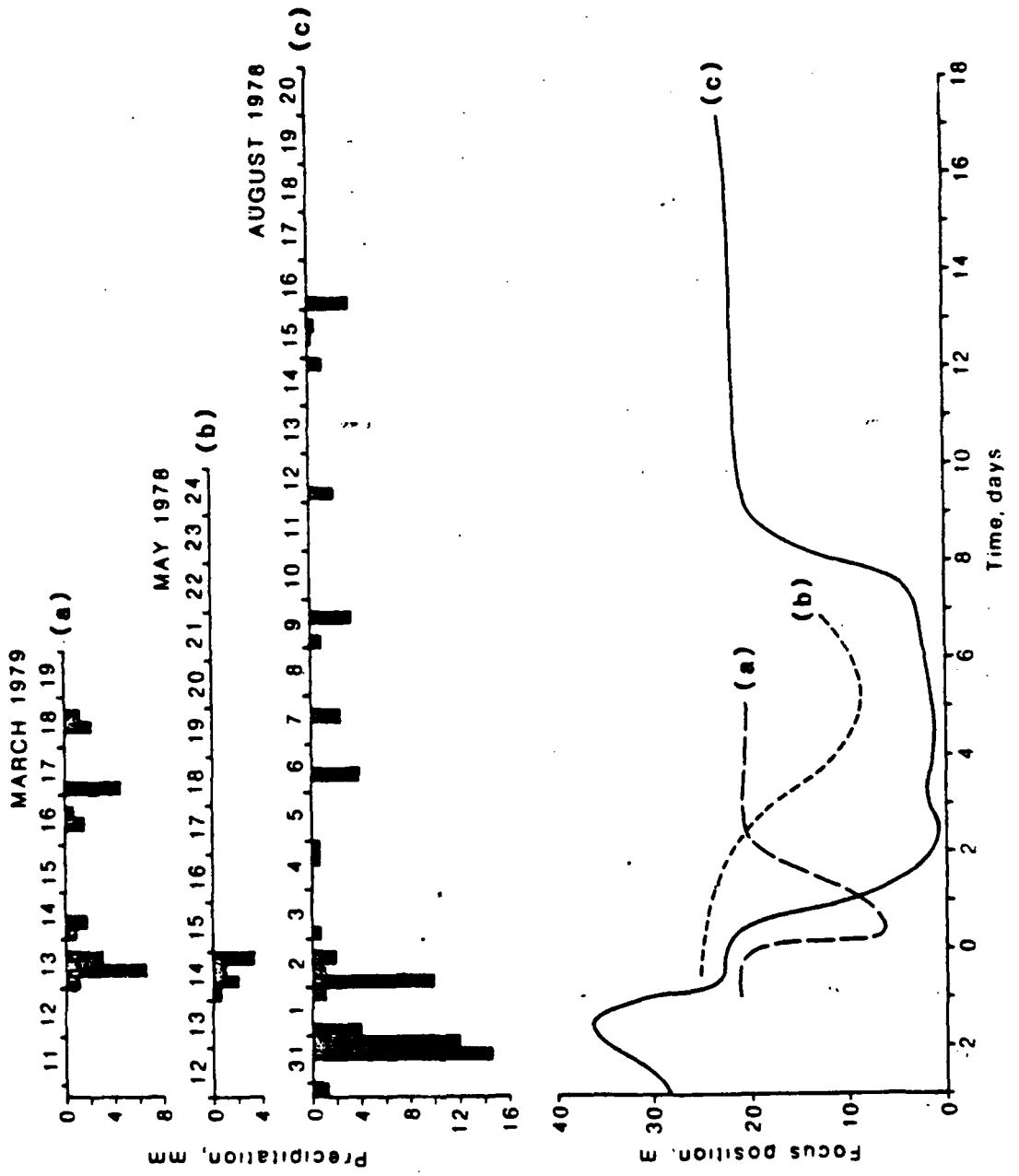

Figure 5.3. Focus position of hillslope soil water for 3 events (Figure 5.1 defines the baseline for measurement)

Here the March 13-16 1979 storm is again represented as are a late Spring and severe Summer precipitation event.

It is important to note the variation in the timing of movement in each case. For the May event which was relatively small, the focus does not reach the downstream spur until five days after rainfall ceased. In terms of the process mechanism described in the last section, this is because lateral throughflow needed to raise the soil water potentials to the horizontal position under the downstream spur took very much longer because the soil was drier (initially unsaturated at 80 cm under the lower spur).

In the case of the heavier August precipitation event, the movement of the focus to the downstream spur takes longer than in the case of the March event although there is greater total precipitation. Again this is explained by reference to the pre-storm pattern of soil saturation. (See Figure 4.2).

On the 1.8.78, 0200 there are two small areas of positive potentials in the centre of the hollow and on the downstream spur. By the 3.8.78, 0100 hr the two areas of saturation at 80 cm depth have amalgamated and the focus is starting to migrate across the hollow reaching its furthest extent on the lower spur on August 5th. The focus was retained on the downstream spur for five days and then slowly migrated back to the hollow position.

This shows that there are considerable temporal variations in the movement of the focus. Also that the timing of focus movement is strongly related to the state of saturation under the downstream spur.

If the area under the downstream spur is unsaturated at the start of the storm event, the "spill over" lateral movement of water into this area will be considerably slower than if the soil was saturated. This being the case, the soil water potentials do not become horizontal in section from hollow to spur until later in the storm event, and focus migration is consequently slower.

Ordinary least squares regression was used to obtain a model to predict the position of the focus at the foot of instrumented slope. The model was based on data for seven independent storm events from all times of the year. The recession periods ranged from three days to twenty days after the end of the precipitation input. The model obtained was:

$$f = 22.37 + 0.097P - 0.527\ Pl - 0.124t + 6.9 \times 10^{-5}\ t_2 - 9.6 \times 10^{-7}\ t_3$$

where: f = focus position at foot of slope, - m see Figure 5.1.

t = time (hours) where t = 0 at the end of the precipitation event see Figure 5.3.

p = precipitation (mm) in the 12 hr period t = -12 to t = 0 hr

p_1 = precipitation (mm) in the 72 hr period t = -84 to t = -12 hr

The model is significant at the p = 0.01 level, $r^2 = 0.32$.
The predicted and observed focus positions for this model are plotted in Figure 5.4 together with error distributions.

The model was then applied to another independent precipitation event in May 1979. This event had not been used in the original model calibration. The actual and predicted positions of the focus of soil water convergence are shown in Figure 5.5.

5.4. Sampling frame for soil water monitoring

Having empirically determined the processes of soil water movement on the study slope and established predictive models for the migration of the focus, it is instructive to re-examine the sampling frame with a view to optimizing data collection at new sites. Parsimony in data collection without a significant loss in data quality has obvious advantages.

Original network

The original tensiometer network was laid out on a grid system encompassing the hillslope hollows and the two adjacent spurs (Figure 3.1). Tensiometers were installed at up to three depths 40 cm 80 cm, and 150 cm depth, with complete cover over the slope at 80 cm depth. This was in anticipation of finding the active throughflow zone clearly expressed, expanding, and contracting, at this level. The soil water potential maps shown in previous chapters indicate this installation cover.

In this section, the spatial sampling frame at 80 cm depth is reduced by the ommission of certain tensiometer points and the resulting computer drawn maps of soil water potential are analyzed. Implicit in the spatial optimization is a sectional optimazation of points. It is worth noting here that three depths of tensiometers is almost the minimal sampling frame for the determination of hydraulic gradients in different parts of the slope and for the construction of cross sectional soil water profiles.

Figure 5.6A shows in diagrammatic form the field network of tensiometers at 80 cm depth. Data from these points were used to construct the soil water maps. Figures 5.5B, C, and D show three alternative sampling frames which were

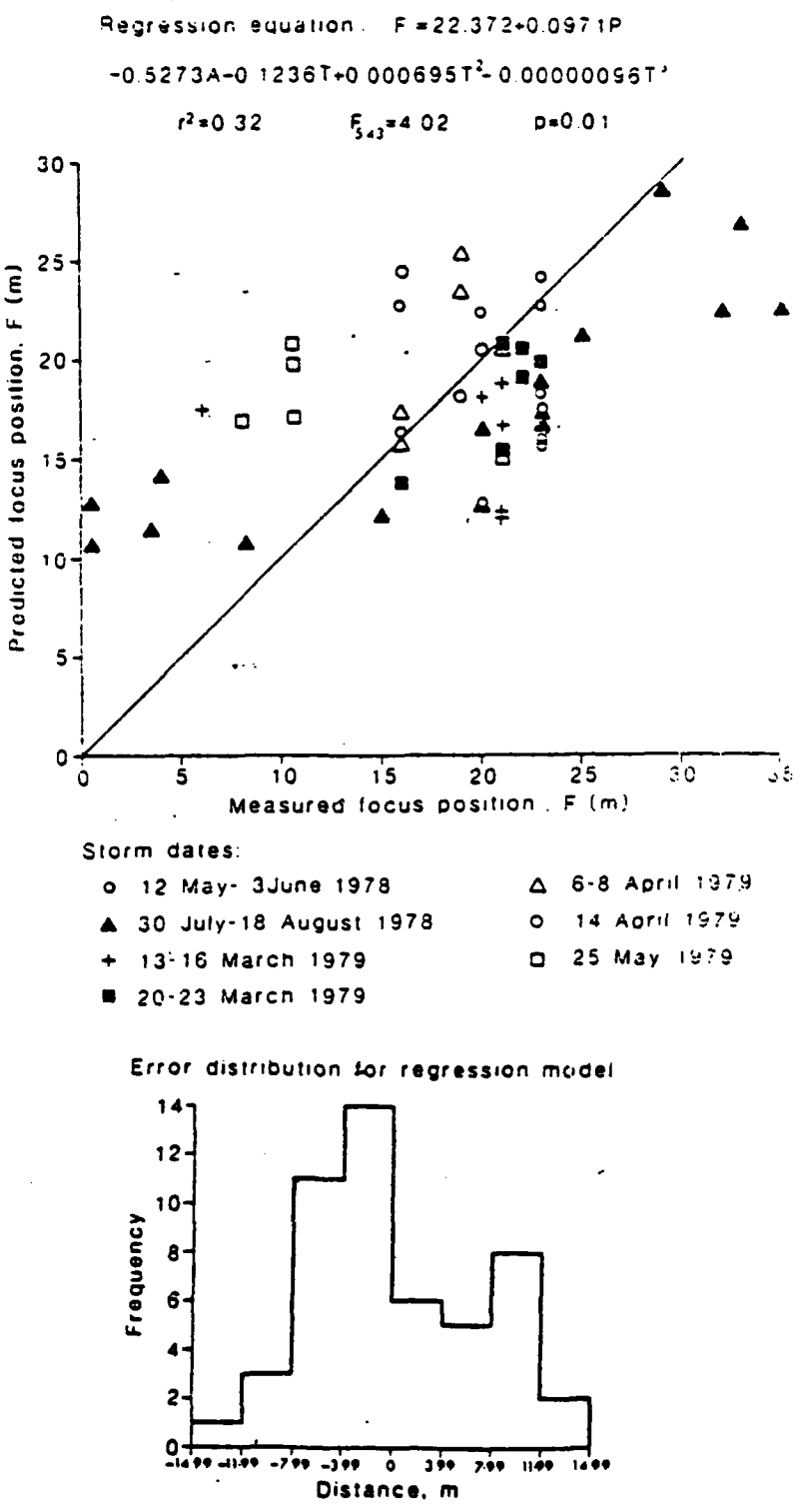

Figure 5.4. Regression plot and error distribution plot of focus prediction model.

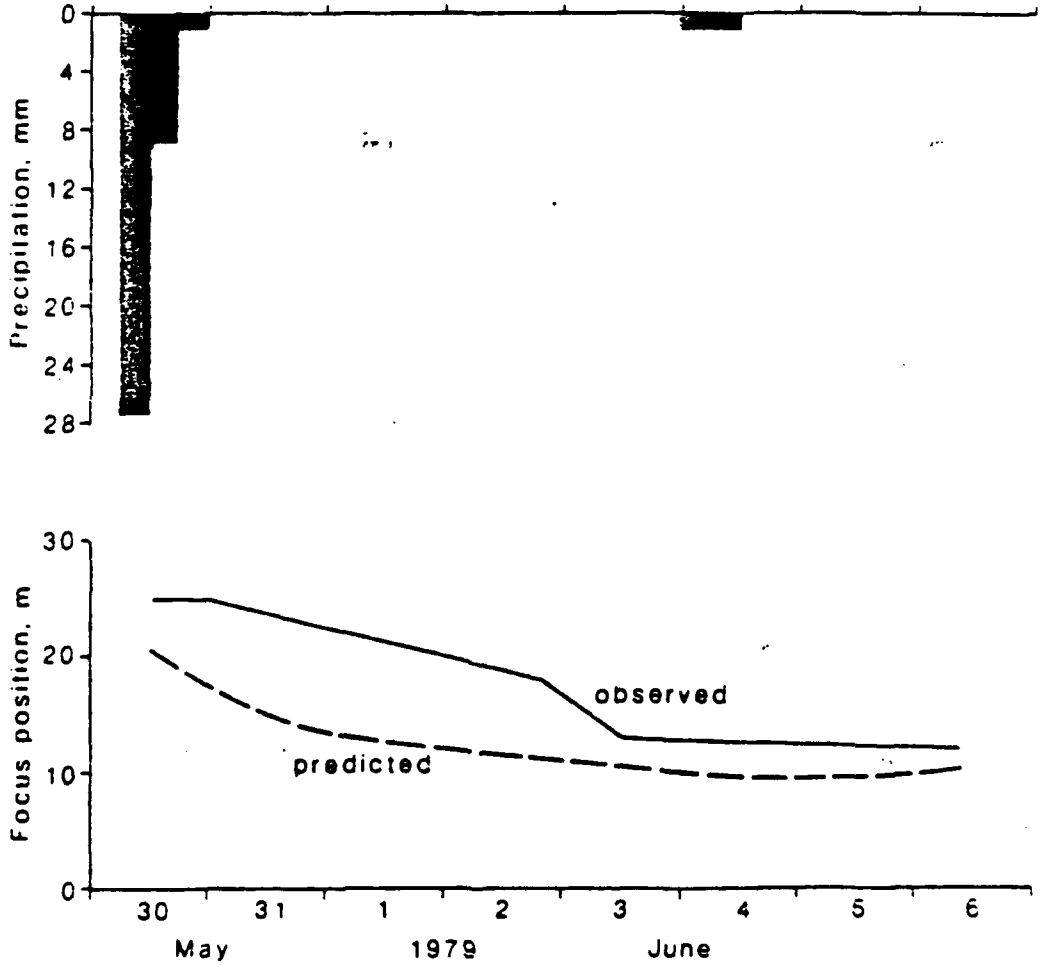

Figure 5.5. Focus position predicted by model for a storm event not used in the model calibration.

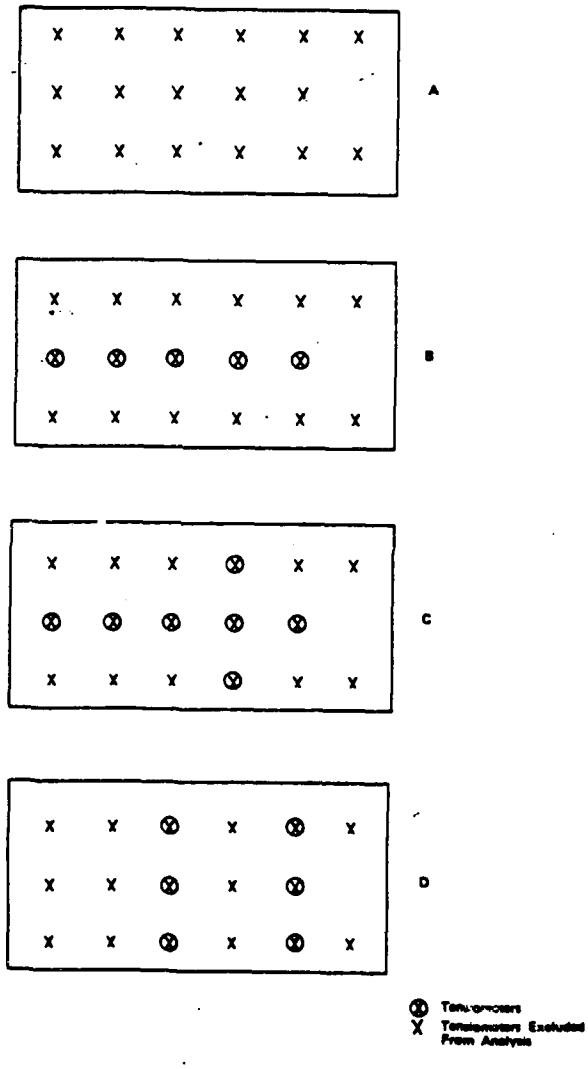

Figure 5.6. Diagrammatic plot of tensiometer sampling schemes for convergence plots in Figure 5.7.

tested to optimize the monitoring procedures. In case B, the middle row of tensiometers have been omitted. In case C, the middle row of tensiometers together with the central tensiometers on the upper and lower rows are excluded. Finally in sample D, the tensiometers parallel to the slope gradient on the lower part of the upstream spur and immediately downstream of the hollow are removed.

Figure 5.7 summarizes the results obtained for each of the sampling frames for the storm period 13-16 March 1979. This storm has already been referred to and the actual soil water potentials examined (Figure 4.2). For ease of examination therefore only the orthogonals to the total potentials in each case have been mapped.

The full sampling frame A shows the soil water position (13.3.79, 00.00) with convergence into the centre of the hollow and the focus at the foot of the hillslope concavity. At 21.00 on the 13.3.79, the focus has migrated across the hollow and convergence is achieved on the downstream spur. Three days later the pattern has reverted to convergence towards the slope hollow again.

Reducing the sampling frame, we find that grid B provides a very adequate approximation to the grid A pattern. The focus of convergence is observed to migrate across the slope and return to its initial position.

Grid C also gives promising results, but with the tensiometers from the hollow centre missing the focus position is initially displaced further downstream than is the case with grid A. Again the focus migration is observed.

This is not however the case with grid D. Removing the tensiometer on the downstream side of the hollow suggests that the soil water focus is to be found on the downstream spur at all times. Moreover the focus is not observed to migrate. This sample frame therefore indicates the importance of the tensiometer data from t4 of accurate predictions of the focus movement are to be made.

Clearly either grid patterns B or C could be substituted for the original sampling pattern, A, without a significant loss in the data quality. The importance of correctly assessing the soil water potentials on the slopes adjacent to (or between) the spur and the hollow is emphasized by the failure of grid D to indicate the actual soil water potential movements.

5.5. Indirect identification of partial source areas

Complementing direct measurements of saturated partial contributing areas (Weyman 1973,(14) Anderson and Burt 1978)(3) are a series of studies which attempt to identify the partial source areas from topographic, soils and vegetation indices.

For example Latshaw and Thompson (1968)(45) and Simonson and Boersma (1972)(46) showed that soil gleying could be related to soil saturation and Moore (1974)(47) mapped the extent of mottled clay to estimate the distribution of the saturated soil zone (Figure 5.8). Zimmerman (1967)(48) showed that plant species can be good indicators of soil drainage conditions and the broad water regime of an area. In his study catchment, the sedge distribution outlined the minimum extent of the saturated area in the early autumn. Further attempts at indirectly predicting soil water fluctuations were made by Boersma (1967)(49) using a water budget method, and by Nelson et al. (1973)(50) who used multiple regression of a range of meteorological parameters. Dunne et al. (1975)(51) used some of the above methods together with field mapping of the saturated areas during storm events to identify the zones of soil saturation. However, this type of data is obviously only available for limited periods during field visits and more importantly it is restricted to a two dimensional observation of soil saturation. No data could be available of the extent of the saturated wedge upslope beneath the soil surface, nor of the depth of saturation. The depth of saturated areas could be particularly important where materials of different permeabilities are interdigitated. Examination of gleyed areas of soil would require extensive field investigations and again only give a very general guide to the time extent of saturation. This is because gleyed soils infer that the soil is almost permenantly near saturation and of course the saturated area expands and contracts in response to individual storm events over a wider area. Kirkby and Chorley (1967)(21) have shown theoretically that the largest contributions to discharge come from slopes which are concave in both plan and section. This is implicit in the index: a/s

where a = area drained per unit contour length

s = slope angle

and has been used by Kirkby (1976)(52) and Beven and Kirkby (1979)(53) to identify the hollow slope areas which are then assumed to saturate preferentially.

In steep sloped areas Anderson and Burt (1978)(3) and Beven (1978)(43) have shown empirically that concave hollow slopes do saturate preferentially and are the major source of throughflow discharge. In such areas the soil water movement process is controlled by the evelation potential and therefore the soil water focus must be directed into the hillslope concavities. However in more gentle topographies the dominance of the elevation potential is reduced

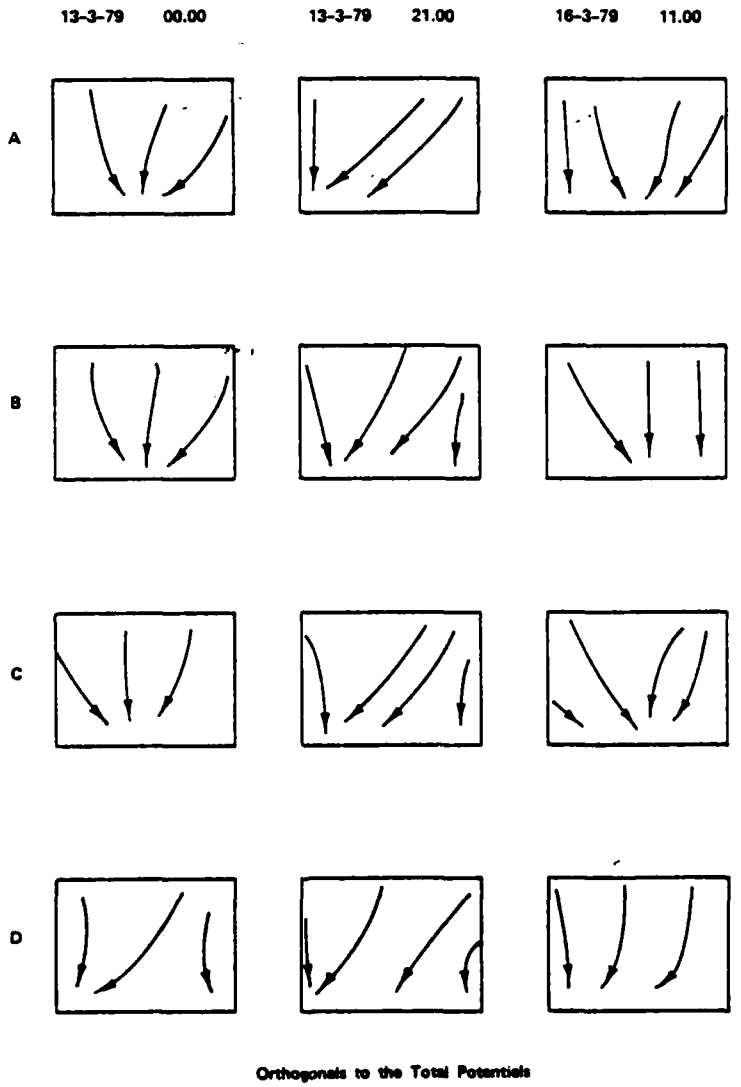

Figure 5.7. Convergence plots from tensiometer configurations shown in Figure 5.6.

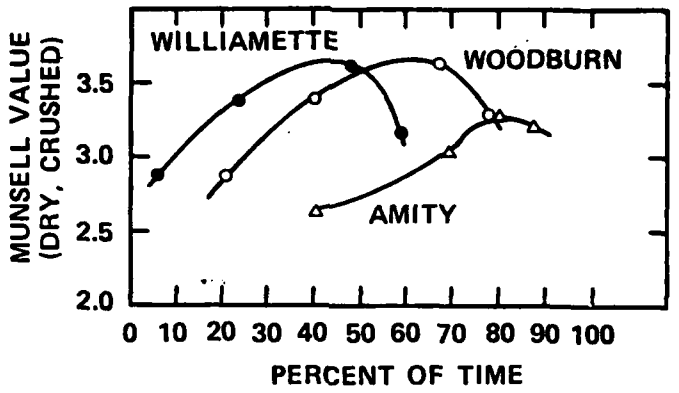

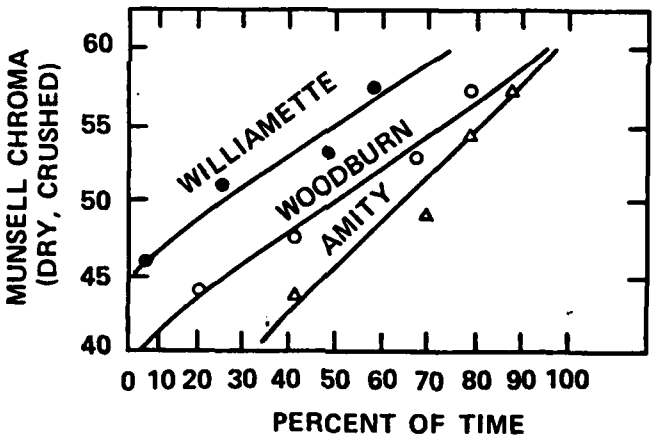

AVERAGE MUNSELL VALUES/CHROMAS

- ● A1 or Ap
- ○ A2 or B1, B2
- △ B3 Horizons

Figure 5.8. Relationships between percent of time soil is saturated and Munsell values and chromas.

and the local topography is considerably less of a control. This has been shown to be the case on the study catchment where the focus of convergence is migrating across the slope after the end of precipitation.

Looking in detail at examples of the use of topographic indices Figure 5.9 shows the Sleepers River experimental watershed studied by Dunne (1969)(44) the a/s isoline is seen to accord reasonably well with the mapped saturated area at the end of a 46 mm storm event. However on this catchment where varved lake deposits are overlain by highly permeable sands, the concave hollows are naturally closer to the underlying clays and intercepting the water table at this level. The permeable sands would drain relatively fast so that saturation partial areas cannot be expected on the upper slope areas. The spatial extent of the partial source areas are therefore a function of both geological structures and slope topography, suggesting the interpretation of a/s results must take account of factors other than topography above.

Beven and Kirkby (1979)(53) in the development of a simple lumped parameter model identified a further topographic index. It is necessary here to follow the derivation in order that the assumptions implicit in the index are clear. The discharge through the soil (Q) for point i in a basin, for which the area drained per unit contour length is A, and the local slope angle B is given by:

$$Q = K_o \exp(Si/M) \tan B$$

were M is a constant, and Si is soil water storage.

and where $Q = K_o \tan B$, when $S = 0$

Now $Q = IA = K_o \exp(Si/M) \tan B$, where I = rainfall rate, and thus

$Si = MLn(IA/K_o \tan B)$.

The saturated area is where $Si > ST$ (the maximum soil water store) or

$A/\tan B > K_o/I \exp(ST/M)$

There are two assumptions in this analysis which are of significance:

(1) that the hydraulic gradient equals the local slope angle B

(2) that the maximum soil water store (ST) is spatially constant.

It is likely that 1. represents less of a restriction on the analysis application than 2. - this I have discussed elsewhere (54). Thus Beven and Kirkby propose that high values of the index A/tan B or In (A/tan B) should be associated with zones of more frequent saturation than areas of a watershed having lesser values. It is necessary to examine the performance of this index in watersheds that have been surveyed in detail and have had detailed records kept of the principal soil water and surface water zones. Figure 5.10 illustrates

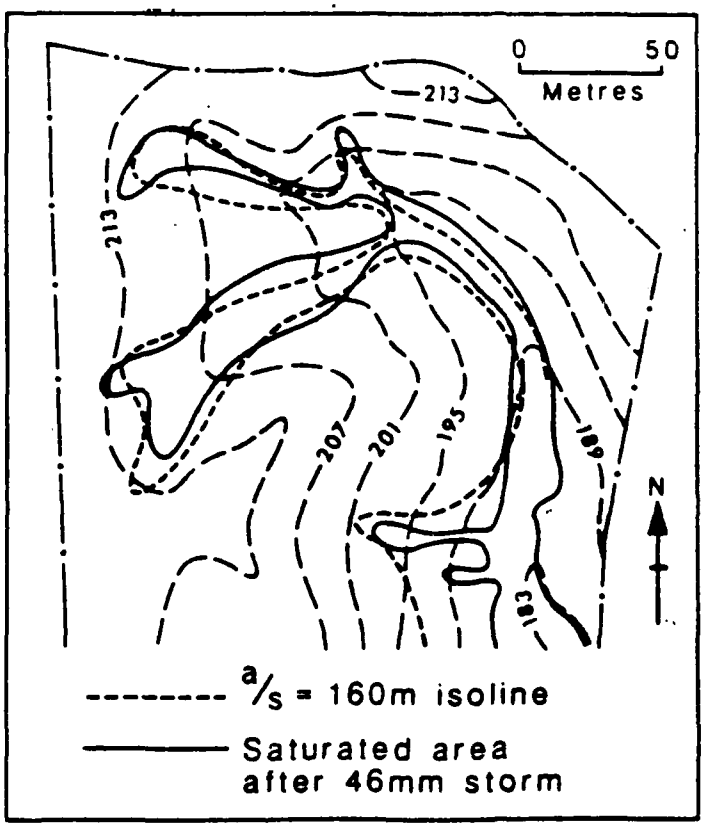

Figure 5.9. Relationship between a/s and saturated areas for a Vermont watershed (after Kirkby, 1978)(55).

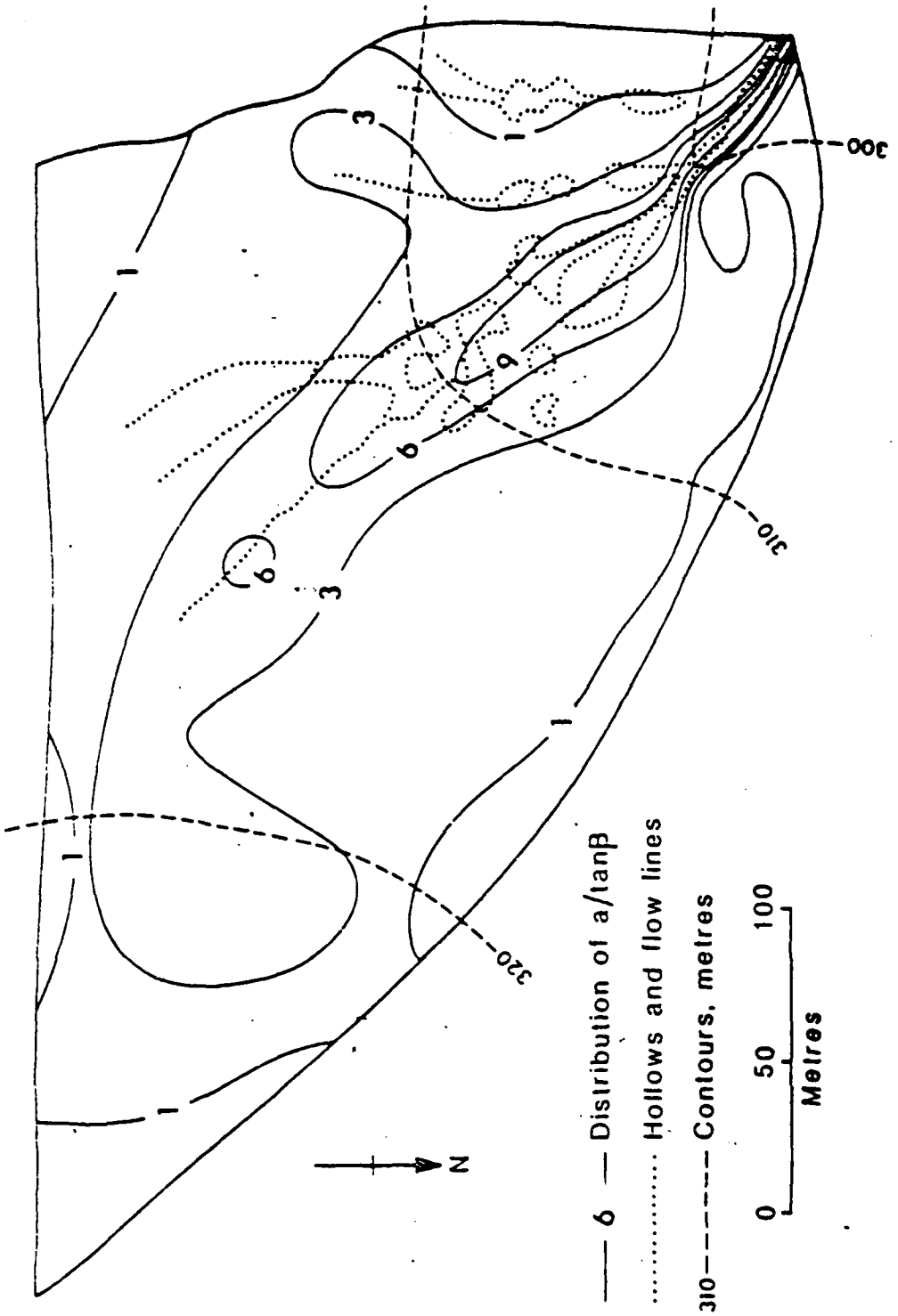

Figure 5.10. Relationship between a/tan B and hollow and flow lines (after Kirkby, 1976)(52).

such a plot of the index for the East Twin Catchment, Somerset, England. In addition Figure 5.11 shows plots of In (a/tan B) for the shallow Winford slopes (6°) (this study) and the steeper slopes at Bicknoller (26°) both of which have hollow and spur topographies. The continuous recording of soil water potentials at both of these sites, over two year periods in each case, allows the maximum upslope extent of the zero pore water pressure line at 80 cm depth to be plotted.

In the 26° slope case the relationship between the maximum saturation pattern and the topographic index is clearly very much better than in the 6° slope case.

Clearly the problem is in deriving indices for soil saturation identification in shallow sloped areas, where the focus of soil water movement is not constant. By their very nature, low lying slopes are likely to be used agriculturally so that indirect vegetation and soil identification, despite all their advantages, cannot be substituted. In addition, the channel gradient can have a significant control on the distortion of flow lines away from the centre of a hillslope concavity if the downstream gradient is large enough.

5.6. Summary

The empirical work reported in this chapter has illustrated several different aspects of the problem of identifying detailed source areas of hillslope discharge in shallow topography:

(i) the dominant effect that soil water potentials can have upon the total potential net. Hence soil water movement convergence zones shift during storms as the soil water potentials themselves change. There is no simple association therefore between zones of convergence and hillslope hollows in shallow topography.

(ii) the prediction of the convergence zone spatially was shown to be a complex function of anticedent precipitation and time after the storm event, (Section 5.3). (This relationship merely reinforces (i) above and is not intended as anything more than supportive evidence since the actual relationship coefficients are in no sense general).

(iii) simple topographically based indices a/s and In (A/tan B) fail to predict the zones of soil water convergence in shallow topography. In the latter case this is of interest since it illustrates the two assumptions by which that index is derived, are invalid. (See Section 5.5). Accordingly it is

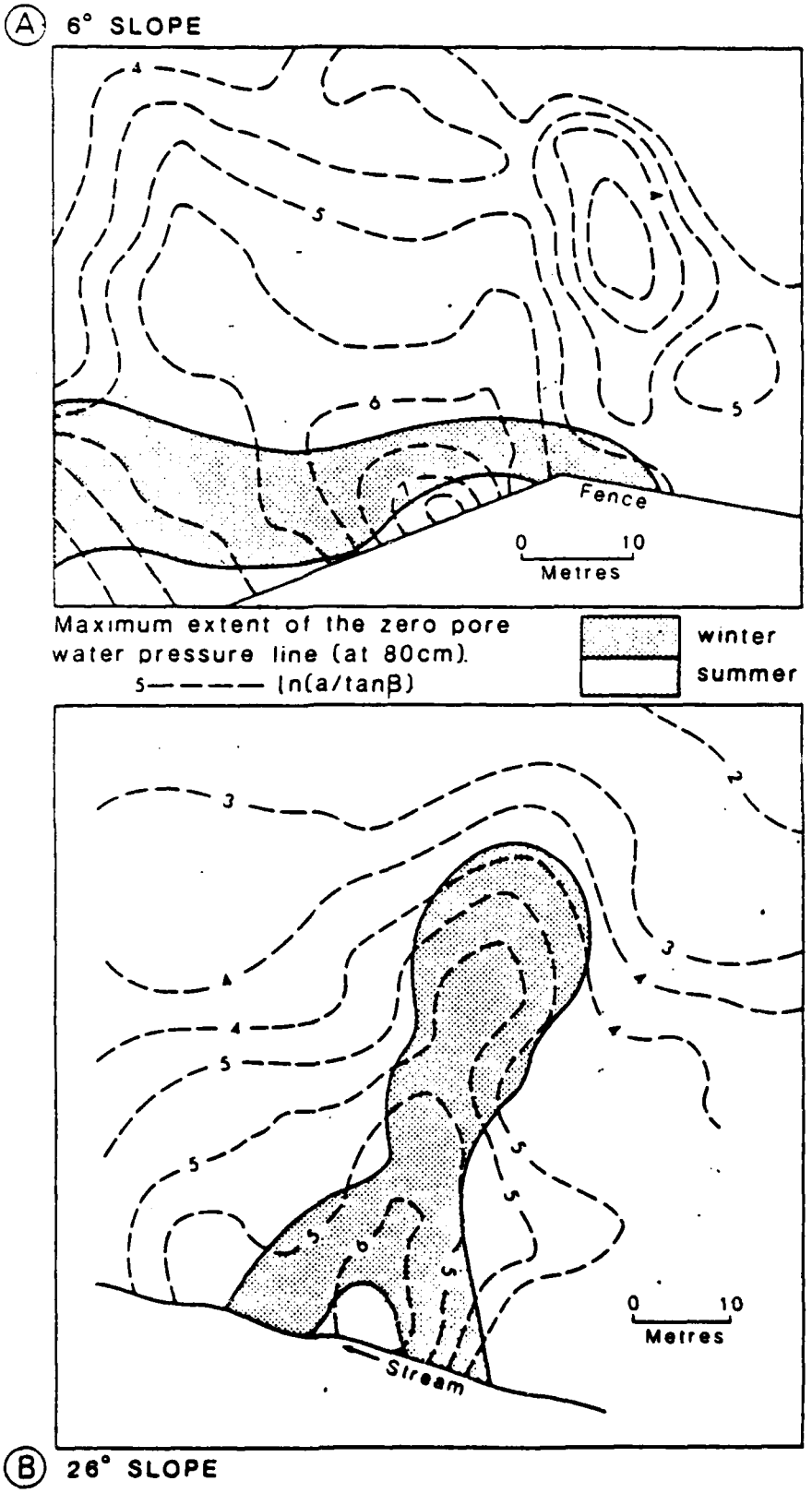

Figure 5.11. Relationship between a/tan B and zero pore pressure line for shallow 6° slope (Figure 3.1) and 26° slope detailed in Burt (1978)(19).

evident that such simple topographic indices cannot hope to provide predictions of saturated areas in shallow topography because of (i) and (ii) above.

(iv) given the complexity of soil water movement and patterns in shallow topography, their generation and prediction is seen to be only possible by simulating the actual soil water processes, thus circumventing certain of the basic assumptions of index measures (attractive as they of course are in being capable of being extracted from topographic maps; e.g., their static nature and assumptions of equality between topographic slope and hydraulic gradient). Thus Chapter 6 is devoted to the establishment of a simulation model which seeks to define conditions that lead to soil water convergence patterns on hillslopes with a wide a variety of start conditions.

PART III

Chapter 6

Modelling Soil Water Movement on Hillslopes

6.1. Introduction

Empirical evidence has been presented to show two contrasting soil water conditions on hillslopes. Firstly, where the soils are permeable (1×10^{-3} cm sec^{-1}) and the topography is steep (30°) soil water conveyance is shown to always occur into hillslope hollows irrespective of antecedent conditions (Anderson and Burt 1977)(2). Secondly, for a shallow topography (6°) with less permeable soils (1×10^{-5} cm sec^{-1}) is has been shown that the focus of soil water convergence may oscillate across hollow-spur topography, inducing, in extreme cases, higher soil water potentials on downstream spur location than in the hillslope hollow centre (Chapter 4). Available evidence from these two sources indicates that while, during the storm event itself, there is near uniformity of response in terms of hollow convergence, it is the drainage characteristics that differ significantly.

This chapter, by the application of a drainage simulation model, seeks to determine the nature of the thresholds for the initiation of the higher soil water potential zones. It is evident that the two principal factors that interact in this context in hollow and spur topographies are hydraulic conductivity and hillslope angle, based on the empirical evidence referred to above. However, it is of particular interest to be able to isolate

a. those conditions of hydraulic conductivity and slope angle that, following storm cessation, maintain down-hollow soil water convergence, and those conditions that maintain cross hollow-spur movement, and

b. those conditions of hydraulic conductivity and slope angle that, on drainage, occasion high soil water potentials in the hollow centre, and those that give rise to higher values on the downstream spur.

While instrumented hillslope sites can provide an important base from which this work can begin, the combination of parameter requirements necessary to identify threshold values of hydraulic conductivity and hillslope angle are too large to be examined empirically. Accordingly, this investigation is based

upon a drainage simulation model, calibrated and tested from data obtained in the study reported by Anderson and Kneale (1982)(54), and Chapters 4 and 5 in this report.

Previous work in this field has been more concerned with estimating peak hillslope discharge by means of simulation (Beven 1977(56), Freeze 1978)(57) than with an examination of control thresholds on hillslope soil water status during drainage. The contention here is that if it can be shown that a wide range of specified circumstances can induce soil water flow paths to migrate across slope with attendant changes in the soil water potentials, then it may be possible to be more specific concerning the true location and controls of variable source areas during recession.

6.2 Simulation procedure and experimental design

The equation determining the flux from one point to another in the soil is

$$F = K \text{ grad } \emptyset \qquad (6.1)$$

where F is the flux of moisture per unit area
K is the hydraulic conductivity
and $\emptyset$ is the total potential.

If K was known throughout the entire hillside and for all moisture states, then the flux could be predicted at all points. However, hydraulic conductivity is not constant but varies with soil moisture content (θ). Campbell (1974)(39) illustrated a method of determining unsaturated hydraulic conductivity directly from the moisture retention function and a single measurement of hydraulic conductivity at some water content. If the moisture retention function can be represented by:

$$\Psi = \Psi_e \, (\theta/\theta_s)^{-b} \qquad (6.2)$$

where Ψ_e is the air entry water potential
θ_e is the saturated water content
Ψ is the soil water potential

then the hydraulic conductivity is given by

$$K = K_s \, (\theta/\theta_s)^{2b+3} \qquad (6.3)$$

where K_s is the saturated hydraulic conductivity.

The moisture retention function is well known to contain hysteresis dependent upon the anticedent wetting and drying states (Poulovassilis 1962)(58). However, certain writers have ignored such hysteresis in the establishment of initial modelling thresholds as distinct from specific accurate numerical simulations (e.g., Hillel 1977)(59). In any case, the argument for not incorporating hysteresis is that the concern here is with simulating drainage only. Having established the moisture retention function on the drying cycle, together with K_s, then it is possible to predict θ and K for given values of ϕ and hence predict the flux F.

The initial conditions requiring specification are the initial ϕ, K_s, depth of each cell, distance from cell midpoint to cell midpoint, the moisture retention function, and the utilization of the Campbell method for obtaining K. Clapp and Hornberger (1978)(60) and Brakensiek (1979)(61) have commented on the applicability of the Campbell procedure, which, among other requirements, necessitates that since equation (6.2) describes the moisture retention function for the soil, the data points plotted on a log-log scale should produce a straight line with slope equal to -b. If this condition is not met equation (6.3) will not produce valid estimates of K.

Following other similar simulation formulations, and especially that of Hillel (1977)(58), a number of dynamic conditions can be specified:

a. The volume of water in each cell is the time integral of the net flux (difference between influx and outflux).

b. θ is the ration of the water volume to the cell volume per unit area.

c. Total potential $\phi = \Psi + Z$. (Z is elevation above arbitrary datum)

d. Average hydraulic conductivity (AK) for flow through boundary I between adjoining cells I and I-1 is weighted according to their length L.

e. The bottom boundary is taken as an impervious plane, the upslope boundary as the divide and the downslope boundary is the channel.

f. the flux between each cell follows Darcy's Law in discrete form:

$$F = \frac{\phi_1 - \phi_2}{L} AK \qquad (6.4)$$

AD-A118 687 BRISTOL UNIV (ENGLAND) F/G 8/8
THE ROLE OF HILLSLOPE HOLLOWS IN GENERATING RIVER DISCHARGE.(U)
APR 82 M G ANDERSON. DA-ERO-78-G-104
UNCLASSIFIED NL

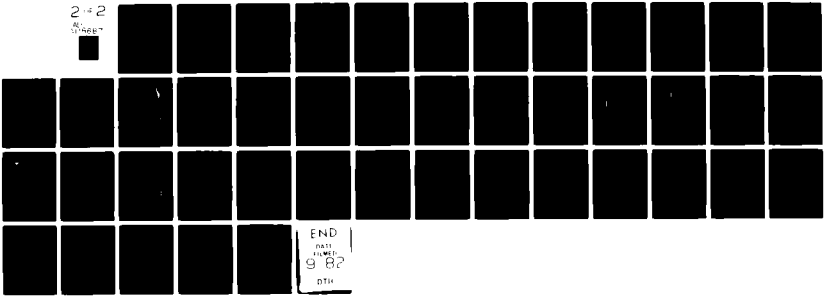

g. The change in water content for each cell obeys the continuity equation, providing a return entry in (a) above entering into the determination of water volume at the next time increment.

At this point the revised estimates of $\emptyset$ and K are made based upon the empirically fitted equations (2) and (3). In the application of the model, the grid size and configuration found to be sufficiently precise and conservative of computational time was one cell deep (1 m) and 63 (9 x 7) 10 m square cells in plan on the instrumented site. In the simulations undertaken a variety of time step increments were used ranging from 300 to 3×10^5 secs with drainage being simulated to 1000 hours (approximately 42 days) from start.

Figure 3.1 shows the nature of the shallow topography for which detailed soil water potential data is available as outlined in Anderson and Kneale (1980, 1982)(24)(54) and Chapters 4 and 5. From the contours shown it is evident that there is only a very slight departure from a pure planar slope, but this departure, although slight in the center and lower center sections of the slope, is sufficient to induce hollow-spur topographic controls on soil water movement (Kneale 1981)(41). Hillel (1977)(58) has outlined and provided a full derivation of the now general finite difference techniques for flux calculation on a cell basis, based exactly on the above assumptions, and it is this scheme that is followed here. Thus the simulation technique is a simplified version of pre-existing procedures, in that only drainage conditions are considered.

The experimental design for the simulation drainage comprised five principal elements:

a. The procedure was validated on the 6° hillslope sector illustrated in Figure 3.1 for periods for which long recession data on soil water potential was available.

b. This slope configuration was then tilted up through 30° with simulations being undertaken at intermediate slope angles. All remaining conditions of K_s, soil moisture retention function, and start potentials were kept constant.

c. The procedure in b. was repeated with the slope tilted 2° in the downstream direction (referred to below as "asymmetrical" topography).

d. Simulations as detailed in b. and c. were then repeated for varying values of K_s in the range 10^{-6} to 10^{-1} cm sec, with the attendant changes in K (equation (5.3)).

This overall procedure was used to identify those conditions of hydraulic conductivity and slope angle which occasion significantly different soil water convergence patterns and soil water potential values as outlined above.

6.3. Catchment Details and Instrumentation

The principal catchment details have been fully described in two previous papers (Anderson and Kneale 1980 and 1982) (24, 54) and Chapter 3 and it is only necessary here to outline elements pertinent to the simulation study. Figure 6.1 illustrates the moisture retention function for the clay loam with $K_s = 1 \times 10^{-5}$ cm sec^{-1} to 1.0 m depth being determined by both laboratory and field determinations (Kneale 1981)(41). Immediately below this depth, K_s decreased to 1×10^{-9} cm sec^{-1}, effectively thereby representing an impermeable lower boundary. On the 90 m by 70 m hillslope sector a network of 44 tensiometers continuously recorded soil water potentials at 50 cm depth of a transducer-chart recorder system (Anderson and Kneale 1980)(24). Such data in providing an accurate and continuous record, provides and ideal base for the evaluation and testing of the drainage simulation model.

The topographic slopes, both within the instrumented sector and elsewhere within the catchment were in the 6-8° range, with the landuse being pasture (Chapter 3). The principal storm and anticedent conditions used as starting values for the drainage simulation illustrated below related to the storm of August 1978, full details of which are given in Chapter 4. This storm was selected for presentation because the long 1-month recession that followed would allow a full assessment of the drainage simulation to be made. The model, however, was also run successfully on other, shorter duration, recessions.

6.4. Simulation Results

Model verification

Figure 6.2 shows the simulation of drainage for a storm on 6 August 1978, whilst Figure 6.3 shows a similar simulation commencing on 1 August 1979. Examining both of these simulations, the results accord well with the observed data. At the base of the slope the observed 0 cm soil water potential contour is not coincident with the predicted line approximately 1 month after the start of drainage. The discrepancy at that time is less severe than it appears in the figure since the maximum error (predicted-observed) is 20 cm of water in this

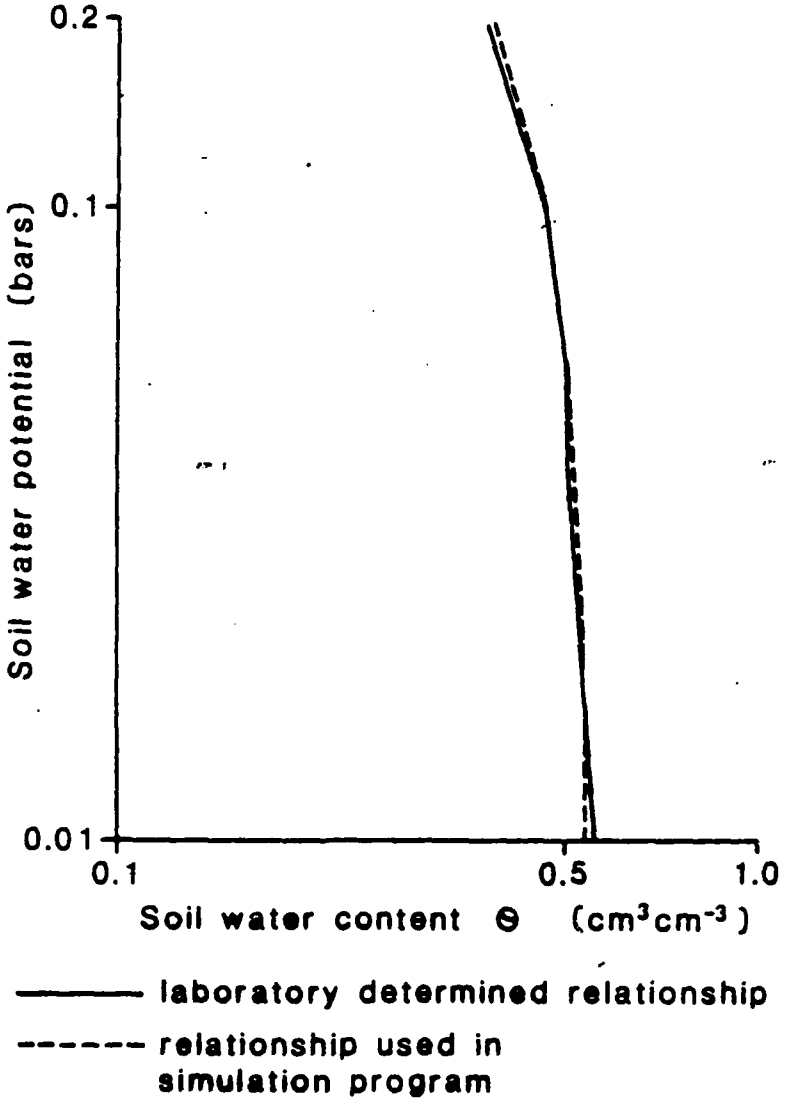

Figure 6.1. Field soil moisture retention curve together with the approximated relationship used in the simulation model

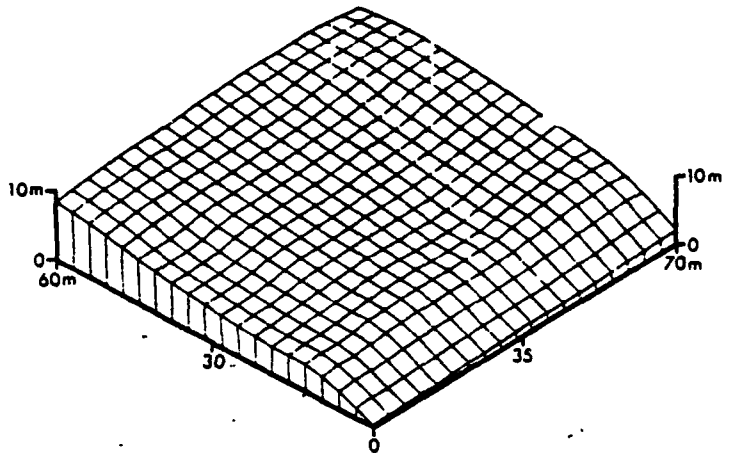

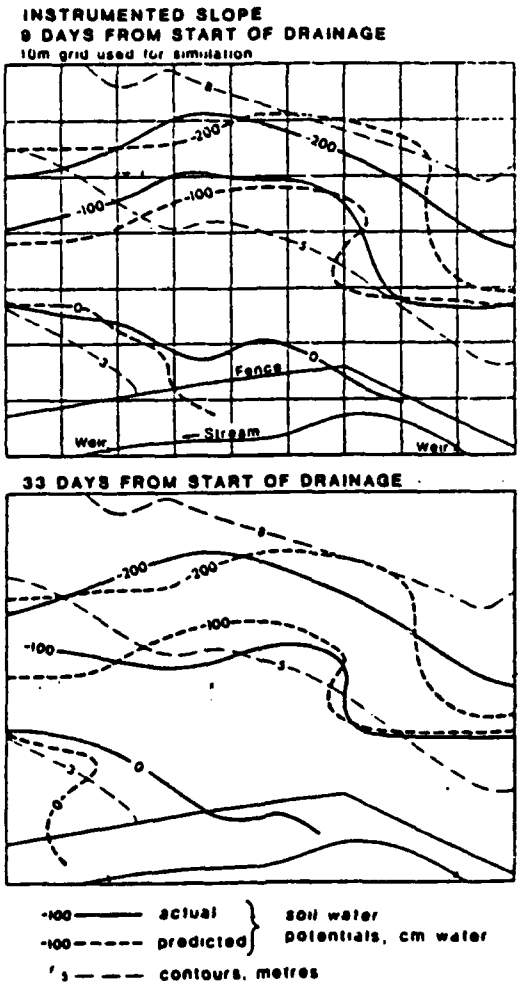

Figure 6.2. Drainage simulation (with start date 6 August 1978) together with measured soil water potential data. The simulation grid frame is also shown.

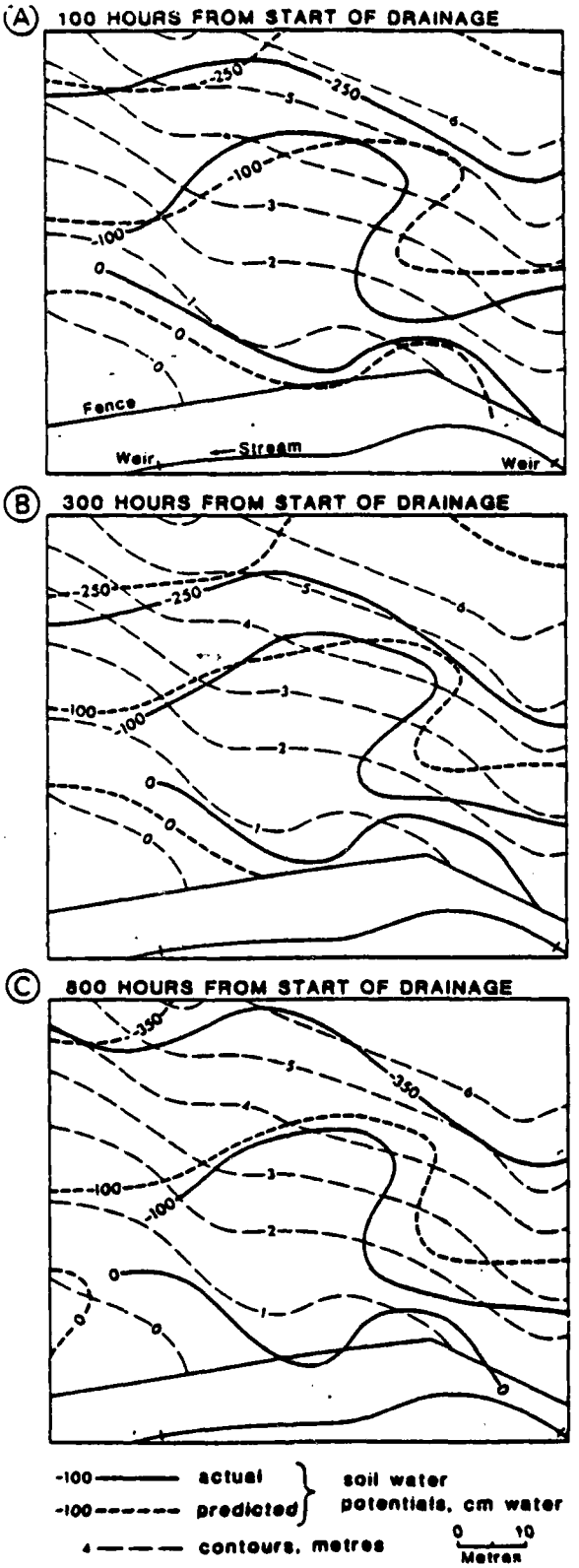

Figure 6.3. Drainage simulation (with start date 1 August 1979) together with measured soil water potential data.

region of the hillslope. Similarly, with Figure 6.3c, the predicted values in the vicinity of observed values of -350 cm, are -320 cm. The salient point here is that for 91 percent of the grid area, the simulated soil water potentials are within a value of ±5 cm of the measured values, and that the figure is maintained for test simulation runs in excess of 30 days. The principal deviations (maximum 30 cm) occur in the top right hand grid cell on the slope. This reflects boundary effects from the immediately adjacent noninstrumented upslope zone and upstream hillslope spur area. This deviation is however confined to this single cell. The evidence therefore suggests the model to be replicatively valid (Zeigler 1976)(62) in that it matches data already acquired. Having used long recession data to validate the model it becomes possible to draw certain limited conclusions from the simulation experiments that follow. These conclusions, as Hillel (1977) observes, must be based on the systematic testing of explicit hypotheses over a realistic range of values of input variables and parameters.

Hillslope angle and hydraulic conductivity changes

Simulation were undertaken for the following conditions:

a. Slope angle: 2°, and then every 3° to 14°, 18° and every 3° to 30° (Figure 6.4 shows the 5° and 30° slopes used in the simulation).

b. $K_s = 10^{-6}$, 10^{-5}, 10^{-4}, 10^{-3}, 10^{-2} cm sec^{-1} for each of the above slope angles.

c. A downstream 2° tilt (asymmetrical condition) was imposed on the above initial symmetrical topography start conditions and all above simulations in a. and b. rerun.

Thus, 100 simulations in all were undertaken. From these resulting drainage conditions, the dominant soil water flow paths were calculated (using orthogonals to total potential lines, since infiltration was assumed to have ceased [see Anderson and Burt 1978])(3) and soil water potential data at the key locations of hollow centre and downstream spur abstracted (see Figure 3.1).

Figures 6.5 and 6.6 illustrate the soil water potential status for slopes of 15° and 30° with all the conditions identical to that of the 6° slope (actual) simulation in Figure 6.2. Comparison of these three figures illustrate the enlargement of the zone of 0 cm soil water potential at the slope base as the slope angle is increased, combined with more rapid drainage in upslope locations.

Figure 6.7 illustrates the reversal of soil water conditions, induced by decreasing K_s, that occur on the downslope spur location (5° slope - site 8 in Figure 3.1c). In this zone the draining process gives way to wetting at approximately $K_s = 10^{-4}$ cm sec^{-1}, while the hollow centre (site 10 in Figure 3.1c) is seen to be draining throughout for equivalent conditions. Figure 6.8 and 6.9 and Table 6.1 present summaries of the principal results. In the case of $K_s = 10^{-5}$ cm sec^{-1} the slope is seen to be "safe" against sudden increases in soil water potential until the slope angle is raised to approximately 15°. For angles around and above this value, significant increases in Ψ are seen to occur for all cases except that of the downstream spur location, where the increase is gradual in the case of "symmetrical" topography (0° downstream tilt imposed on the original slope surface).

The effect of tilting the slope by 2° in the downstream direction is shown by the difference between predicted soil water potentials for these cases (asymmetrical-symmetrical). The principal source of difference is in the downstream spur with increased soil water potentials occurring in the asymmetrical topography case, especially with lower hydraulic conductivities (Figure 6.10). The soil water status in the hollow centre is seen to remain relatively unaltered by such tilt effects irrespective of hillslope angle, hydraulic conductivity and time of drainage.

From Figure 6.9 an additional feature worthy of comment, is that for shallow angles the hollow centre has relatively high Ψ, since with a low hydraulic gradient, drainage is slower than angles in the 15-20° range. High slope angles (25°-30°) again see a return to high Ψ in the hollow, this time occasioned by relatively rapid drainage to that zone from upslope areas (this phenomenon is also illustrated by a comparison of Figure 6.5 and 6.6). The summary of results in Table 6.1 holds good irrespective of the time increment used in the simulation model. Model sensitivity to changes in the time increment used, showed that over a 40 day drainage period, changes from 5 minutes to 8 hours as the basic unit showed maximum discrepancies of only 5 cm of water.

We have already observed the potential for stream gradient effects to manifestly 'control' the hillslope soil water convergence processes. However simulations undertaken, increasing the stream gradient from 0° to 3.5° with a range of different soil permeabilities, slope and topography configurations, suggest such gradient effects to be relatively minor. Figure 6.11 illustrates for the

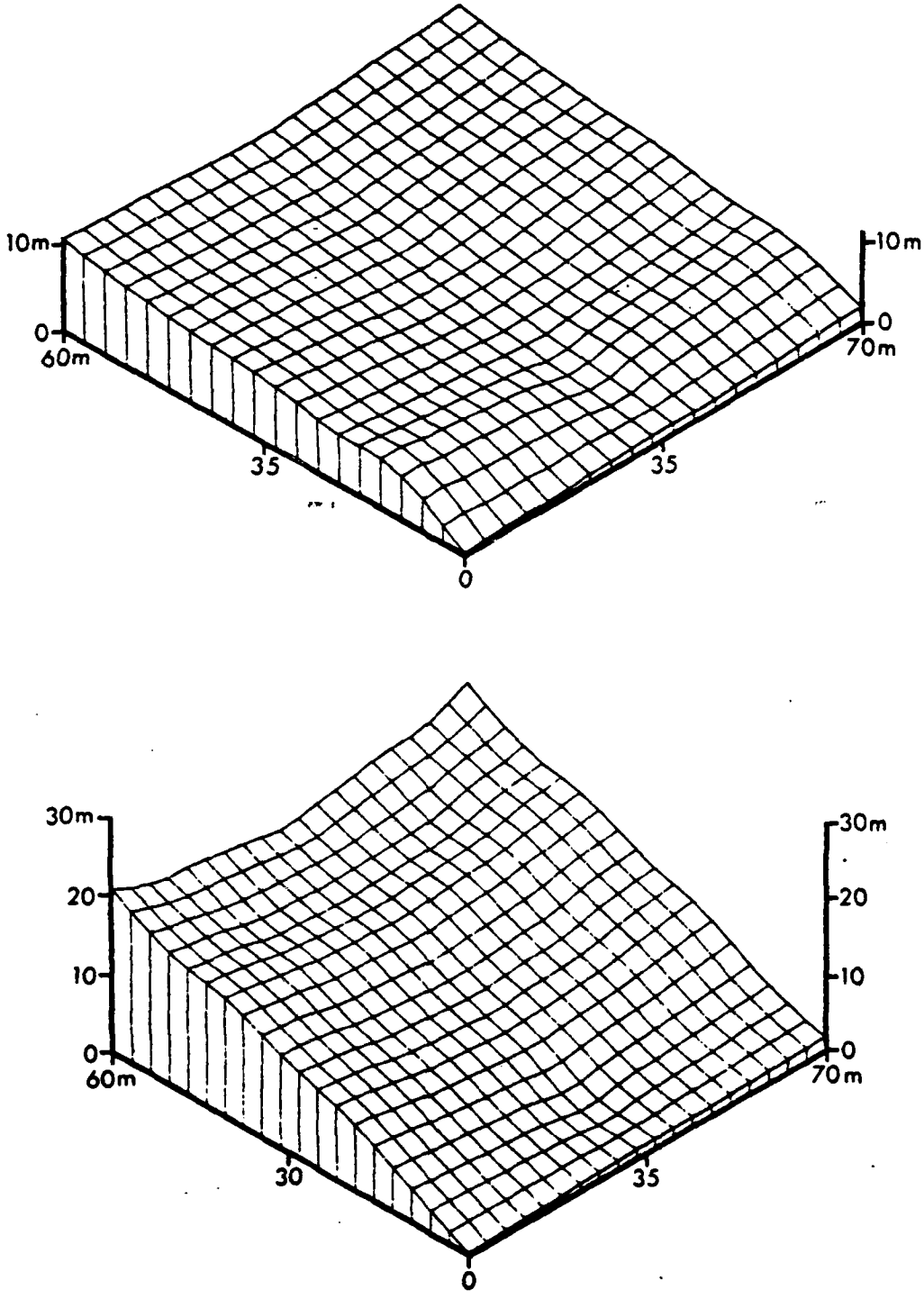

Figure 6.4. The 5^{o} and 15^{o} slopes used in the simulation.

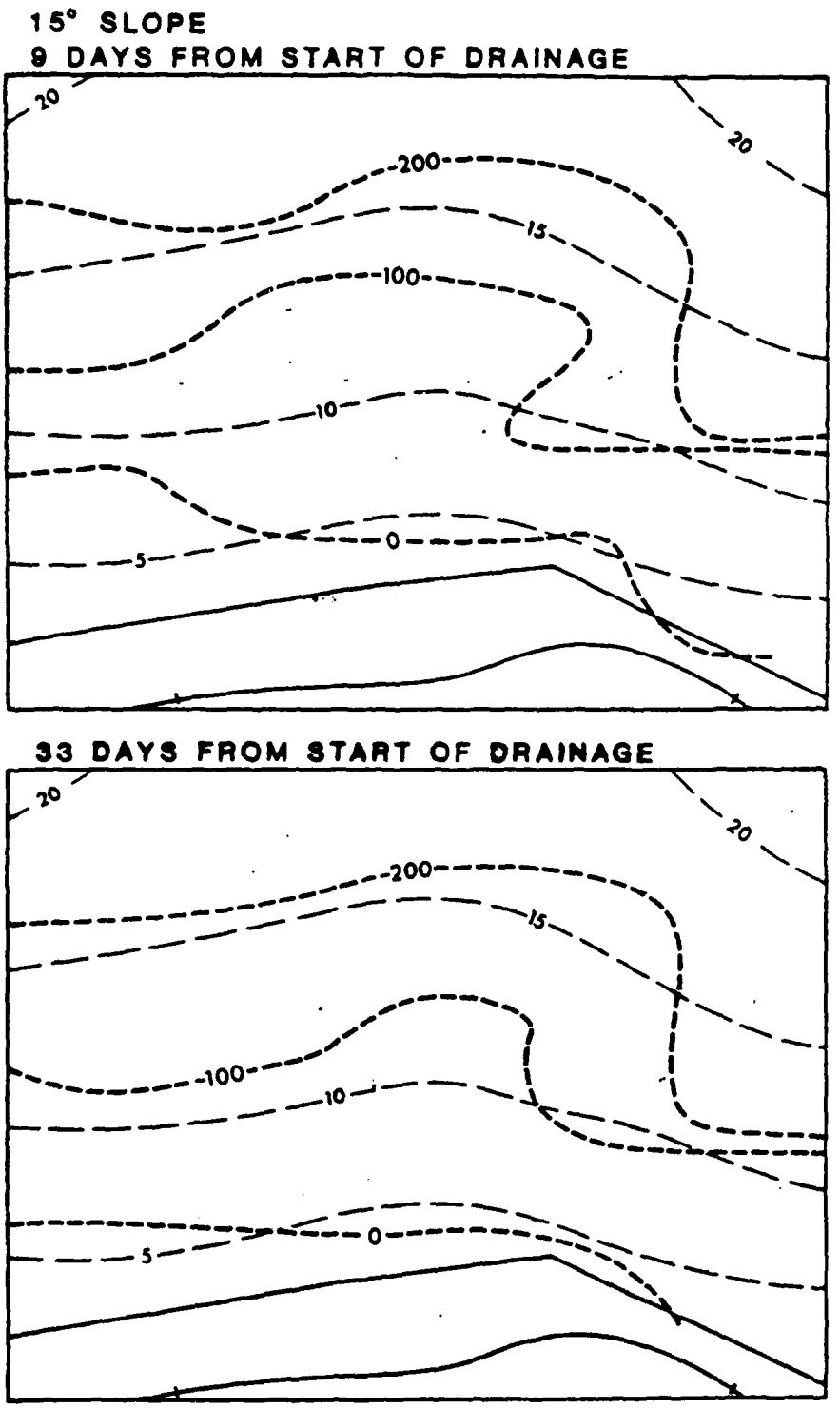

Figure 6.5. Drainage simulation on a hypothetical 15° slope (all conditions otherwise identical to those in Figure 6.2).

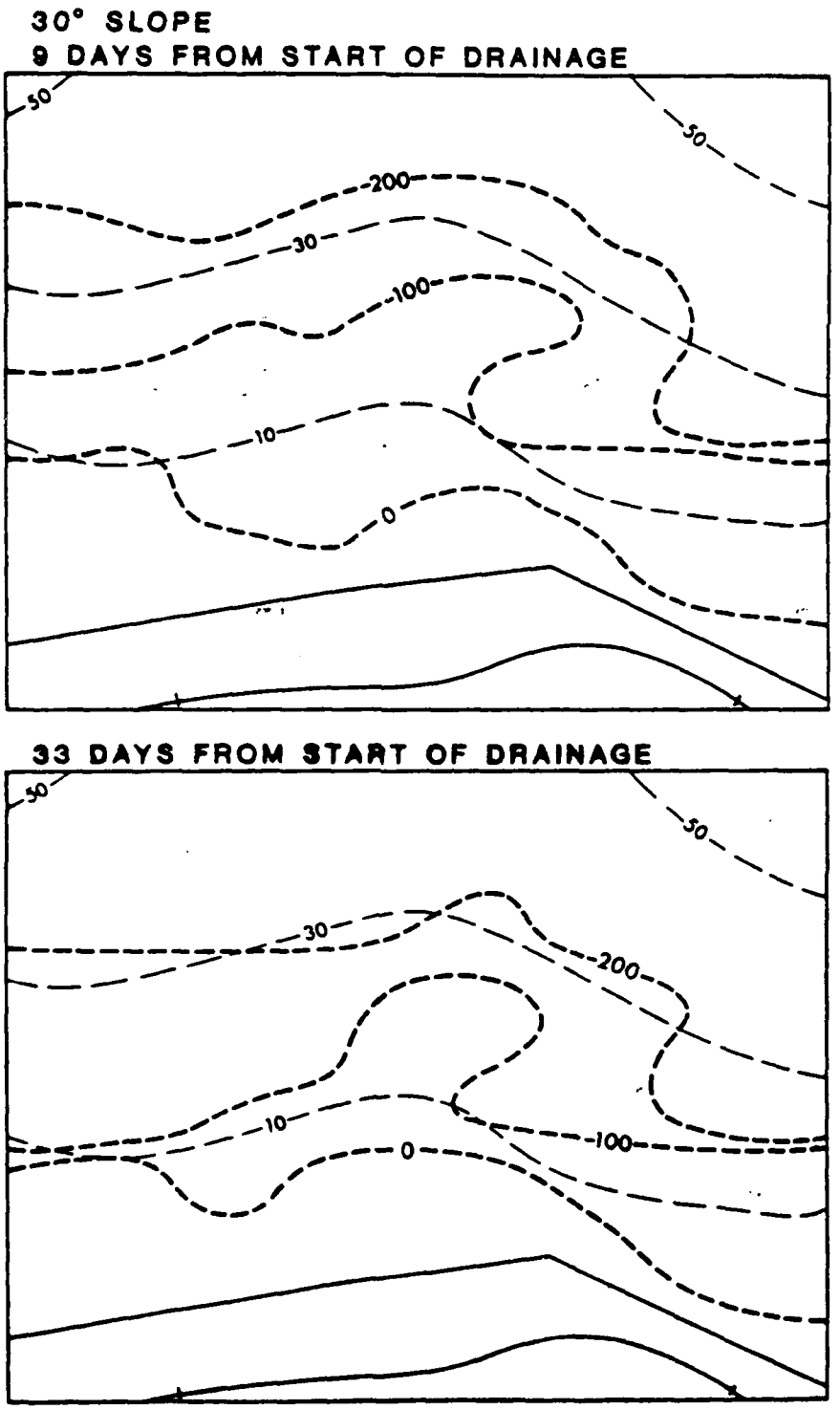

Figure 6.6. Drainage simulation on a hypothetical 30° slope (all conditions otherwise identical to these in Figure 6.2).

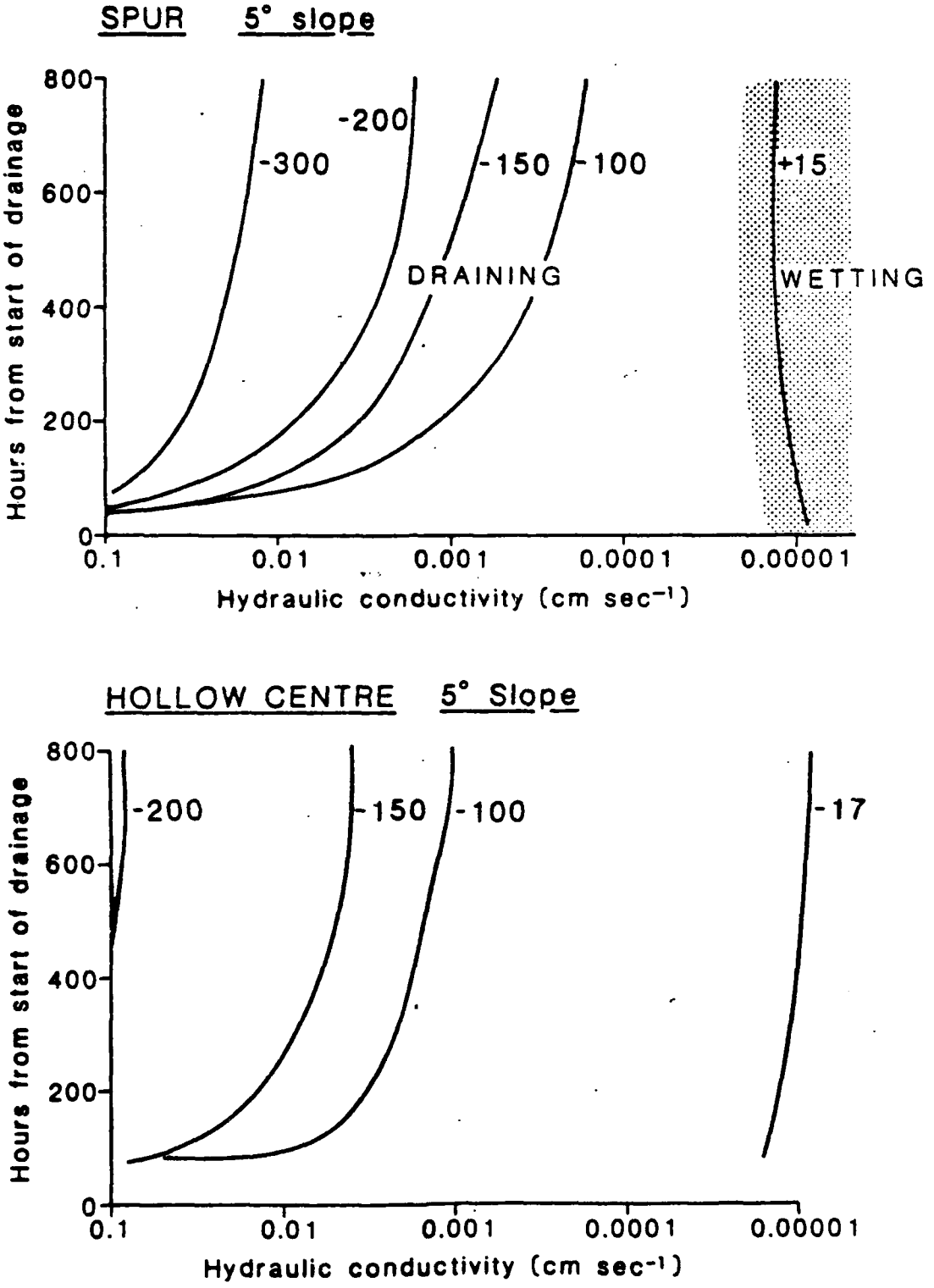

Figure 6.7. Contrasting soil water conditions in the hollow spur (locations 10 and 8, respectively, on Figure 3.1).

stated conditions when $K_s = 1 \times 10^{-5}$ cm sec^{-1}, that the 0 cm soil water potential contour is similar in respective of stream gradient. Soil permeability and slope angle have much greater impacts on the location and extent of hillslope zones of saturation.

In summary, the findings from the simulations (given in Table 6.1) highlight that only in the restricted conditions of high K_s and high slope angle is the soil water flow always into the hollow centre. Secondly, the wide range of circumstances under which it is possible to encounter high soil water potentials at a downstream spur location than in the hollow are illustrated.

Table 6.1

Summary of Simulation Results

Control Variables*		Resulting Conditions		
Slope Angle Range	K (unsaturated hydraulic conductivity defined by equation 6.3)	Dominant Soil water flow path	Downstream spur and hollow Ψ comparison	Remarks
25°-30°	$>10^{-4}$ cm sec^{-1}	always converging into hollow	Ψ highest in hollow	Simulation data confirmed by empirical results (Anderson and Burt 1977)(2).
	$<10^{-4}$ cm sec^{-1}	Cross hollow-spur	Ψ highest in hollow	With 2° downstream tilt, downstream spur continues to "wet up" throughout drainage.
10°-24°	10^{-2}-10^{-6} cm sec^{-1}	Cross hollow-spur but somewhat diffuse flow paths	Ψ highest on downstream spur to 400 hours drainage,	Tilting the slope in downstream direction makes very little difference to drainage rate or to Ψ values for any K_s value.
2°- 9°	$>10^{-4}$ cm sec^{-1}	Always cross hollow-spur	Ψ highest in hollow	
	$<10^{-4}$ cm sec^{-1}	Always cross hollow-spur	Ψ highest on downstream spur	Simulation data confirmed by empirical results (Anderson and Kneale 1982)(54).

* The additional effects of inducing a downstream tilt on the topography are included in the "remarks" column where relevant.

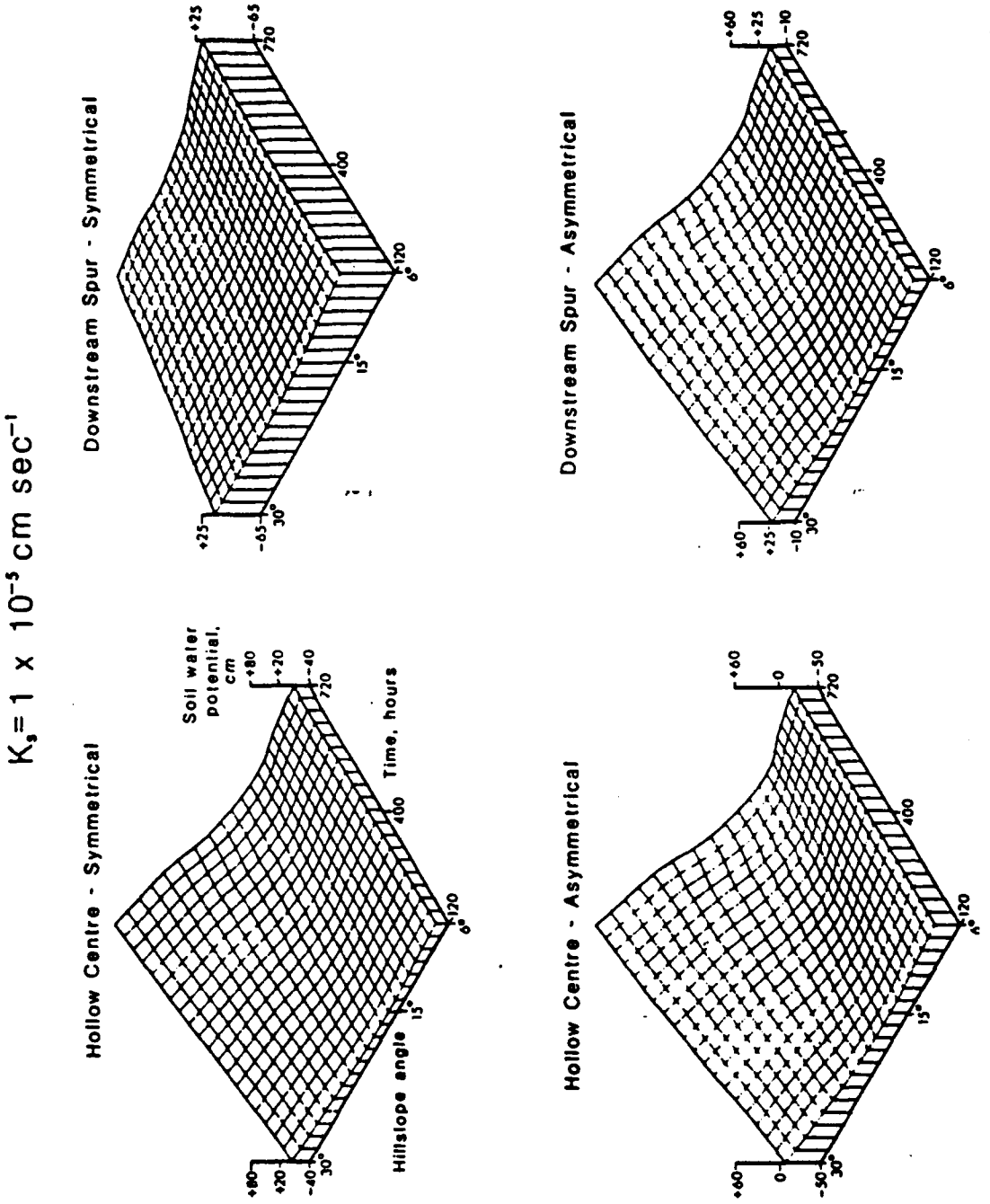

Figure 6.8. Summary of soil water potential responses for simulations undertaken with $K_s = 10^{-5}$ cm sec^{-1} (for spur and hollow location points (8 and 10) - see Figure 3.1).

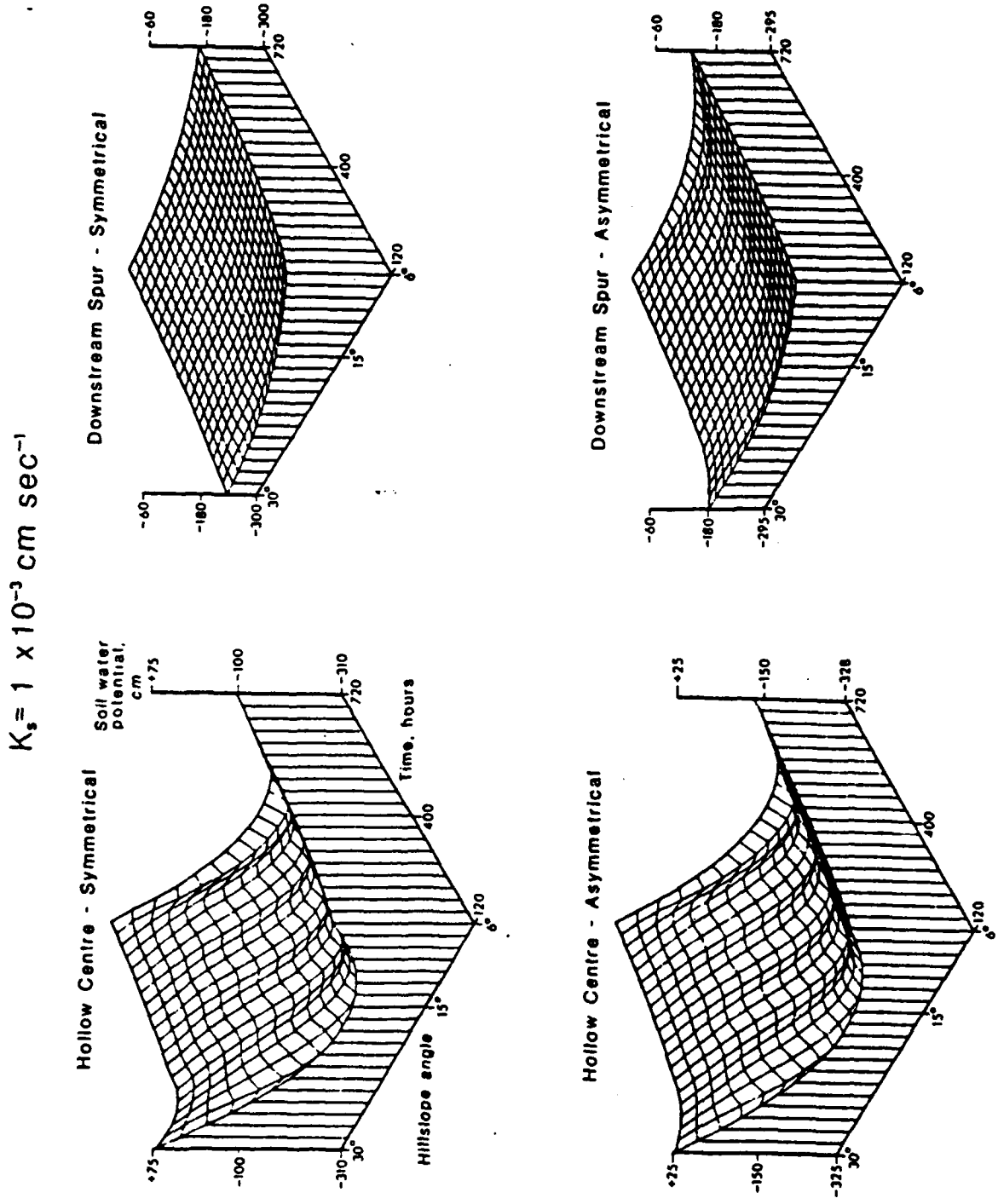

Figure 6.9. Summary of soil water potential responses for simulation undertaken with $K_s = 10^{-3}$ cm sec^{-1}.

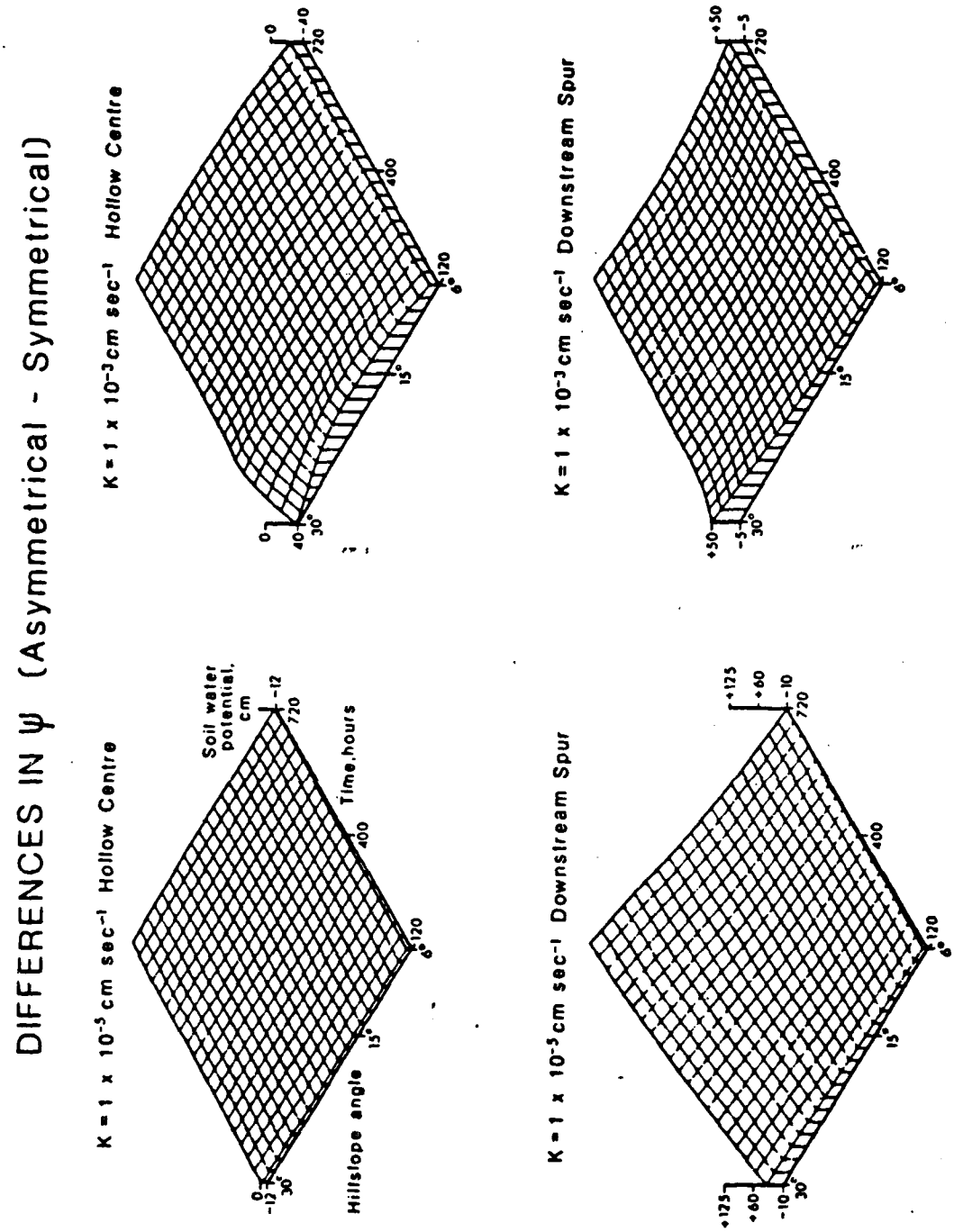

Figure 6.10. Summary of differences in soil water potentials between simulations undertaken with a 2° downstream tilt imposed on original topography (asymmetrical) and the condition of zero downstream tilt (original topography (symmetrical)).

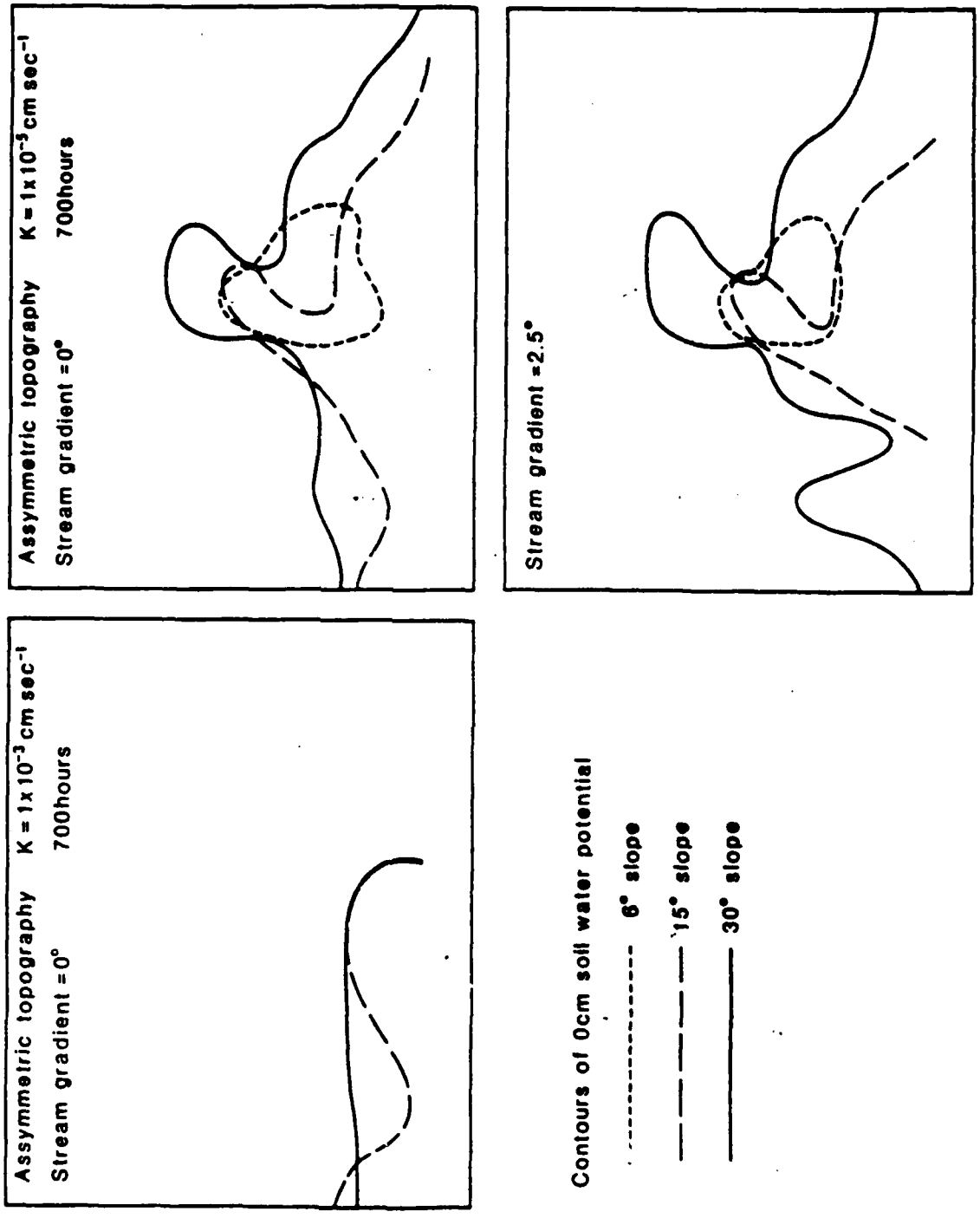

Figure 6.11. Summary of selected simulations to illustrate the effect of different stream gradients on the extent of 0 cm soil water potential contour.

6.5. Discussion

The hydrological implications of the model study, in highlighting certain circumstances in which soil water potential surfaces do not accord with topographic contours has strong implications for the study of hillslope outflow hydrograph source areas as well as for soil water residence time studies. The single tracer study for example, dependent upon the time it is undertaken, may well provide misleading information regarding the dominant soil water flow direction, since several subtle but significant changes of spur-hollow soil water potential balances are seen to occur during drainage. Secondly, the potential margin of error for extrapolation of soil water flow paths and responses in drainage from one topographic-soil property combination to another, is seen to be very large. Coarse differences between those circumstances inducing down-hollow convergence and cross hollow-spur flow have been identified, but within this division the simulation results highlight the particular importance of unsaturated and saturated hydraulic conductivity in the determination of hollow and spur zone soil water potential values.

This chapter has illustrated and validated simulation data that testify to subtle flux changes between spur and hollow sectors that imply fundamental changes in the soil water travel times in the unsaturated zone during recession. Thus, it is possible to comment on Beven's (1977)(56) assertion, (based on a hypothetical data base and finite element simulation) that the unsaturated zone is of fundamental importance in controlling the nonlinear discharge response from hillslopes. While Beven simulated the evident control the unsaturated zone should have, the work reported here provides detailed and verified evidence of the mechanism of that control.

It is these general themes which are seen as the principal findings from the simulation procedure. The drainage simulation results presented omitted potential important phenomena such as spatial heterogeneity and soil moisture hysteresis, although the model has the capacity to include these if required. Secondly, the data used an initial topographic form which was then subjected to tilting both parallel and orthogonal to the stream. A further range of start topographies could be examined. However, the topography used was selected on the basis that it should facilitate the maximum potential soil water movement shifts due to the shallow nature of the hollow and spur topography.

Hillel (1977)(58) has observed that the traditional tendency has been to isolate phenomena and study them separately in arbitrarily disjointed segments of the field environment. While the work reported here has attempted to integrate variable controls in attempting to define particular requirements for differing soil water flow configurations, it is important to recall that refinement of such procedures depends increasingly on the identification of stochastic effects such as local variation in soil parameter values. It is encouraging that work is now being undertaken in just this area (e.g., Sharma et al. 1980)(63) and it is to be hoped that this will lead to refinement of the type of results presented in Table 6.1.

Chapter 7

Hillslope Discharge Contributions - Empirical and Modelling Evidence

7.1. Introduction to empirical evidence

Where there is shallow spur-and-hollow topography, the effect of the movement of the focus of convergence (Figure 5.1) may be to change the timing and volume of soil-water flow (by both overland flow and throughflow) to a much greater degree than in a straight rectilinear slope where there is no comparable convergence.

It has already been stated that the study catchment comprised four readily identifiable subcatchments, two with straight slopes and two with hollow-and-spur topographies (Figure 3.1; Section 3.2). Inflow hydrographs for each of the four subcatchments were examined to ascertain whether such topographically induced variation could be isolated. Figure 7.1 illustrates the typical catchment and subcatchment responses to large storms. Four such large events were selected for analysis. Figure 7.2 shows the unit hydrographs for these events for each of the four subcatchments. The unit storm used was 5 mm in 1 hr. It is clear from Figure 7.2 that the unit hydrograph dimensions are relatively constant in the source to D and B to C subcatchments. Thus the subcatchments with predominantly straight rectilinear slopes produce an essentially constant inflow unit hydrograph. This is in marked contrast to the unit hydrographs for the other two subcatchments where the peak discharge, time to peak and hydrograph base length all show greater variation between storms. Comparison of the mean unit hydrographs (Figure 7.3) for the straight rectilinear subcatchments (source to D and B to C) show them to have a similar time base, but with the steeper sloped area (B to C) producing a greater total discharge. In addition the peak is slightly delayed in this subcatchment with respect to the source to D area.

The derivation of mean unit hydrographs for the A to B and D to C reaches is less satisfactory because of the wider variation between storm responses. However, it is useful to use the unit hydrographs to predict the form of the total stream hydrograph for the full stream length, given the actual and hypothetical topographies. Thus, bearing in mind the variation referred to, Figure 7.4 shows the stream response at weir A for an event of 10 mm in 1 hr.

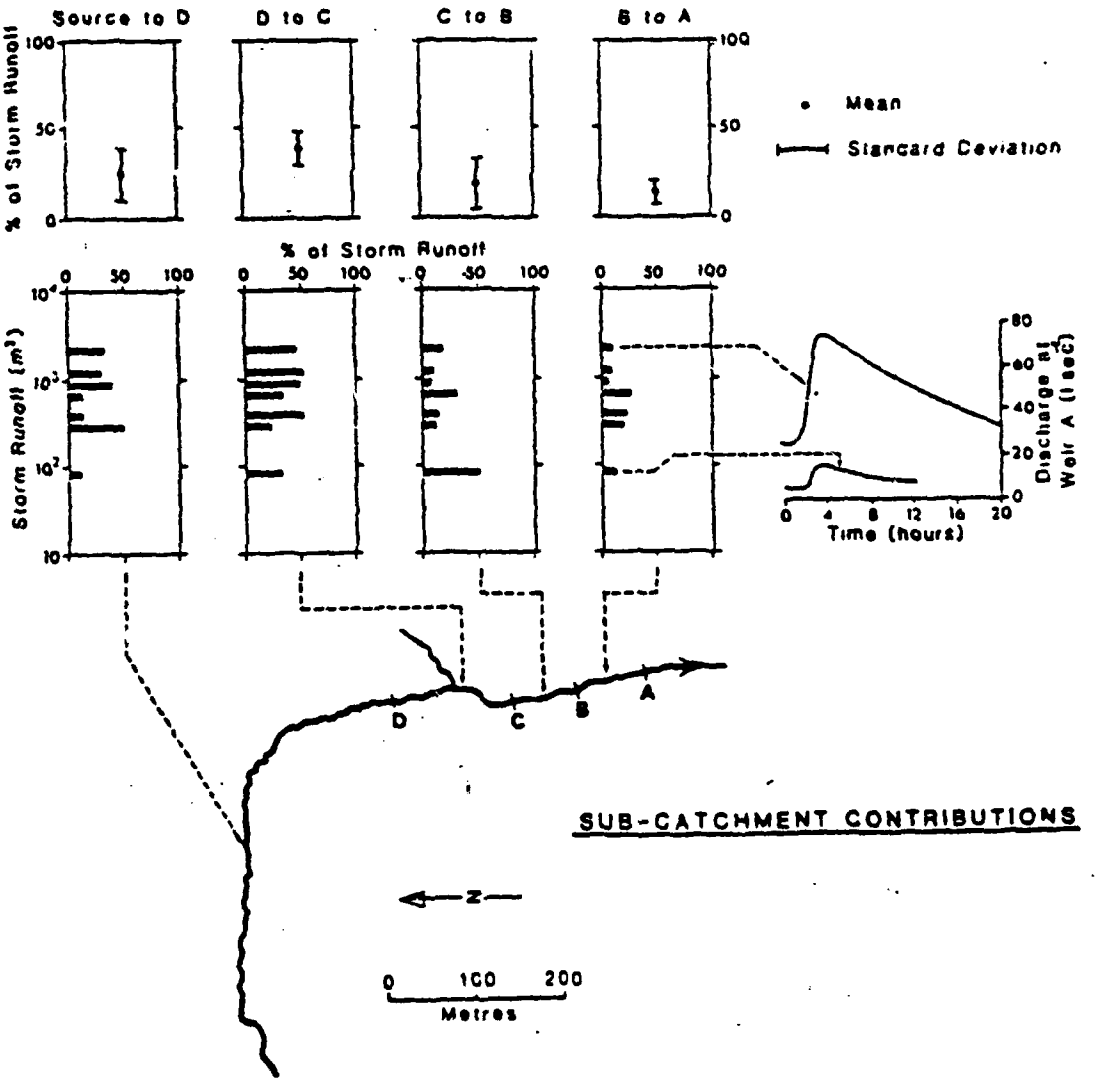

Figure 7.1. Storm runoff for seven winter storm events from each of the 4 subcatchments (Section 3.2).

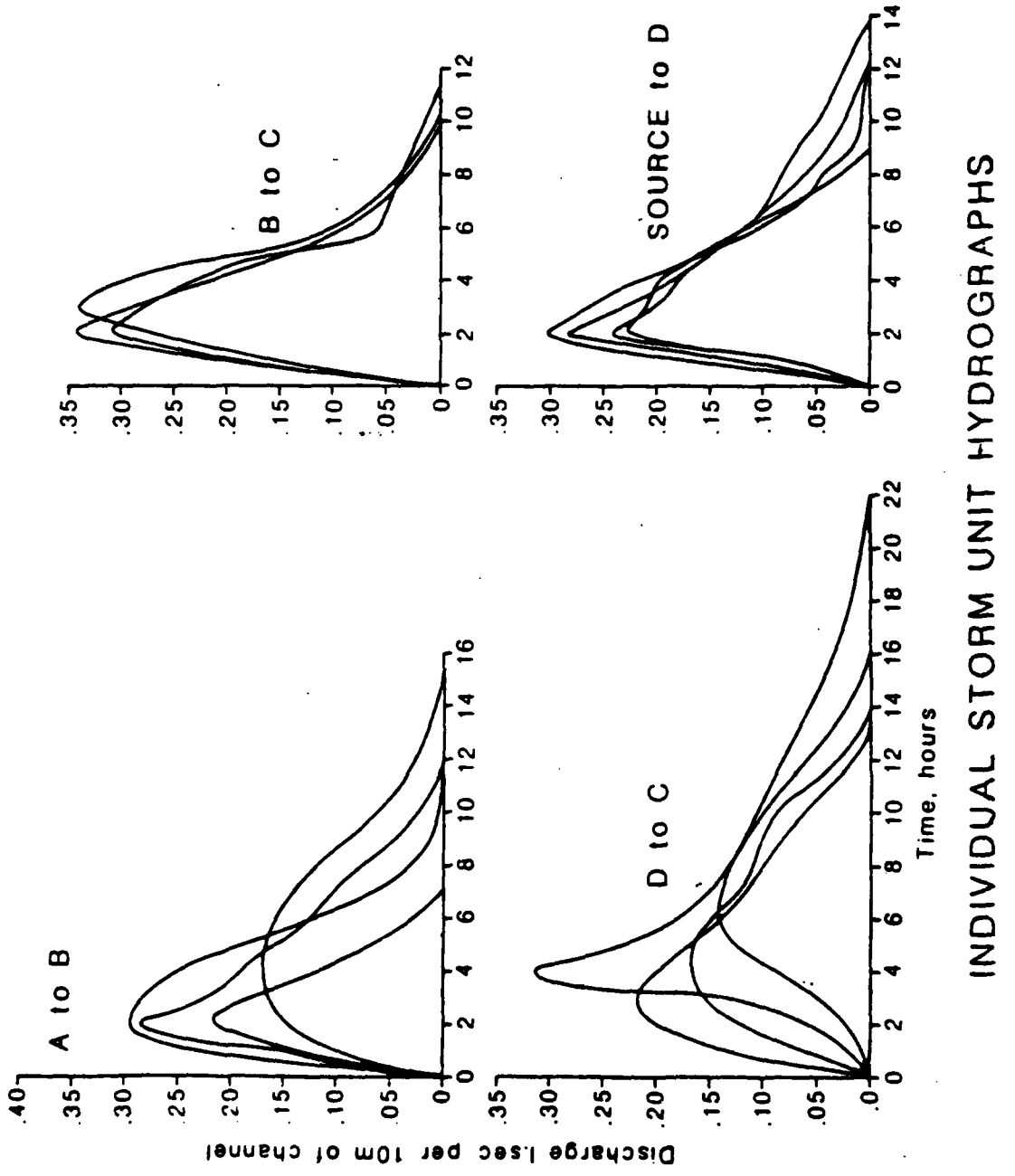

Figure 7.2. Individual storm inflow hydrographs for the 4 subcatchments for 4 large storm events.

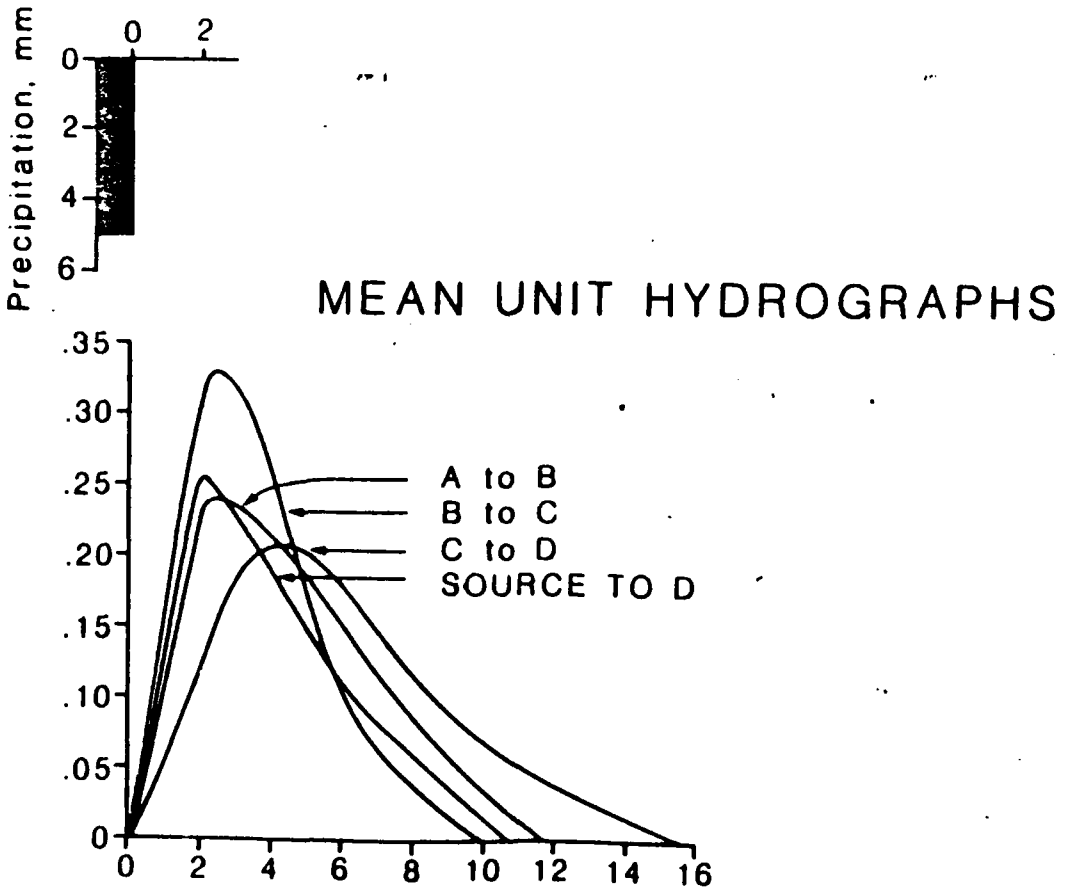

Figure 7.3. Mean unit hydrographs from Figure 7.2 for each of the 4 subcatchments.

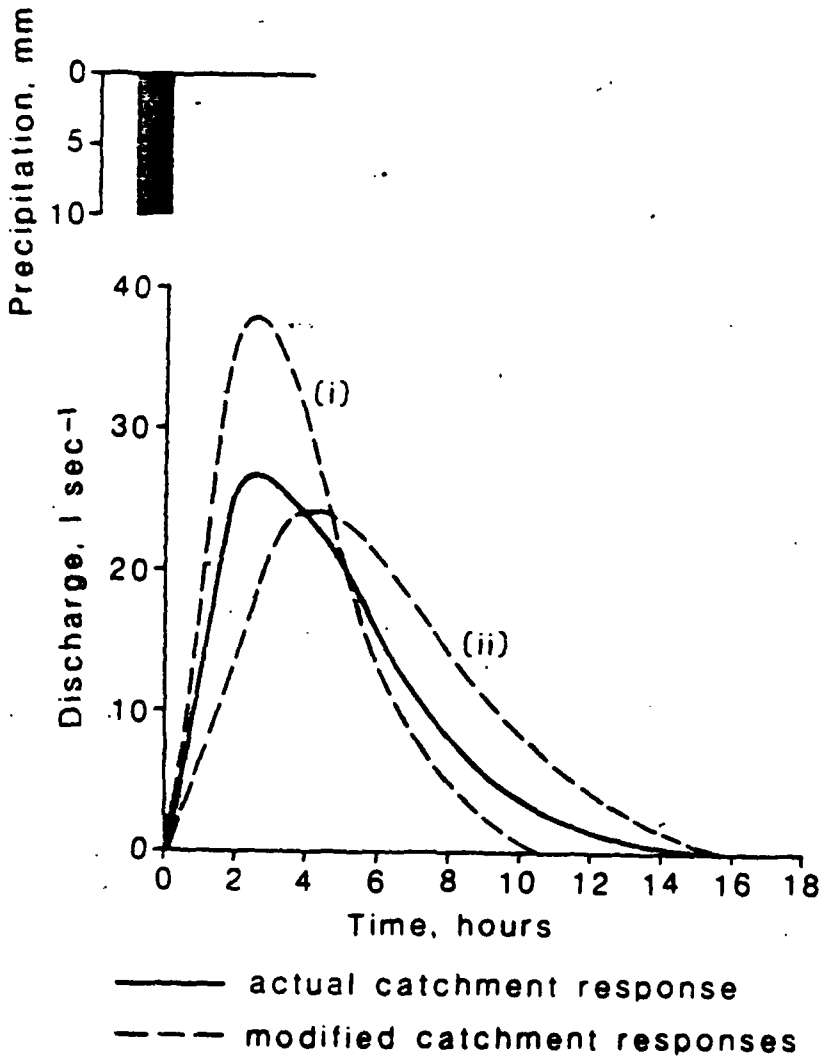

Figure 7.4. Generated catchment responses based upon a 10 mm even in 1 hour for (i) topography having straight rectilinear slopes throughout the entire catchment (mean unit hydrograph 8-C, Figure 7.3) and with (ii) hillslope and spur topography typical of the source to D subcatchment assumed to exist throughout the entire catchment.

This figure shows the response from the actual catchment, together with the predicted response assuming all channel sideslopes were: (1) straight and rectilinear with 6° - 10° slopes (i.e., B to C characteristics); and (2) were shallow hollow-spur topography (D to C characteristics).

In the case of straight rectilinear slopes the peak discharge is increased by 30 percent and the hydrograph time base reduced by 30 percent. However, when the catchment is assumed to comprise all hollow-spur topography (D to C) the time to peak increases by 2 hr. and there is a marginal reduction in peak discharge.

The broad implication is thus that relatively minor topographic "alterations" yield measurable differences in discharge characteristics (Figure 7.4), and such differences may eventually be shown to indicate a scale which, for certain topographic-discharge relationships, should not be exceeded when the topography is shallow.

7.2. Secondary streamflow peaks

Figures 7.5 and 7.6 show the discharge hydrographs obtained from the electrical stage recorder for periods in April 1979. Evident in these and other records are the initial overland flow generated peak (coincident with precipitation) and a subsequent delayed smaller peak. It is seen that the summation of these smaller peaks (throughflow generated) determines the nature of the stream hydrograph recession. Similar peaks have not been identified and reported in the hydrograph records of watersheds with shallow slopes as far as the author is aware. The generating process for these secondary peaks is that of throughflow induced by the detailed and sensitive configuration of the saturated zone at the hillslope base (Sections 4.2 and 4.3). Thus the complete stream hydrograph for an individual storm has a rising limb and peak associated with overland flow, but topographically dependent (See Figures 7.2 and 7.3). By contrast, the tail of the falling limb and entire recession characteristics are generated by the saturated wedge at the slope base (See Figures 7.5 and 7.6) which we have observed to be capable of significant spatial shifts within coarsely defined subcatchment zones (Figure 5.1).

7.3. Baseflow recession

The combination of shallow topography and low permeability has been observed to cause saturation to remain for up to several weeks at the base of the hillslope sector under study (Figure 4.2). This association manifests

itself in the capacity of the shallow topography to maintain baseflow for protracted periods of time fed from shallow soil depths (0-1 m). Figure 7.7 testifies to the existance of maintained areas of saturation at 80 cm depth for up to 3 weeks in the absence of further precipitation. Empirical evidence for the hillslope source area providing the major contribution to the hydrograph at and beyond the peak has suggested that such areas may well undergo a spatial shift during the drainage process. We have already noted that during the commencement and early stages of storm events, shallow and steep slopes respond similarly in the context that convergence of hillslope soil water is seen to occur into topographic hollows. Using an extended version of the study slope sector, together with the simulation program outlined in Chapter 6, the outflow discharge from defined topographic slope elements can be isolated. Figure 7.8 defines the hollow-spur configuration used, with the left hand spur and hollow representing the instrumented study section (Figure 3.1). Start soil water conditions for this subsector were as defined in Figure 7.9, and interpolation of these values and field values provided suitable start data for comparative, as distinct from absolute, comparisons. Figures 7.8 and 7.10 illustrate soil water flow paths for different K_s values at 800 hr into drainage. Whilst at this time such paths appear relatively coincident with the topographic structure, Figure 7.11 is the more revealing. This illustrates in the case of $K_s = 1 \times 10^{-3}$ cm sec^{-1} the initial relative importance of spur locations in providing stream discharge at 100 hr, contrasted with the significant reduction in the significance of these source areas by 800 hours. In the case of $K_s = 1 \times 10^{-5}$ cm sec^{-1}, the important role of hillslope spur sectors in providing stream discharge is again evident, with the only discernable change in emphasis being the relative reduction in contribution from the centre hollow zone. This however is a small, but never the less evident shift which is of course confirmed by empirical results of shifts in the zones of hillslope saturation (Figure 4.2).

7.4. Summary

This analysis has done more than serve to illustrate the relatively complex formulation of hillslope hydrographs from small watershed with shallow topography and low permeability sorts. Specifically it has been shown that

(i) minor relative relief features in terms of undulating topography can induce very significant changes in the hillslope unit hydrograph discharging to the stream (Figures 7.2 and 7.3)

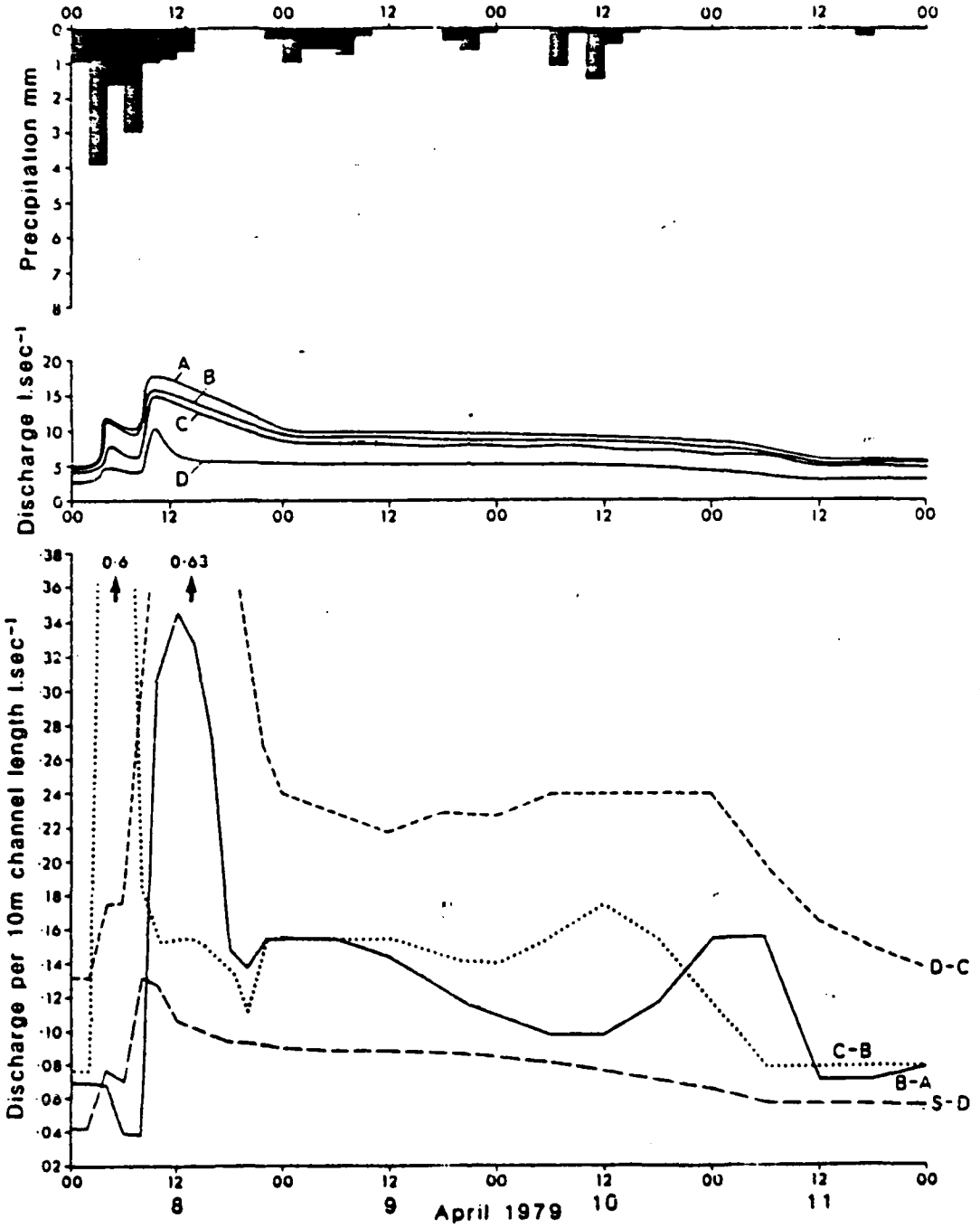

Figure 7.5. Subcatchment hydrographs 8-11 April 1979.

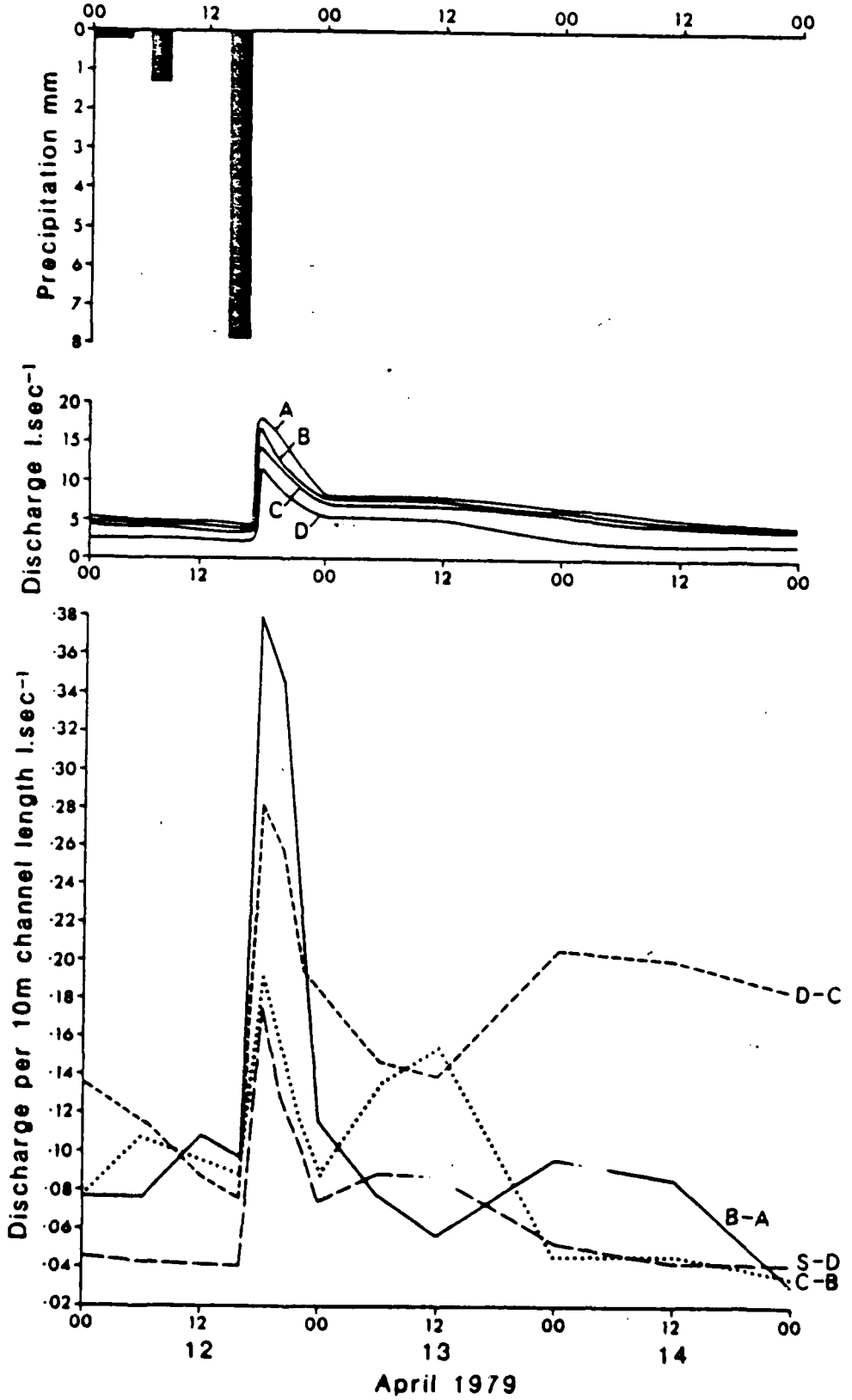

Figure 7.6. Subcatchment hydrographs 12-14 April 1979.

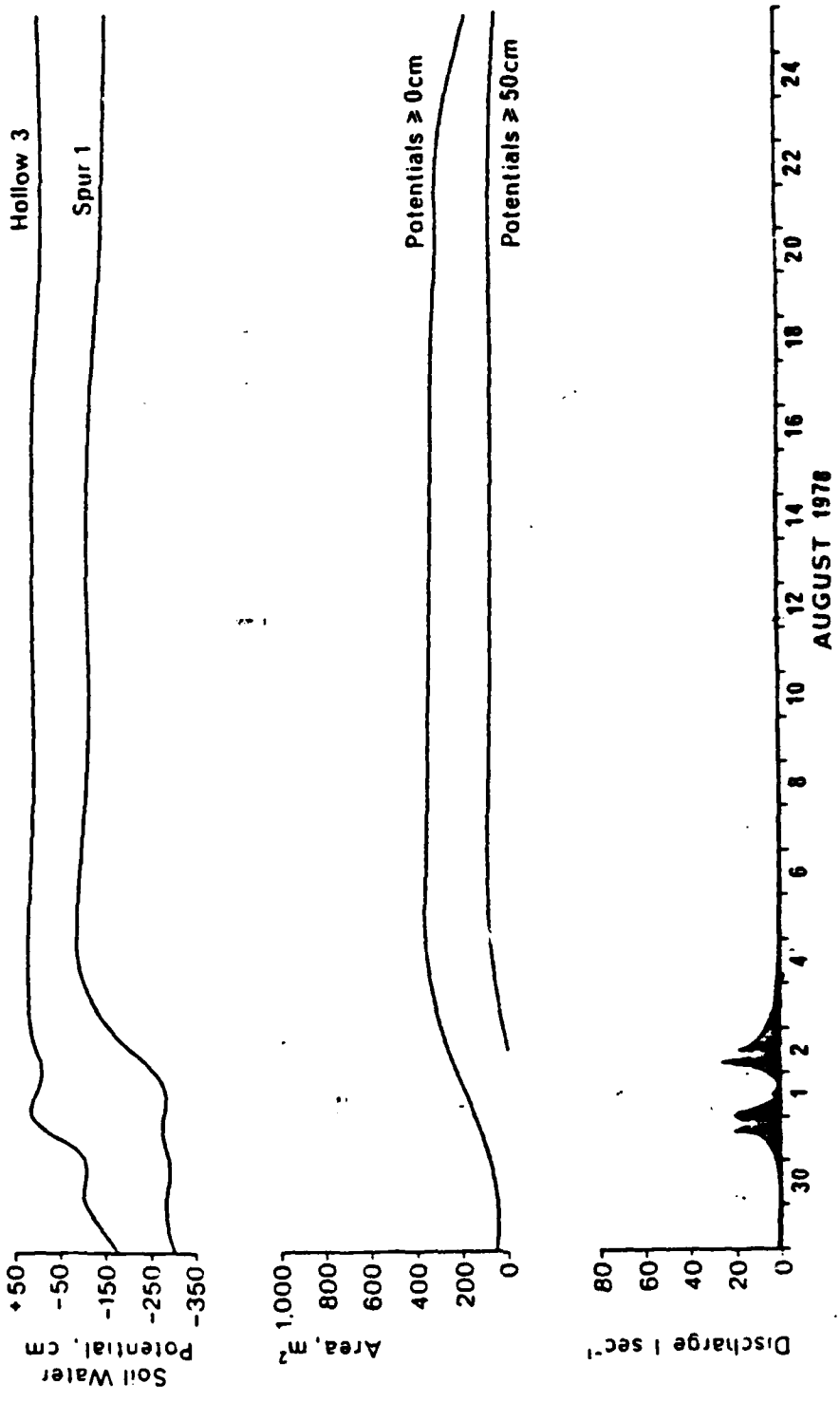

Figure 7.7. Selected soil water potential responses, and hillslope area with soil water potentials above 0 cm for the storm in Figure 4.1.

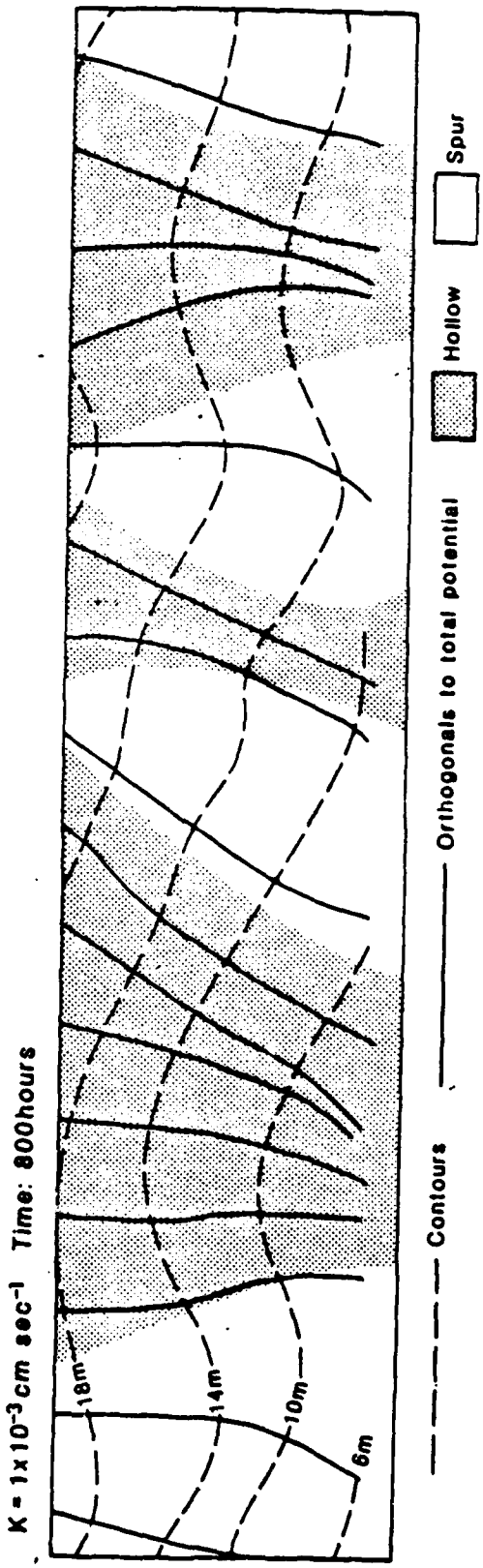

Figure 7.8. Resulting soil water flow paths for enlarged simulation area for the conditions specified.

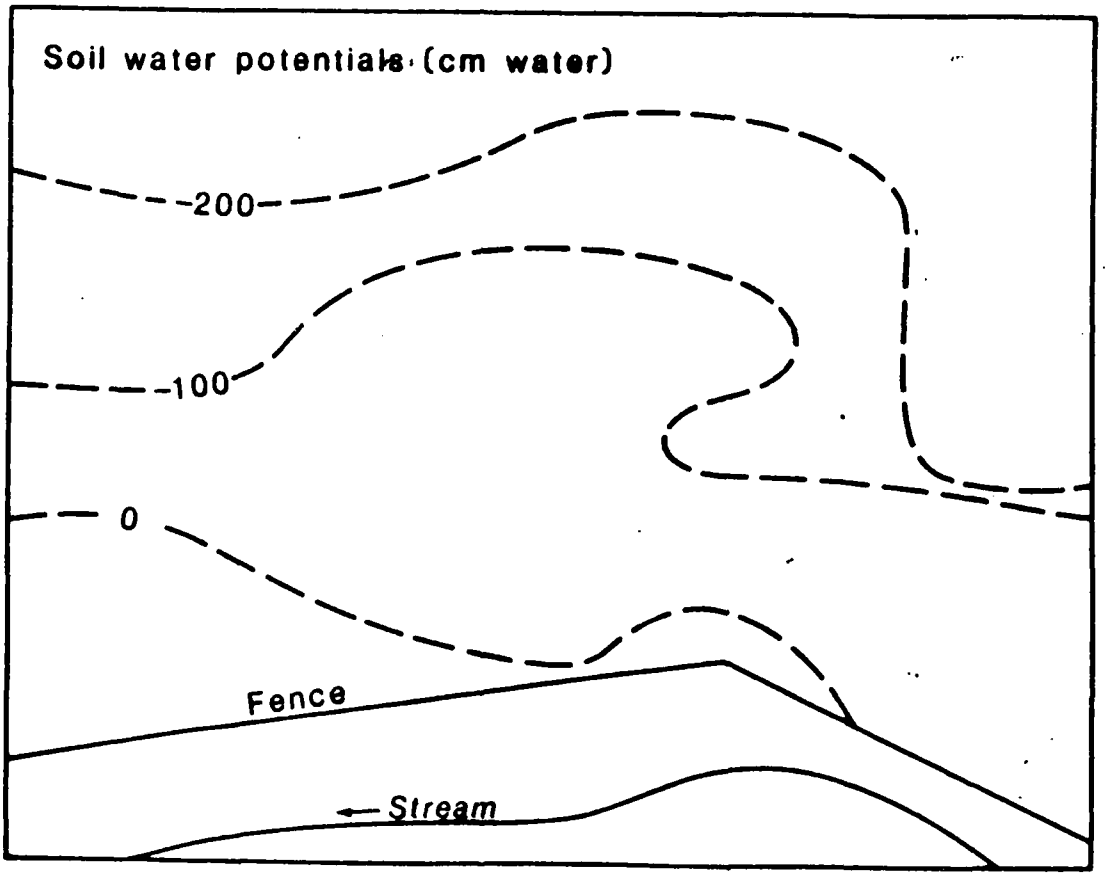

Figure 7.9. Start conditions for the instrumented spur-hollow zone used for the simulations reported in Figures 7.8 and 7.10.

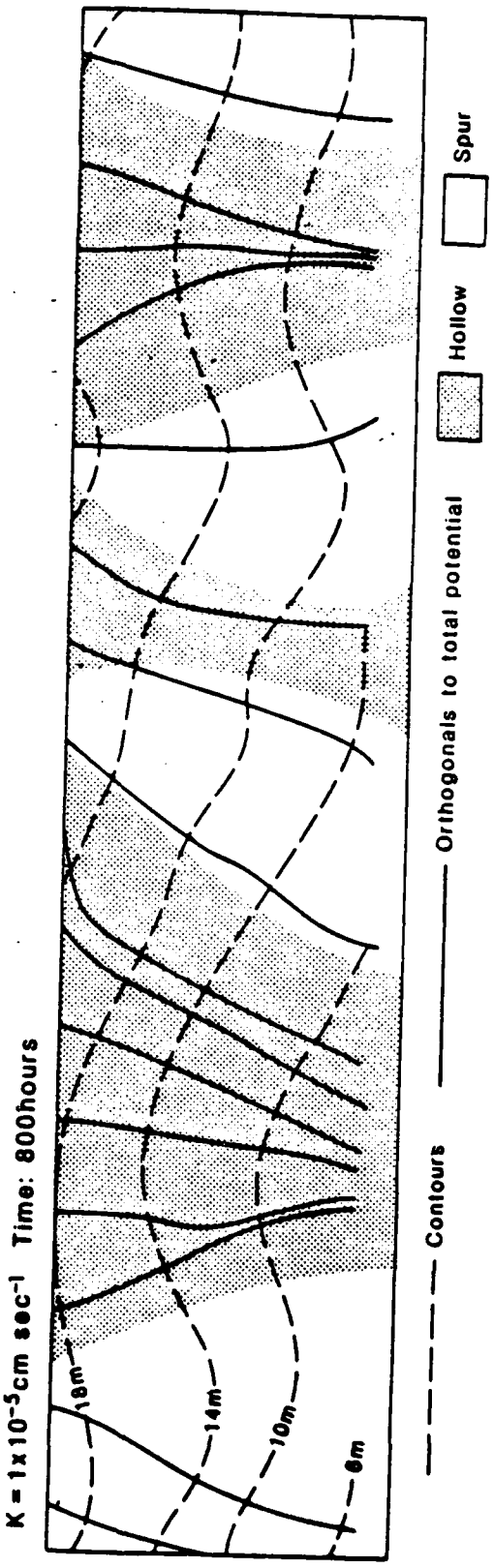

Figure 7.10. Resulting soil water potential orthogonals with $K_s = 1 \times 10^{-5}$ cm sec^{-1}.

(ii) the falling limb of the total catchment outflow is a summation of small, but significant, throughflow pulse peaks (Figures 7.5 and 7.6), the exact timing of which is a function of the spatial location of the saturated zone.

(iii) in recession, the simulation procedure (Chapter 6) has testified to the relative importance of spur slope sections contributing to stream discharge. Two specifics are important here.

(a) the relative contribution is time dependent as the recession takes place (Figure 7.11) and (b) this is the exact opposite of steeper sloped, more permeable soils where hollows dominate the discharge contribution (See Figure 7.12).

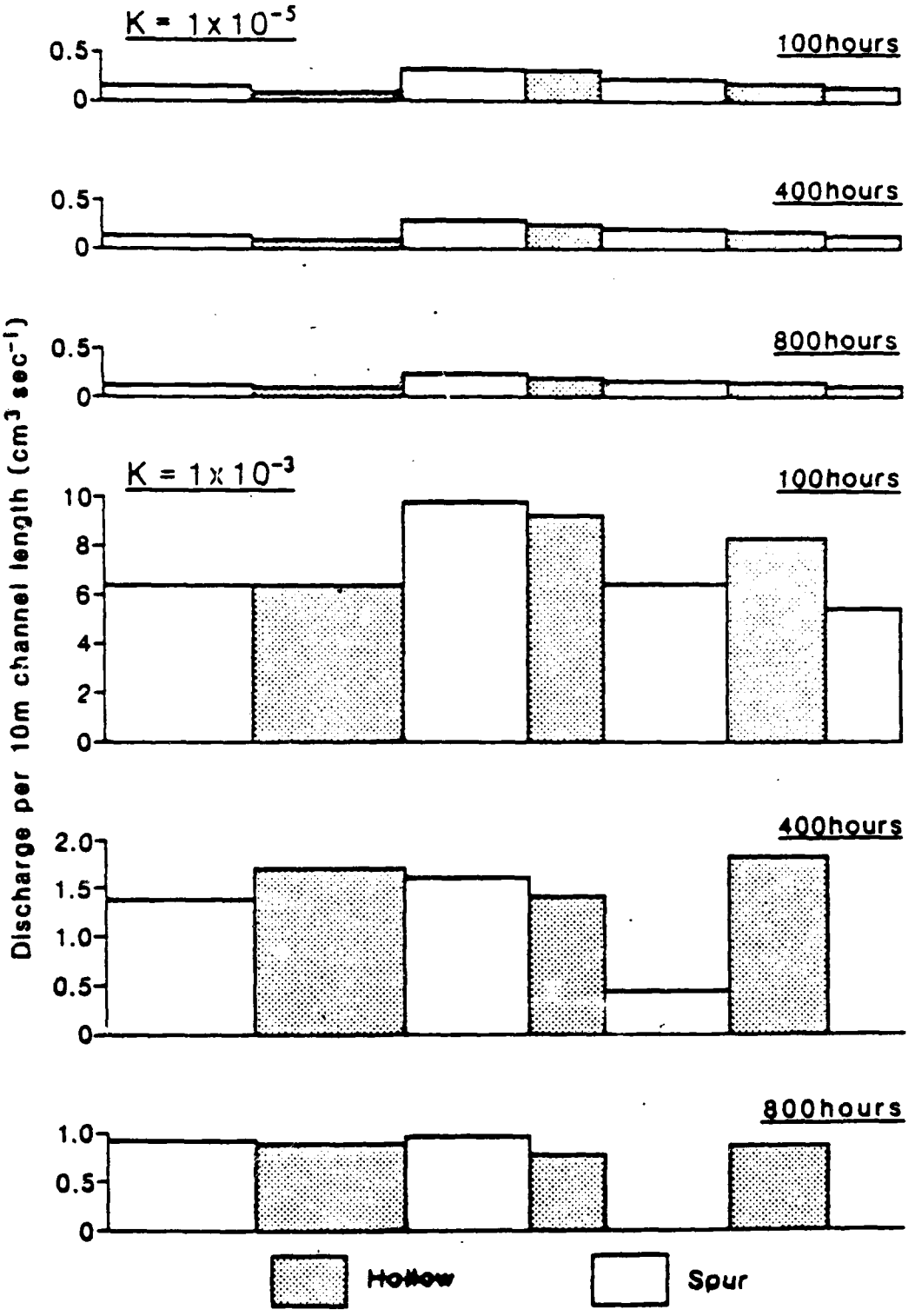

Figure 7.11. Stream inflow from the zones shown in Figures 7.8 and 7.10 at different times during drainage.

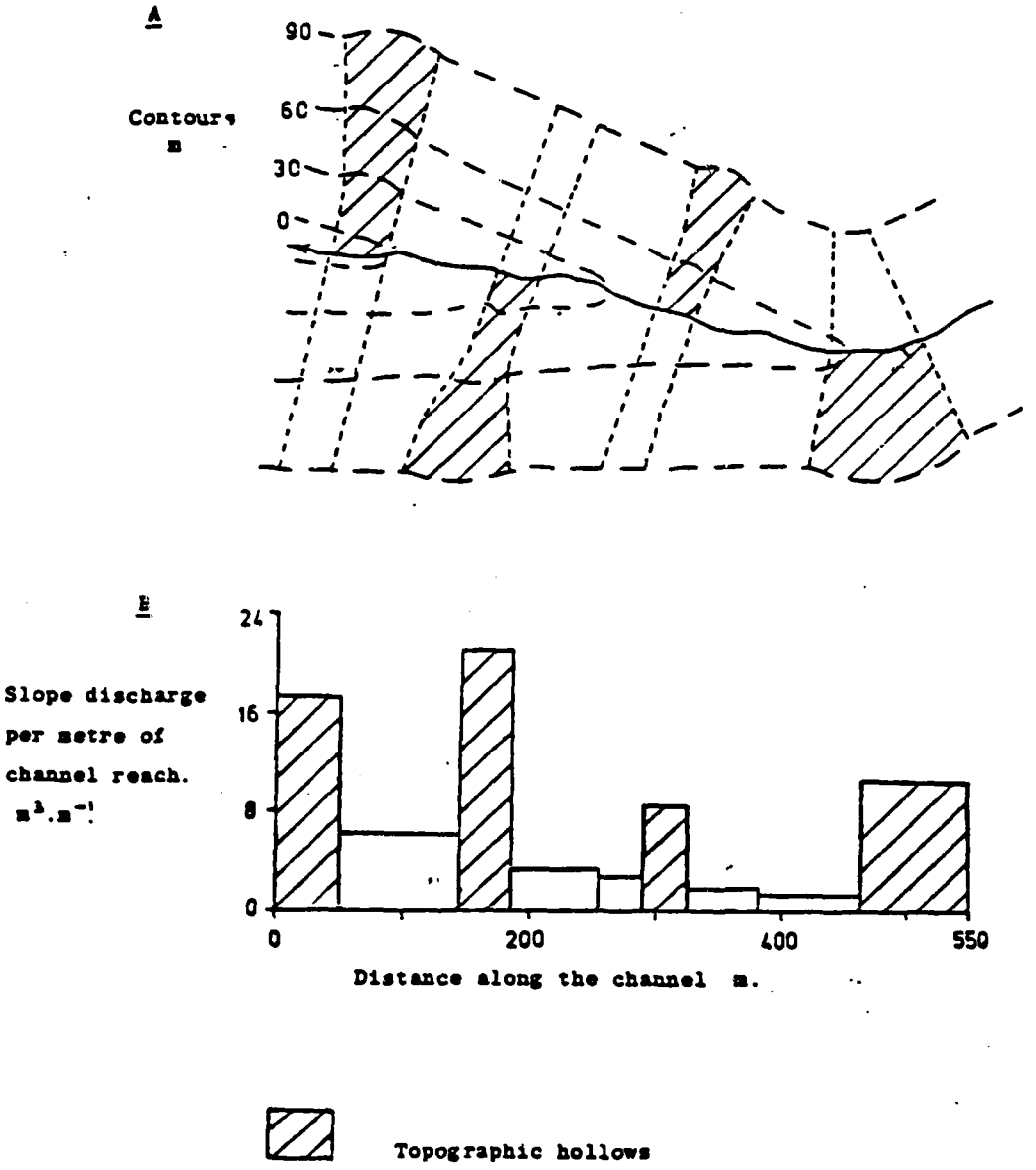

Figure 7.12. A Plan of 26° study site reported in Anderson and Burt (1978)(18), with
B Hillslope discharge inputs for spur and hollow zones.

PART IV

Chapter 8

Conclusions and Recommendations

8.1. Background

Previous detailed investigations showed that on steep, relatively permeable slopes, soil water convergence was always directed into hillslope hollows. This fact has two important implications:

(i) zones of saturation, and hence major streamflow contributing areas in such conditions will be found in hillslope hollows, and

(ii) that because of the dominant effect of elevation potential in the total potential equation, simple topographic indices (e.g., In A/tan B) are seen to perform tolerably well in the identification of zones known to saturate preferentially.

This investigation has sought to broaden this pre-existing investigation in two principal ways:

(i) to examine the nature of soil water potentials and soil water convergence on a comparatively shallow (6°-10°) and less permeable topography, and

(ii) to identify those conditions under which soil water convergence is directed into hillslope hollows and those which it is not. This element was undertaken by a simulation program in recognition of the facts that (a) all possible combinations of relevant factors could not be accommodated by instrumented field sites and (b) the data obtained from the empirical study forming part of this project, and the findings from a previous investigation, provided calibration data representing markedly contrasting topography and soil conditions (i.e., permeable soil and steep togography, low permeability soil and shallow undulating topography).

8.2. Principal findings

(i) That zones of soil water convergence on hillslopes with shallow undulating topography (6-10°) and low permeability soils (1×10^{-6} cm sec^{-1}) are not always coincident with topographic hollows (Figure 4.1 and Chapter 4).

(ii) The zones of soil water convergence in such topography are seen to migrate, during the progress of a storm, from the hollow centre, to the downstream hillslope spur, and, on occasions to return to the hollow (Figures 5.1 and Chapter 5).

(iii) The mechanisms controlling such saturated zone movement, are seen to be in a very fine state of balance at any one time, since with the elevation potential being relatively small, comparatively minor soil water potential changes induced by convergence can cause significant spatial shifts in the location of saturated areas on the hillslope. (Figure 5.2).

(iv) Due to the migrating nature of zones of hillslope saturation in such topography, the performance of topographically derived indices (attractive from the standpoint of military hydrology) to identify such zones is very poor. This is seen to be the case even when the index is derived in the context of only two assumptions relating to water table slope and the soil moisture store. (Figure 5.11 and Chapter 5).

(v) A simulation of hillslope soil water drainage processes has shown, for the controlling variables of hydraulic conductivity, slope angle and stream gradient, that for permeable soils ($K_s > 1 \times 10^{-4}$ cm sec^{-1}) the highest soil water potentials are found in hillslope hollows for all hillslope angles. By contrast, for less permeable soils for slope angles <12° highest soil water potentials occur on the downstream spur. (These findings subject to the boundary and other conditions given in Chapter 6 (See Table 6.1 and Figure 6.2).

(vi) It therefore follows implicitly that this drainage simulation has specified the broad topography/soil permeability groups that static, topographically based indices for hillslope saturated zone identification must be limited to for adequate performance. The evidence here is that such indices (Chapter 5) can only be expected to provide accurate ' a priori' locations of hillslope saturated areas for relatively permeable soils ($K_s > 1 \times 10^{-4}$ cm sec^{-1}) on hillslopes steeper than 12°.

(vii) The zones of saturation on the shallow topography examined were shown to control:

(a) the falling limb of the stream hydrograph by the complex summation of throughflow pulses from the topographically distinct subcatchments (Figure 7.5), and (b) the entire form of the streamflow recession which may, in summer,

last several weeks (Figure 7.7). Of greater importance perhaps is the illustration (Figure 7.2) of the degree of variation in the inflow unit hydrographs for the four topographically distinct subcatchments. Minor topographic changes in shallow topography (i.e., the presence or absence of undulating hollow/spur topography with maximum relative relief of 1 m, on otherwise shallow (6°-10°) rectilinear slopes) have been shown to effect changes in the inflow unit hydrographs for those subcatchments which can produce peak flow variations in excess of 40 percent and a lag in the timing of the peak flow by as much as 2 hr in the 0.74 km^2 catchment.

8.3. Recommendations

(i) Given the complexities of shallow topography hillslope soil water movement, priority should be given to the establishment of more elaborate simulation procedures than that reported here, for the identification of zones of hillslope saturation. (It is evident from this study that streamflow source areas in such topography cannot be identified by static measures).

(ii) That a coordinated recommendation be made for all topographic and soil types, based upon (i), as to the optimum emplacement of soil moisture sensors, either remotely or directly by field operators, for a suite of specific needs e.g., real time models or the identification of saturated hillslope areas.

(iii) That models of the type outlined in Chapter 6 be selectively incorporated into larger scale watershed hydrology models to improve the accuracy of prediction in shallow topography, where, as we have seen, minor variations in topography can yield major changes in the hillslope discharge unit hydrograph (Figure 7.4).

REFERENCES

1. Fleming, G. (1975). Computer simulation techniques in hydrology. Elsevier

2. Anderson, M. G., and Burt, T. P. (1977): Automatic monitoring of soil moisture conditions in a hillslope spur and hollow; J. of Hyd. 33, pp. 27-36.

3. Anderson, M. G., and Burt, T. P. (1978): Toward more detailed field monitoring of variable source areas; Water Resource Res. 14, pp. 1123-1131.

4. Bates, C. G., and Henry, A. J. (1928): Forest and streamflow experiments at Wagon Wheel Gap, Colorado; U. S. Weather Bureau, Mon. Wea. Rev., Suppl. No.30, pp. 79.

5. Hewlett, J. D. (1961): Soil moisture as a source of base flow from steep mountain watersheds; U. S. Forest Serv., Southeast Forest Expt. Sta. Paper 132, pp. 11.

6. Pereira, H. C. (1962): Hydrological effects of changes in land use in some South African catchment areas; East African Agricultural and Forestry Journal Spec. Issue 27, pp. 131.

7. Hewlett, J. D., and Hibbert, A. R. (1967): Factors affecting the response of small watersheds to precipitation in humid areas; in Sopper, W. E. and Lull, H. W., International Symp. on Forest Hydrology, Pergamon Press, New York, pp. 275-290.

8. Whipkey, R. Z. (1965): Subsurface stormflow from forested slopes; Bull. Int. Ass. Sci. Hyd. 10(2), pp. 74-85.

9. Whipkey, R. Z. (1967): Theory and mechanics of subsurface stormflow; in Sopper, W. E. and Lull, H. W., International Symp. on Forest Hydrology, Pergamon Press, New York, pp. 255-259.

10. Ragan, R. M. (1968): An experimental investigation of partial area contributions; Int. Ass. Sci. Hydrol. Pub. No. 76, pp. 241-251.

11. Dunne, T., and Black, R. D. (1970): An experimental investigation of runoff production in permeable soils; Water Resources Res. 6(2), pp. 478-490.

12. Hewlett, J. D., and Nutter, W. L. (1970): The varying source area of streamflow from upland basins; in Proceedings of a symposium on the interdisciplinary aspects of watershed management, Am. Soc. Civ. Eng., New York, pp. 65-83.

13. Wilson, T. V., and Lignon, J. T. (1973): The interflow process on sloping watershed areas; Report No. 38, Water Resources Res. Inst., Clemson University, Clemson, S. Carolina, pp. 58.

14. Weyman, D. R. (1973): Measurements of the downslope flow of water in a soil; J. of Hyd. 20, pp. 267-288.

15. Arnett, R. (1974): Environmental factors affecting the speed and volume of topsoil interflow; Inst. Brit. Geog. Spec. Pub. No. 6, pp. 7-22.

16. Knapp, B. J. (1974): Hillslope throughflow observation and the problem of modelling; in Gregory, K. J., and Walling, D. E. Fluvial Processes in Instrumented Watersheds, Inst. Brit. Geog. Spec. Pub. No. 6, pp. 23-31.

17. Harr, R. D. (1977): Water flux in soil and subsoil on a steep forested slope; J. of Hyd. 33, pp. 37-58.

18. Anderson, M. G., and Burt, T. P. (1978): The role of topography in controlling throughflow generation; Earth Surface Processes 3, pp. 331-344.

19. Burt, T. P. (1978): Runoff processes in a small upland catchment with special reference to the role of hillslope hollows; unpub. Ph.D. thesis, University of Bristol.

20. Dunne, T. (1978): Field studies of hillslope flow processes; in Kirkby, M. J. (Ed.) Hillslope Hydrology, John Wiley, London, pp. 227-294.

21. Kirkby, M. J., and Chorley, R. J. (1967): Throughflow, overlandflow and erosion; Bull. Int. Assoc. Sci. Hydrol. 12(2), pp. 5-21.

22. Burt, T. P., and Anderson, M. G. (1980): Soil moisture conditions on an instrumented slope, Somerset, March to October 1976; in Doornkamp, J. C., and Gregory, K. J. Atlas of Drought in Britain 1975-1976, p. 44.

23. Anderson, M. G., and Burt, T. P. (1978): Time synchronised stage recorders for the monitoring of incremental discharge inputs in small streams; J. of Hyd. 37, pp. 101-109.

24. Anderson, M. G., and Kneale, P. E. (1980): Topography and hillslope soil water relationships in a catchment of low relief. J. Hydrology, 47, pp. 115-128.

25. Rice, R. (1969): A fast response field tensiometer system; Trans. Am. Soc. Agric. Eng. 12, pp. 48-50.

26. Williams, T. H. Lee (1978): An automatic scanning and recording tensiometer system; J. of Hyd. 39, pp. 175-183.

27. Watson, K. K. (1965): Some operating characteristics of a rapid response tensiometer system; Water Resources Res. 1. pp. 577-586.

28. Colbeck, S. C. (1976): On the use of tensiometers in snow hydrology. J. of Glaciology, 17, pp. 135-140.

29. Ingersoll, J. E. (1980): Soil tensiometers for use at temperatures below freezing (unpublished report).

30. Ingersoll, J. E. (1981): Laboratory and field use of soil tensiometers above and below 0°C. CRREL Special Report 81-7.

31. McKim, H. L., Berg, R. L., McGraw, R. W., Atkins, R. T., and Ingersoll, J. (1976): Development of a remote-reading tensiometer/transducer system for use in subfreezing temperatures. Conference on Soil Water Problems in Cold Regions, Edmartan, pp. 31-45.

32. McKim, H. L., Walsh, J. E., and Arion, D. N. (1980): Review of techniques for measuring soil moisture in situ. CRREL Special Report 80-31.

33. Schmugge, T. J., Jackson, T. J., and McKim, H. L. (1980): Survey of methods for soil moisture determination. Water Res. Res., 16, pp. 961-979.

34. Klute, A., and Peters, D. B. (1962): A recording tensiometer with a short response time; Proc. Soil Sci. Soc. Am. 26, pp. 87-88.

35. Watson, K. K., and Jackson, R. J. (1967): Temperature effects on a tensiometer-pressure transducer system; Proc. Soil Sci. Soc. Am. 31, pp. 156-160.

36. Young, N. C. (1968): Using a tensiometer-pressure transducer apparatus to study one and two-dimensional imbibition; M. Sc. thesis, Univ. Idaho, Moscow, Idaho.

37. Fitzsimmons, D. W., and Young, N. C. (1972): Tensiometer-pressure transducer system for studying unsteady flow through soils; Trans. Am. Soc. Agric. Eng. 15, pp. 272-275.

38. Boels, D., Van Gils, J. B. H. M., Veerman, G. J., and Wit, K. E. (1978): Theory and system of automatic determination of soil moisture characteristics and unsaturated hydraulic conductivities; Soil Sci. 126, pp. 191-199.

39. Campbell, G. S. (1974): A simple method for determining unsaturated conductivity from moisture retention data; Soil Science 117, pp. 311-314.

40. Kneale, P. E. (1981) Soil water processes in low permeability soils with reference to hillslope hydrology and slope stability. Unpublished Ph.D thesis, University of Bristol.

41. Hewlett, J. D., and Hibbert, A. R. (1963): Moisture and energy conditions within a sloping soil mass during drainage; J. of Geophysical Res. Vol. 68, pp. 1081-1087.

42. Anderson, M. G., and Burt, T. P. (1977): A laboratory model to investigate the soil moisture conditions on a draining slope; J. of Hyd. 33, pp. 383-390.

43. Beven, K. (1978): The hydrological response of headwater and sideslope areas; Hydrol. Sci. Bull. 23, pp. 419-437.

44. Dunne, T. (1969): Runoff production in a humid area; unpub. Ph.D. thesis, John Hopkins University, Maryland.

45. Latshaw, G. J., and Thomspon, R. F. (1968): Water table study verifies soil interpretations; J. Soil Wat. Conserv. 23, pp. 65-67.

46. Simonson, G. H., and Boersma, L. (1972): Soil morphology and water table relations II: correlation between annual water table fluctuations and profile features; Proc. Soil Sci. Soc. Am. 36, pp. 649-653.

47. Moore, T. R. (1974): Gley morphology and soil water regimes in some soil in south-central England; Geoderma 11, pp. 297-304.

48. Zimmerman, R. C. (1967): Forests of the Sleepers River watersheds. Unpublished USDA report, Danville, Vermont.

49. Boersma, L. (1967): Water table fluctuations in the soil series of the Williamette catena; Trans. Am. Soc. Agric. Eng., 10(3), pp. 405-406.

50. Nelson, L. A., Daniels, R. B., and Gamble, E. E. (1973): Generalizing water table data; Proc. Soil Sci. Soc. Am. 37, pp. 74-78.

51. Dunne. T., Moore, T. R., and Taylor, C. H. (1975): Recognition and prediction of runoff-producing zones in humid regions; Hydrol. Sci. Bull. 20, pp. 305-327.

52. Kirkby, M. J. (1976): Hydrograph modelling strategies. Chapter 3 in Processes in Physical and Human Geography (R. Beel, M. Chisholm, and P. Haggett eds), Heinemann.

53. Beven, K., and Kirkby, M. J. (1979): A physically based, variable contributing area model of basin hydrology; Hydrol. Sci. Bull. 24, pp. 43-69.

54. Anderson, M. G., and Kneale, P. E. (1982): The influence of low angled topography on hillslope soil water and stream discharge. J. Hydrology, (in press).

55. Kirkby, M. J. (1978): Implications for sediment transport; in Kirkby, M. J. (ed.) Hillslope Hydrology, John Wiley, London, pp. 325-362.

56. Beven, K. (1977): Hillslope hydrographs by the finite element method. Earth Surface Processes, 2, pp. 13-28.

57. Freeze, R. A. (1978): Mathematical models of hillslope hydrology; in Kirkby, M. J. (Ed.) Hillslope Hydrology, John Wiley, London, pp. 117-226.

58. Poulovassilis, A. (1962): Hysteresis of pore water, on application of the concept of independent domains. Soil Science, 93, pp. 405-412.

59. Hillel, D. (1977): Computer simulation of soil-water dynamics. IDRC Ottawa.

60. Clapp, R. B., and Hornberger, G. M. (1978): Empirical equations for some soil hydraulic properties. Water Res. Res., 14, pp. 601-604.

61. Brakensiek, D. L. (1979): Comments on empirical equations for some soil hydraulic properties by Roger B. Clapp and George M. Hornberger. Water Res. Res., 15, pp. 989-900.

62. Zeigler, B. P. (1976): Theory of modelling and simulation. John Wiley.

63. Sharma, M. L., Gander, G. A., and Hunt, C. G (1980): Spatial variability of infiltration in a watershed. J. Hydrology, 45, pp. 101-122.

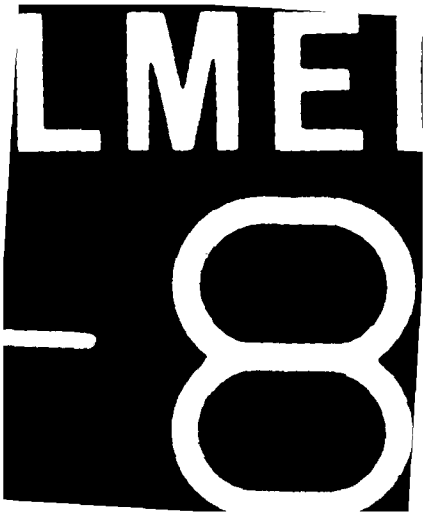
LME
8